Supporting Information

for

Diverse Structural Reactivity Pattern of a POCOP Ligand with Coinage Metals

Moushakhi Ghosh[a], Nasrina Parvin[b], Prakash Panwaria[a], Srinu Tothadi[c], Rangarajan Bakthavatsalam[c], Arshad Therambram[a], Shabana Khan[a]*

[a]Department of Chemistry, Indian Institute of Science Education and Research Pune, Dr. Homi Bhabha Road, Pashan, Pune-411008, India.

[b]CSIR-Central Salt and Marine Chemicals Research Institute, Gijub Badheka Marg, Bhavnagar-364002, India

[c] Indian Institute of Science Education and Research (IISER) Tirupati, Tirupati, India

*Corresponding author. E-mail: shabana@iiserpune.ac.in

Contents

S1. Experimental Details

All experiments were carried out under an atmosphere of dry argon or in vacuo using a standard Schlenk technique and in a dinitrogen filled MBRAUN MB 150-G1 glovebox. The solvents used were purified by an MBRAUN solvent purification system MB SPS-800. All other chemicals purchased from Aldrich were used without further purification. ^{1}H, ^{13}C, ^{19}F and $BF_3 \cdot OEt_2$ for ^{11}B NMR spectra were recorded with the Bruker 400 MHz spectrometer, using $CDCl_3$ and DMSO-d_6 as a solvent with an external standard ($SiMe_4$ for ^{1}H, ^{13}C; 85% H_3PO_4 for ^{31}P and CHF_3 for ^{19}F).

❖ Synthesis of 1

We modified the existing procedure. 4,6-di-*tert*-butyl resorcinol (3.33 g, 15 mmol) was taken in a 100ml schlenk flask and was made soluble in 50 ml anhydrous diethyl ether. 12 ml *n*-BuLi (2.5 M in n-Hexane) was added slowly dropwise to the reaction mixture at -78^{o}C and stirred for 4 hrs at room temperature. Diphenylchlorophosphine (PPh_2Cl) (5.55 ml, 30 mmol) was added to the reaction mixture at -78 ^{o}C. After overnight stirring at room temperature, LiCl was precipitated out from the reaction mixture and was filtered off. The solvent was evaporated, and the oily residue was made soluble in excess *n*-hexane, which afforded colourless crystals. Yield: 6.2 g (70%). The ^{1}H, ^{31}P, and ^{13}C matched well with previously reported literature.[1]

❖ Synthesis of 2

1 (0.295 g, 0.5 mmol) and CuCl (0.067 g, 0.5 mmol) were taken in a flask, and 40 mL of DCM was added to the reaction mixture. After overnight stirring at room temperature, the reaction was filtered off. The colourless crystals suitable for X-ray analysis were obtained from a dichloromethane and n-pentane mixture after 1 day at room temperature. Yield: 450 mg (65 %). ^{1}H NMR (400 MHz, $CDCl_3$, 298K): δ 1.15 (s, 36H, CMe_3), 7.02-7.04 (m, 16H, aromatic CH), 7.12 (s, 2H, aromatic CH), 7.13-7.26 (m, 8H, aromatic CH), 7.32-7.33 (m, 16H, aromatic CH), 8.20 (s, 2H, aromatic CH) ppm. $^{13}C\{^{1}H\}$ NMR (100.6 MHz, $CDCl_3$, 298K): δ 29.40 (CMe_3), 33.30 (CMe_3), 110.72 (resorcinyl aromatic CH, ortho), 123.65 (resorcinyl aromatic CH, meta), 126.80,127.25, 128.85, 129.18, 130.35, 130.45, 130.97, 131.01,131.05,131.09, 134.79, 149.79, 150.57 ppm. $^{31}P\{^{1}H\}$ NMR (161.976 MHz, $CDCl_3$, 298 K): δ 90.74, 92.88 ppm. Mp: 266.9 °C. MALDI TOF: $C_{76}H_{80}Cu_2Cl_2O_4P_4$: m/z 1379.342 Found m/z: 689.0856 (for $C_{38}H_{40}CuClO_2P_2$) (Monomer)

❖ Synthesis of 3

1 (0.295 g, 0.5 mmol) and CuBr (0.14 g, 1 mmol) were taken in a flask, and 40 mL of DCM was added to the reaction mixture. After overnight stirring at room temperature, the reaction was filtered off. The colourless crystals suitable for X-ray analysis were obtained from a dichloromethane and n-pentane mixture after a few days at room temperature. Yield: 700 mg (80 %).^{1}H NMR (400 MHz, $CDCl_3$, 298K): δ 1.12 (s, 36H, C*Me*$_3$), 6.99-7.05 (m, 16H, aromatic CH), 7.09 (s, 2H, aromatic CH), 7.18-7.24 (m, 8H, aromatic CH), 7.28-7.34 (m, 16H, aromatic CH), 8.20 (s, 2H, aromatic CH) ppm. ^{13}C{^{1}H} NMR (100.6 MHz, $CDCl_3$, 298K): δ 29.40 (C*Me*$_3$), 33.29 (C*Me*$_3$), 111.81 (resorcinyl aromatic CH, ortho), 123.72 (resorcinyl aromatic CH, meta), 126.74, 127.20, 128.88, 129.22, 131.16, 131.20, 131.24, 131.29, 134.67, 134.73, 134.79, 149.61, 150.42 ppm. ^{31}P{^{1}H} NMR (161.976 MHz, $CDCl_3$, 298 K): δ 91.40 ppm. Mp: 205.0 °C. ESI MS: $C_{76}H_{80}Cu_4Br_4O_4P_4$: m/z 1755.142 Found m/z: 1755.5341

❖ **Synthesis of 4**

1 (0.295 g, 0.5 mmol) and CuI (0.19 g, 1 mmol) were taken in a flask, and 40 mL of DCM was added to the reaction mixture. After overnight stirring at room temperature, the reaction was filtered off. The colourless crystals suitable for X-ray analysis were obtained from a dichloromethane and n-pentane mixture at room temperature. Yield: 650 mg (67 %). ^{1}H NMR (400 MHz, $CDCl_3$, 298K): δ 1.15 (s, 36H, C*Me*$_3$), 7.02-7.04 (m, 16H, aromatic CH), 7.11 (s, 2H, aromatic CH), 7.21 (m, 8H, aromatic CH), 7.33 (m, 16H, aromatic CH), 8.20 (s, 2H, aromatic CH) ppm. ^{13}C{^{1}H} NMR (100.6 MHz, $CDCl_3$, 298K): δ 29.50 (C*Me*$_3$), 33.29 (C*Me*$_3$), 113.39 (resorcinyl aromatic CH, ortho), 124.02 (resorcinyl aromatic CH, para), 126.65, 127.20, 128.94, 131.59, 134.51, 149.10 ppm. ^{31}P{^{1}H} NMR (161.976 MHz, $CDCl_3$, 298 K): δ 92.9 ppm. Mp: 255.4 °C MALDI TOF: $C_{76}H_{80}Cu_4I_4O_4P_4$: m/z 1943.146 Found m/z: 1980.4334 (for M+K-2)

❖ **Synthesis of 5**

1 (0.295 g, 0.5 mmol) and CuOTf.toluene (0.516 g, 1 mmol) were taken in a flask, and 40 mL of DCM was added to the reaction mixture. After overnight stirring at room temperature, the reaction was filtered off. The colourless crystals suitable for X-ray analysis were obtained from a dichloromethane and n-pentane mixture at room temperature. Yield: 520 mg (51 %).^{1}H NMR (400 MHz, $CDCl_3$, 298K): δ 1.17 (s, 36H, C*Me*$_3$), 6.29 (s, 2H, aromatic H), 7.22-7.28 (m, 16H, phenyl H), 7.29 (s, 2H, aromatic H), 7.32-7.37 (m, 8H, phenyl H), 7.45-7.53 (m, 16H, phenyl H) ppm. ^{31}P{^{1}H} NMR (161.976 MHz, $CDCl_3$, 298 K): δ 98.28 ppm. Mp: 207.6 °C MALDI TOF: $C_{80}H_{80}Cu_4F1_2O_{16}P_4S_4$: m/z 2031.804 Found m/z: 2031.5327

❖ **Synthesis of 6**

Complex **2** (0.690 g, 0.5 mmol) was made soluble in anhydrous THF, and $KPPh_2$ (2 ml in 0.5M solution) was added to the same flask at room temperature. The colour of the reaction instantly changed to bright yellow from colourless. After overnight stirring at room temperature, the reaction was filtered off. The colourless crystals suitable for X-ray analysis were obtained from a THF and toluene mixture at 0°C. Yield: 720 mg (66 %). MALDI TOF: $C_{124}H_{120}Cu_4O_4P_8$: m/z 2175.4287 Found m/z: 2215.4287

❖ **Synthesis of 7**

1 (0.59 g, 1 mmol), $CuBF_4(ACN)_4$ (0.471 g, 1.5 mmol) and 2-2'-bipyridine (0.396 g, 1.5 mmol) were taken in a flask, and 40 mL of DCM was added to the reaction mixture. After overnight stirring at room temperature, the reaction was filtered off. The colourless crystals suitable for X-ray analysis were obtained from a dichloromethane and diethylether mixture at room temperature. Yield: 710 mg (72 %). ^{1}H NMR (400 MHz, DMSO-d_6, 298K): δ 1.09 (s, 36H, C*Me*$_3$), 6.42 (m, 2H, aromatic CH), 7.17 (33H, aromatic CH), 7.31(4H, aromatic CH), 7.49 (8H, aromatic CH), 7.61 (5H, aromatic CH), 8.18 (6H, aromatic CH), 8.53 (m, 6H, aromatic CH) ppm, ^{31}P{^{1}H} NMR (161.976 MHz, $CDCl_3$, 298 K): δ 104.8, 94.3, 91.3, ^{11}B NMR ($CDCl_3$, 128.387 MHz): δ 0.65 ppm, ^{19}F{^{1}H} NMR (376.66 MHz, $CDCl_3$, 298 K): -152.9 ppm. MALDI TOF: $C_{106}H_{104}Cu_3O_4P_4N_6B_3F_{12}$: m/z 2100.9974 Found m/z: 2215.4287

❖ **Synthesis of 8**

1 (0.295 g, 0.5 mmol) and AgBr (0.188 g, 1 mmol) were taken in a flask, and 40 mL of DCM was added to the reaction mixture. After overnight stirring at room temperature, the reaction was filtered off. The colourless crystals suitable for X-ray analysis were obtained from a dichloromethane and n-pentane mixture at room temperature. Yield: 690 mg (70 %).^{1}H NMR (400 MHz, DMSO-d_6, 298K): δ 1.21 (s, 36H, C*Me*$_3$), 6.27 (s, 2H, aromatic CH), 7.22 (s, 2H, aromatic H), 7.35-7.42 (m, 16H, aromatic CH), 7.45-7.51 (m, 8H, aromatic CH), 7.64-7.72 (m, 16H, aromatic CH) ppm. ^{31}P{^{1}H} NMR (161.976 MHz, DMSO-d_6, 298 K): δ 107.24 ppm. Mp: 255.4 °C MALDI TOF: $C_{76}H_{80}Ag_4Br_4O_4P_4$: m/z 1932.431 Found m/z: 1932.431 (for M^+)

❖ **Synthesis of 9**

1 (0.295 g, 0.5 mmol) and AgI (0.232 g, 1 mmol) were taken in a flask, and 40 mL of DCM was added to the reaction mixture. After overnight stirring at room temperature, the reaction was filtered off. The colourless crystals suitable for X-ray analysis were obtained from a

dichloromethane and n-pentane mixture at room temperature. Yield: 730 mg (65 %). Mp: 256.1 °C MALDI TOF: $C_{76}H_{80}Ag_4I_4O_4P_4$: m/z 2119.7383 Found m/z: 2159.4146 (M+K+1)

❖ **Synthesis of 10**

1 (0.59 g, 1 mmol) and $AgSbF_6$ (0.172 g, 0.5 mmol) were taken in a flask, and 40 mL of DCM was added to the reaction mixture. After overnight stirring at room temperature, the reaction was filtered off. The colourless crystals suitable for X-ray analysis were obtained from a THF and n-pentane mixture after two days at room temperature. Yield: 500 mg (65 %).^{1}H NMR (400 MHz, DMSO-d_6, 298K): δ 1.25 (s, 36H, CMe_3), 6.57 (s, 2H, aromatic CH), 7.27 (s, 2H, aromatic CH), 7.40-7.47 (m, 16H, aromatic CH), 7.48-7.57 (m, 24H, aromatic CH) ppm. - ^{13}C{^{1}H} NMR (100.6 MHz, DMSO-d_6, 298K): δ 30.29 (CMe_3), 30.62 (CMe_3), 34.17 (CMe_3), 34.60 (CMe_3), 124.99, 129.40, 129.53, 129.64, 129.74, 130.67, 130.83, 130.87, 131.09, 131.14, 131.33, 131.35, 132.01, 132.34, 132.89, 132.92, 153.04, 154.20 ppm. ^{31}P{^{1}H} NMR (161.976 MHz, DMSO-d_6, 298 K): δ 18.56, 27.68, 111.27 ppm. Mp: 248.1 °C. MALDI TOF: $C_{76}H_{80}AgO_4P_4SbF_6$: m/z 1522.3000 Found m/z: 1329.9229 (M+K-SbF_6)

❖ **Synthesis of 11**

1 (0.295 g, 0.5 mmol) and $AuCl.SMe_2$ (0.298 g, 1 mmol) were taken in a flask, and 40 mL of DCM was added to the reaction mixture. After overnight stirring at room temperature, the reaction was filtered off. The colourless crystals suitable for X-ray analysis were obtained from a THF and n-pentane mixture at room temperature. Yield: 600 mg (75 %).^{1}H NMR (400 MHz, DMSO-d_6, 298K): δ 1.24 (s, 18H, CMe_3), 6.06 (s, 1H, aromatic CH) 7.39 (s, 1H, aromatic CH), 7.55-7.70 (m, 20H, aromatic CH) ppm. ^{13}C{^{1}H} NMR (100.6 MHz, DMSO-d_6, 298K): δ 30.08 (CMe_3), 34.69 (CMe_3), 126.54, 130.33, 130.45, 131.75, 131.92, 133.68, 135.72, 151.44 ppm. ^{31}P{^{1}H} NMR (161.976 MHz, DMSO-d_6, 298 K): δ 110.91 ppm. Mp: 154.2 °C. MALDI TOF: $C_{38}H_{40}AuO_2P_2Cl$: m/z 1060.1681 Found m/z: 1021.9920 (M-1-Cl)

❖ **Synthesis of 12**

1 (0.295 g, 0.5 mmol) and $AuCl.SMe_2$ (0.298 g, 1 mmol) were taken in a flask, and 40 mL of DCM was added to the reaction mixture. After overnight stirring at room temperature, 1 equivalent of $AgSbF_6$ (0.344 g, 1 mmol) was added at 0 °C and stirred at room temperature. The reaction was filtered off. The colourless crystals suitable for X-ray analysis were obtained from a dichloromethane and n-pentane mixture at room temperature. Yield: 600 mg (66 %). ^{1}H NMR (400 MHz, DMSO-d_6, 298K): δ 1.17 (s, 36H, CMe_3), 6.80 (s, 2H, aromatic CH), 7.30-

7.57 (m, 36H, aromatic CH), 7.67-7.76 (m, 8H, aromatic CH) ppm. $^{13}C\{^{1}H\}$ NMR (100.6 MHz, DMSO-d_6, 298K): δ 30.07 (C*Me*$_3$), 34.89 (C*Me*$_3$), 128.28, 130.27, 130.61, 130.82, 130.88, 130.95, 131.68, 131.77, 131.86, 135.11,136.44, 151.25, 165.04 ppm. $^{31}P\{^{1}H\}$ NMR (161.976 MHz, DMSO-d_6, 298 K): δ 127.20 ppm. Mp: 251.9 °C ESI-MS: $C_{76}H_{80}Au_2Sb_2F_{12}O_4P_4$: m/z 1811.08 Found m/z: 1813.6002.

S2. NMR Spectroscopic Data for complexes 2-12

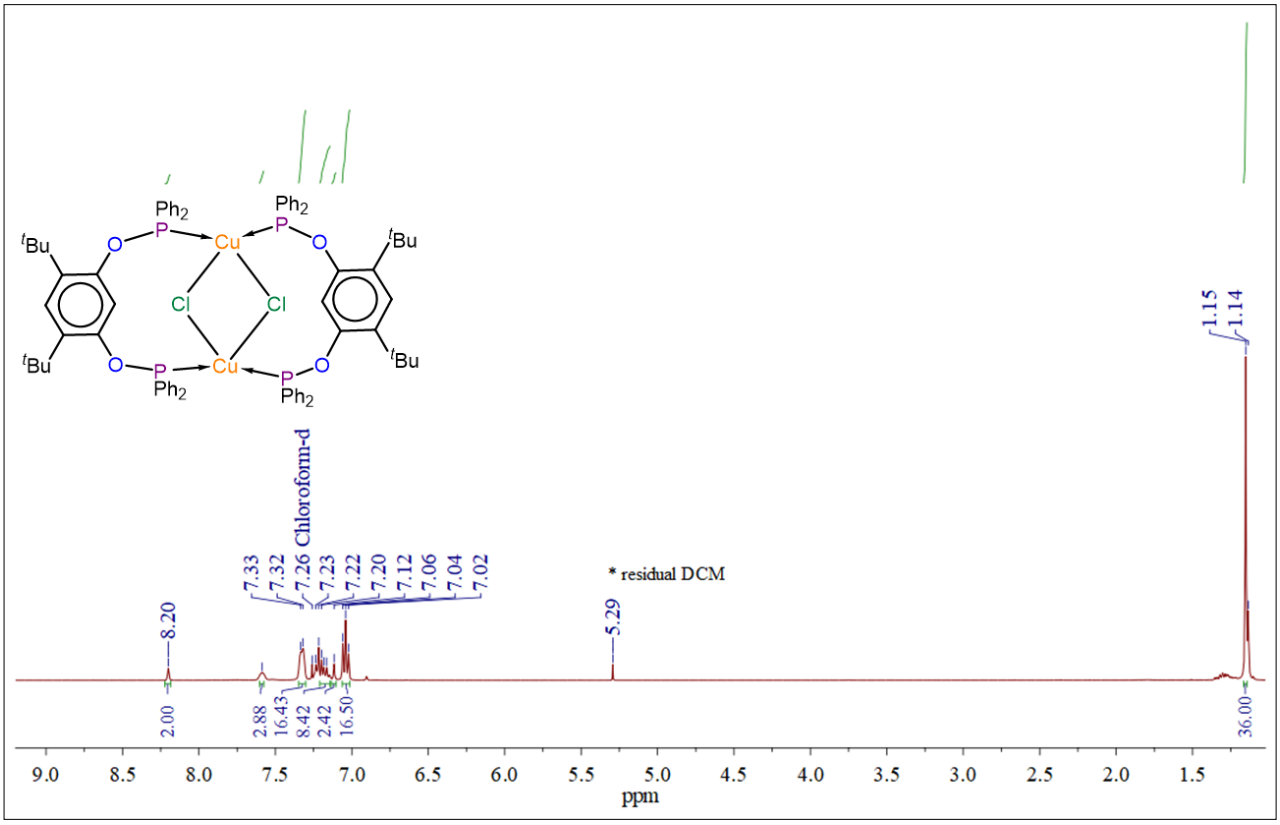

Figure S1. ^{1}H NMR spectrum of **2**

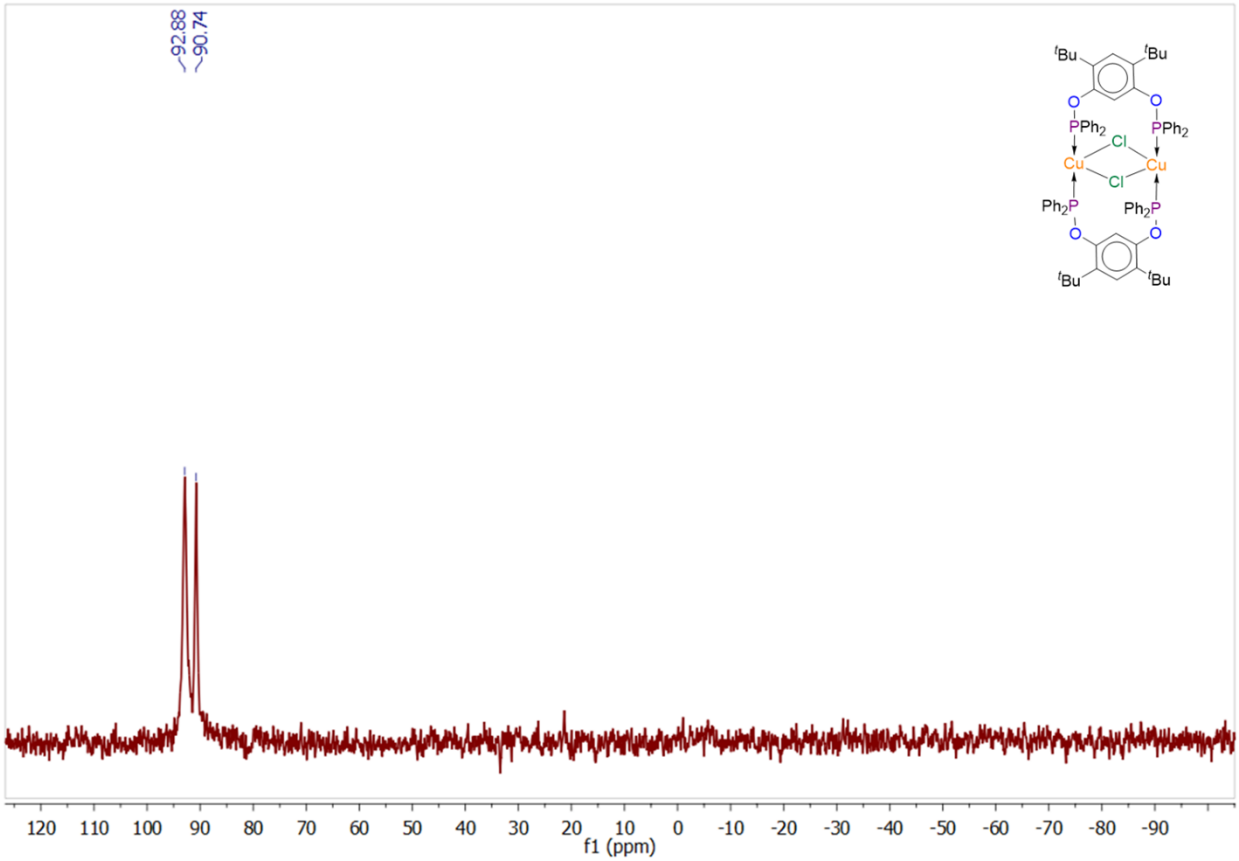

Figure S2. ^{31}P NMR spectrum of **2**

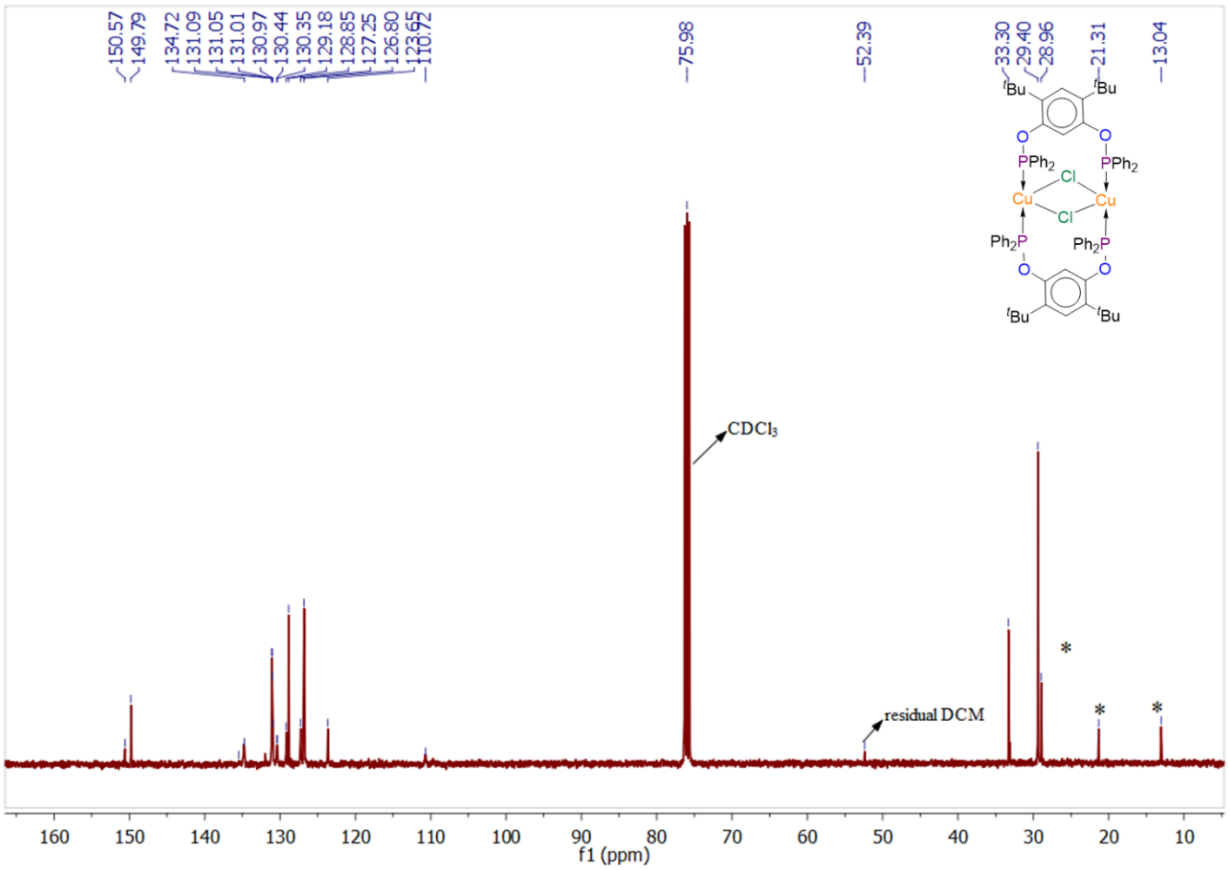

Figure S3. ^{13}C NMR spectrum of **2**

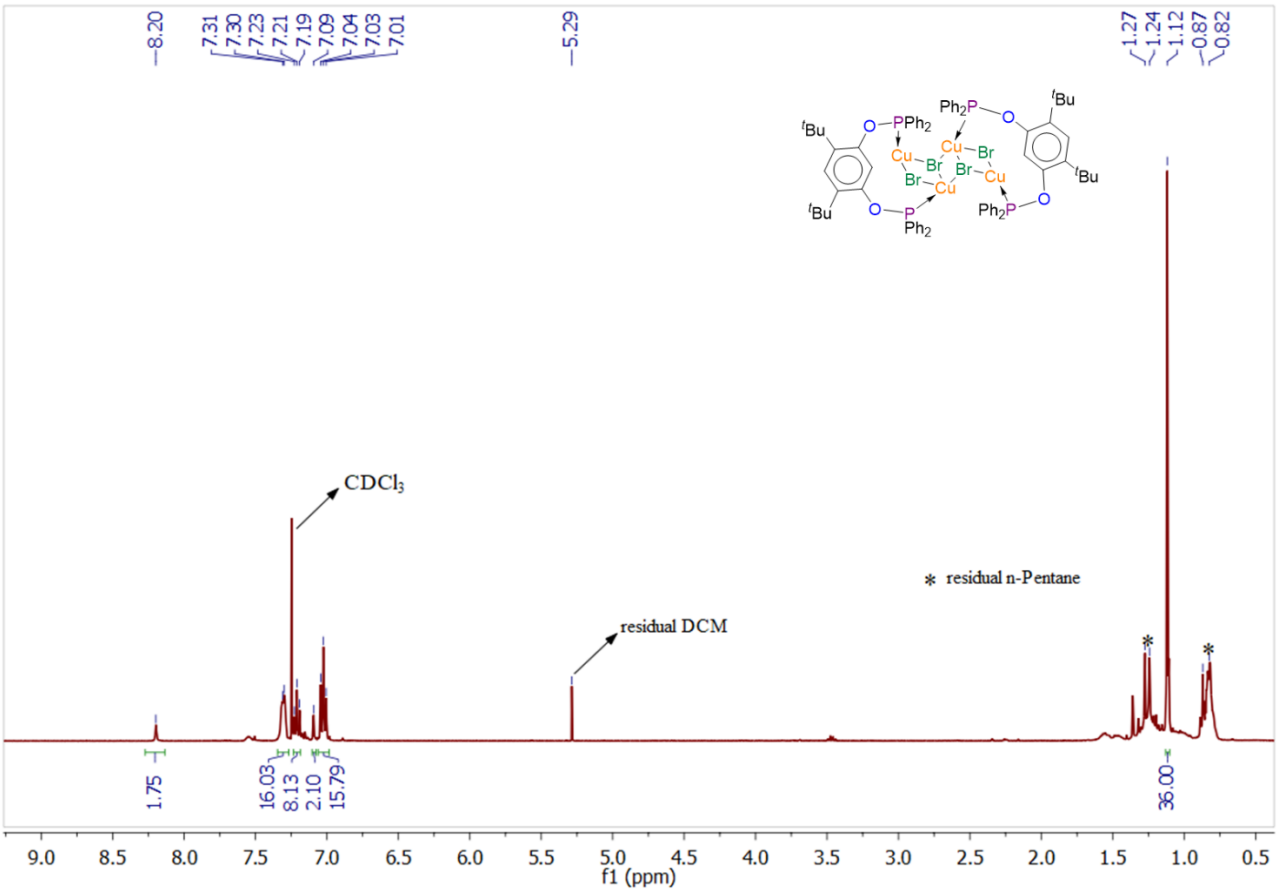

Figure S4. ^{1}H NMR spectrum of **3**

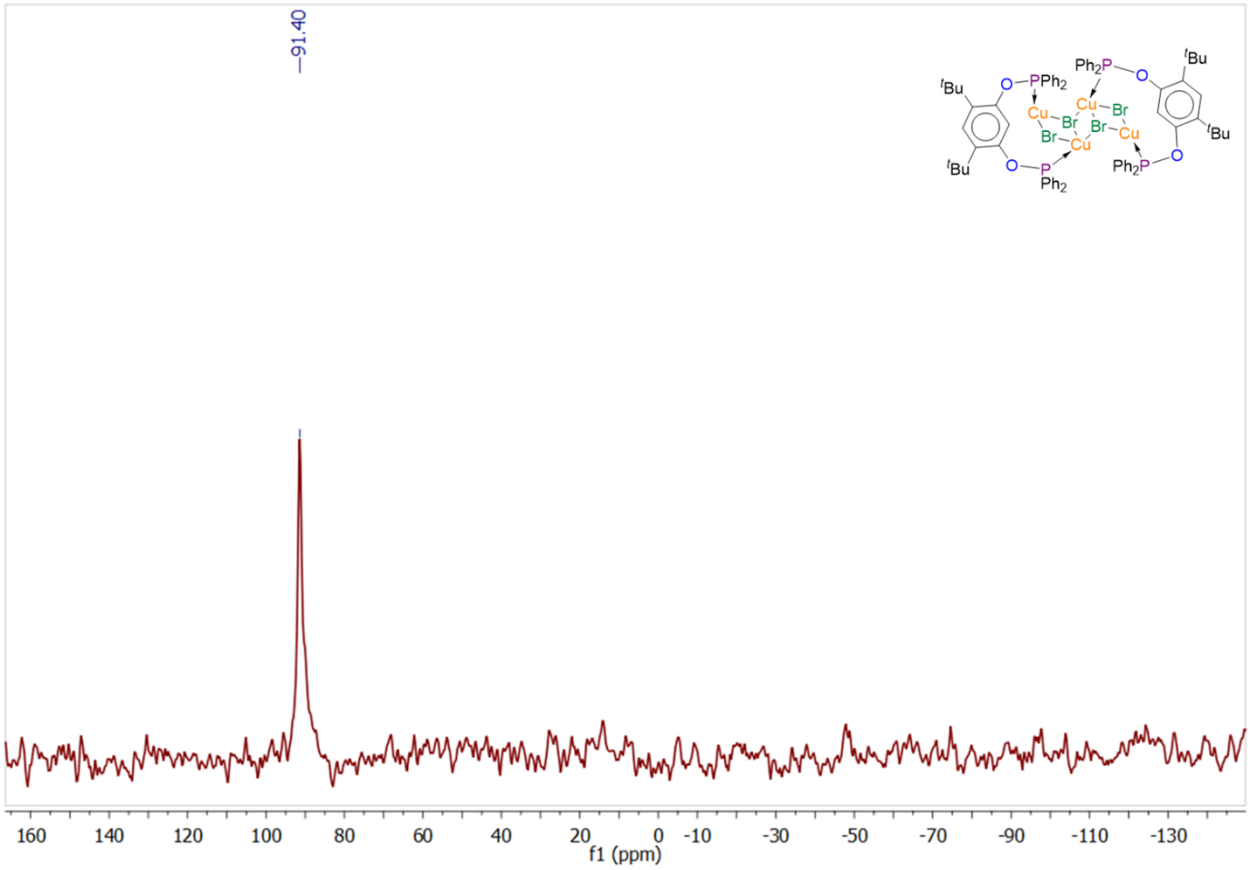

Figure S5. ^{31}P NMR spectrum of **3**

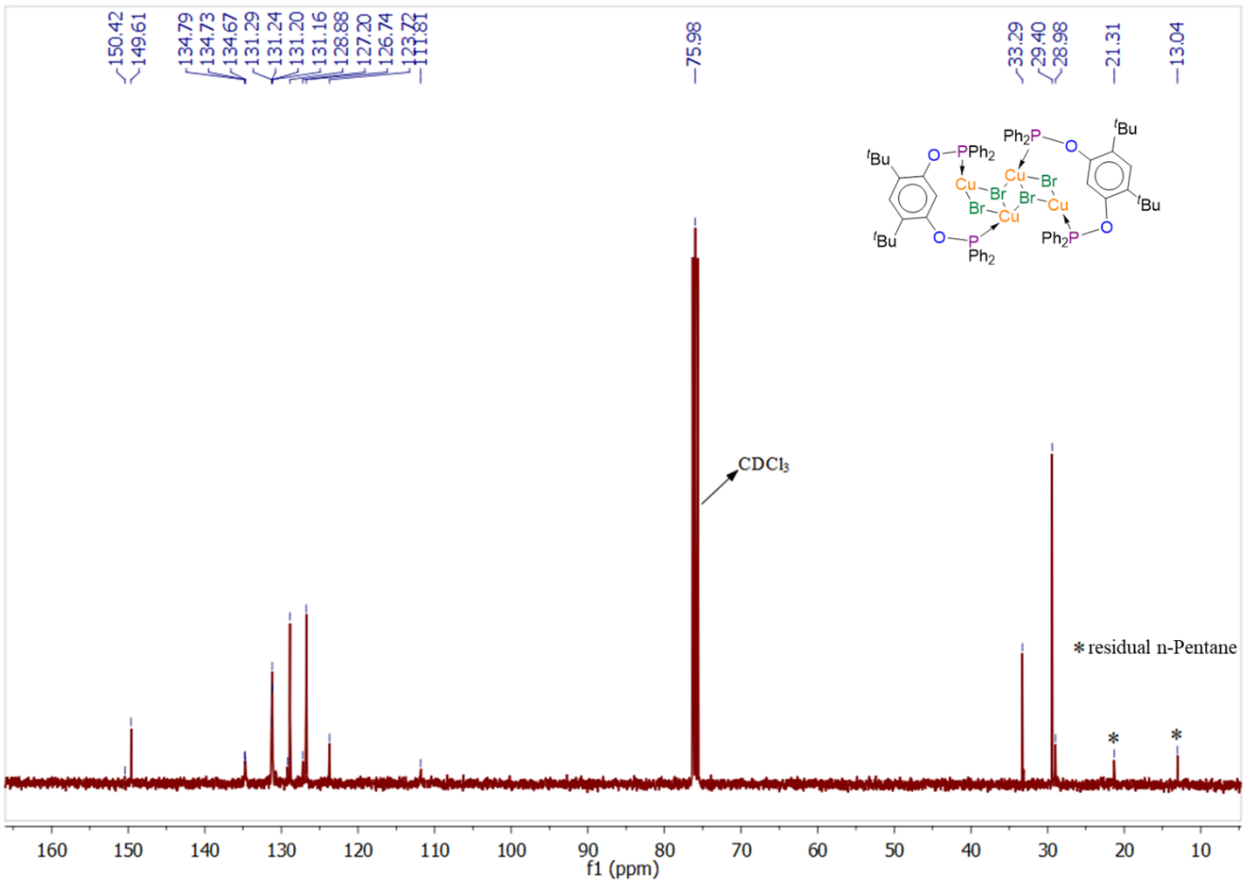

Figure S6. ^{13}C NMR spectrum of **3**

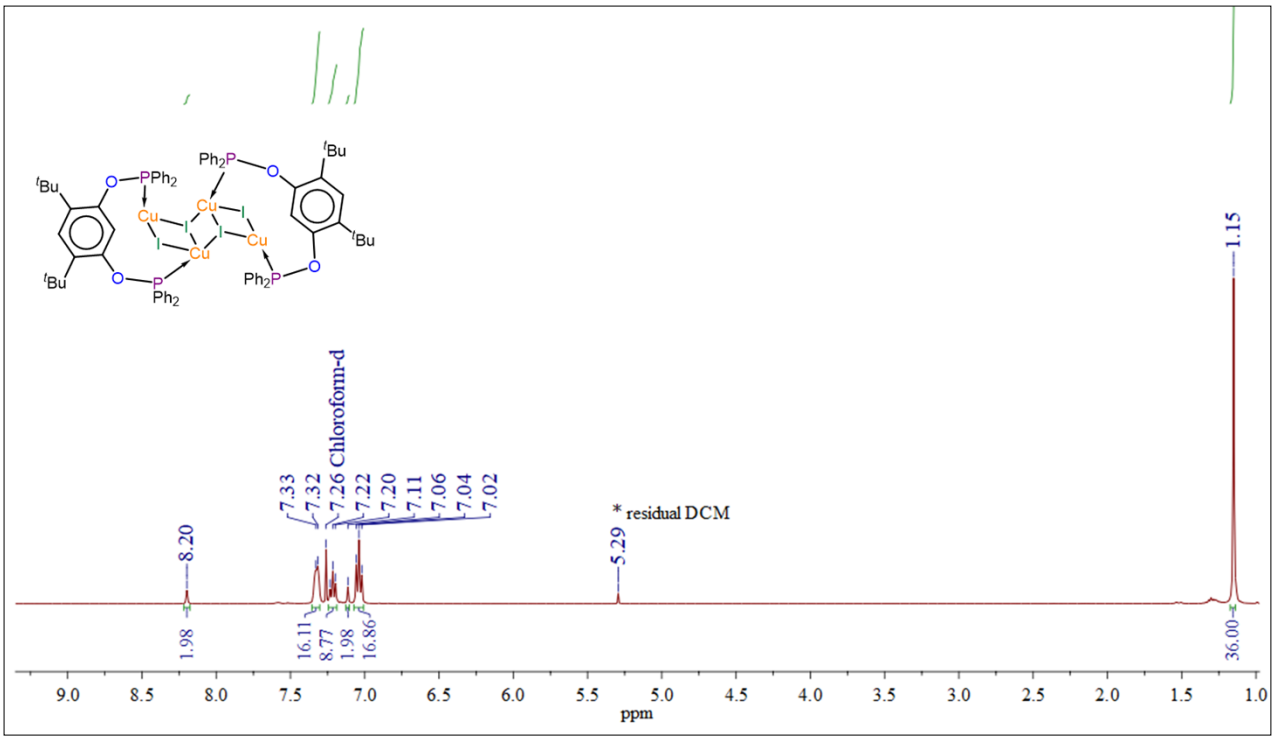

Figure S7. ^{1}H NMR spectrum of **4**

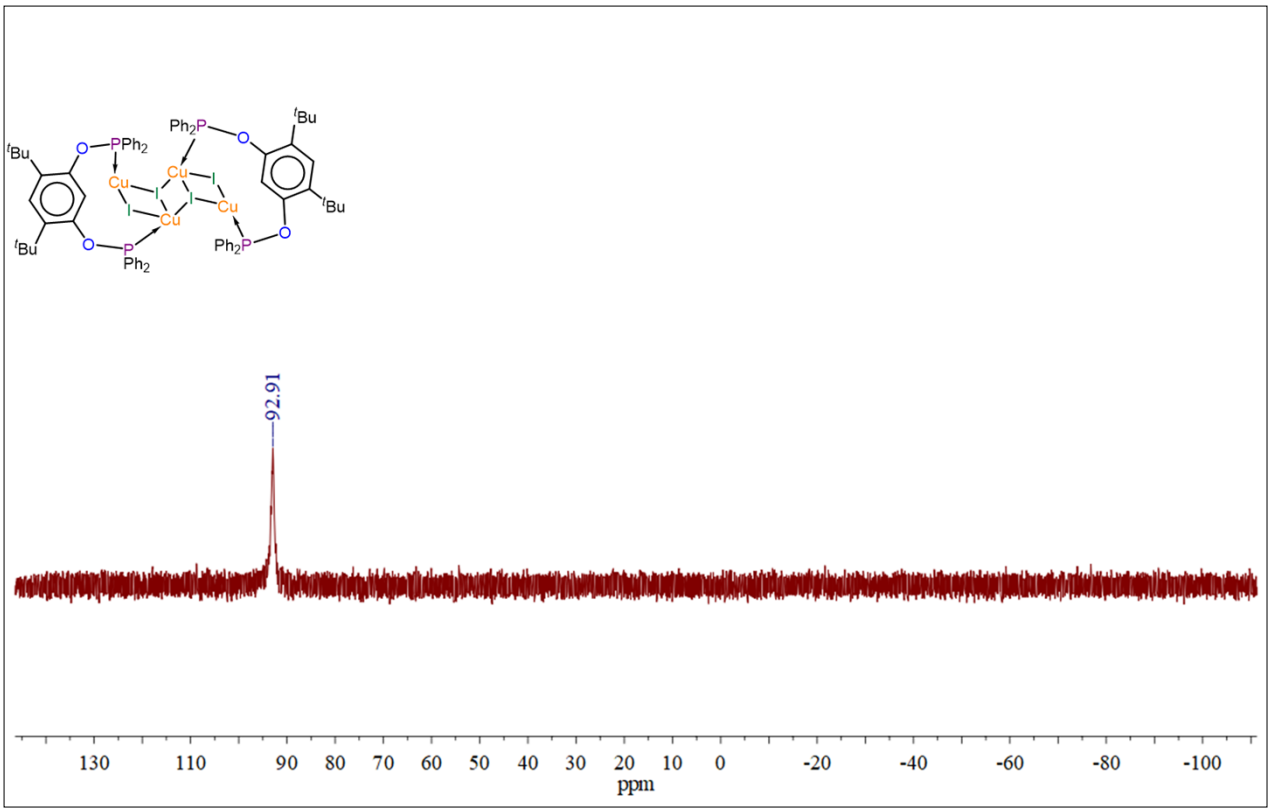

Figure S8. ^{31}P NMR spectrum of **4**

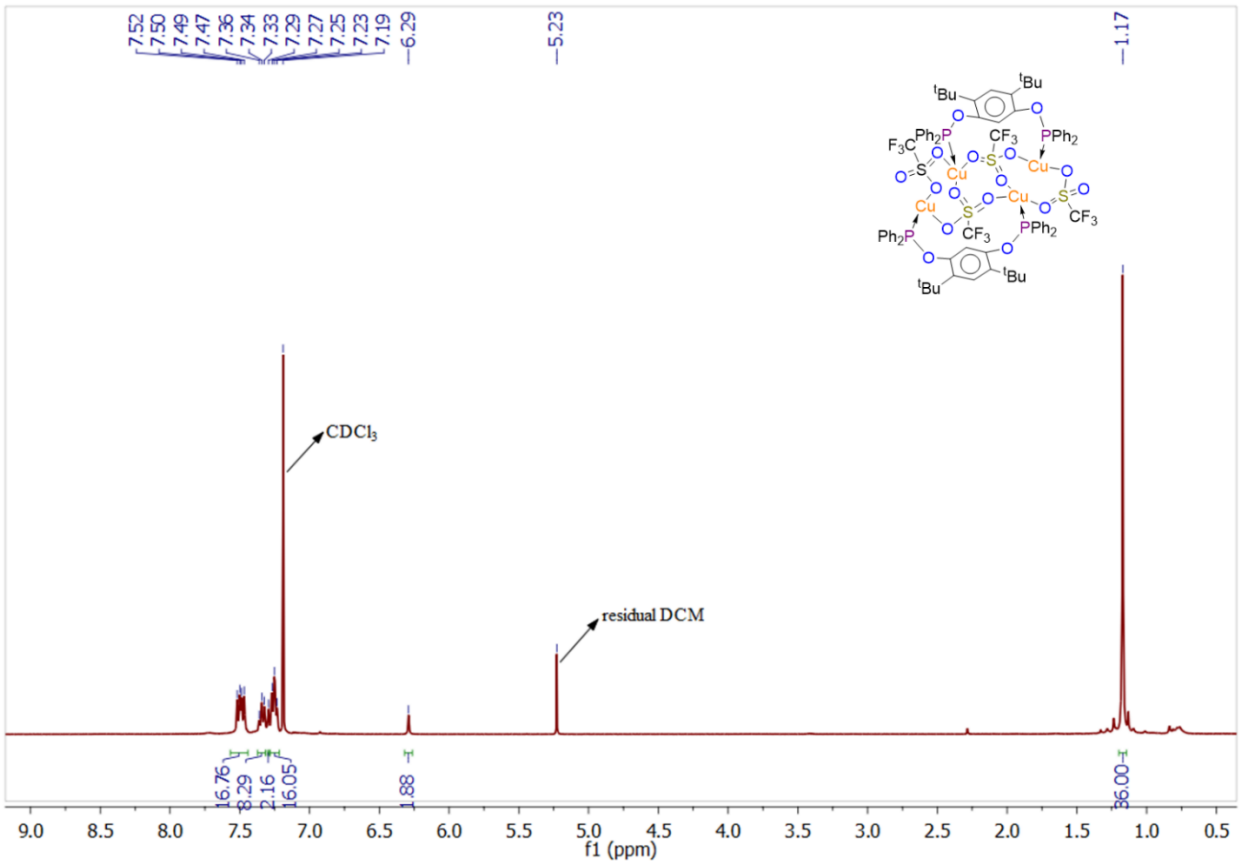

Figure S9. ^{1}H NMR spectrum of **5**

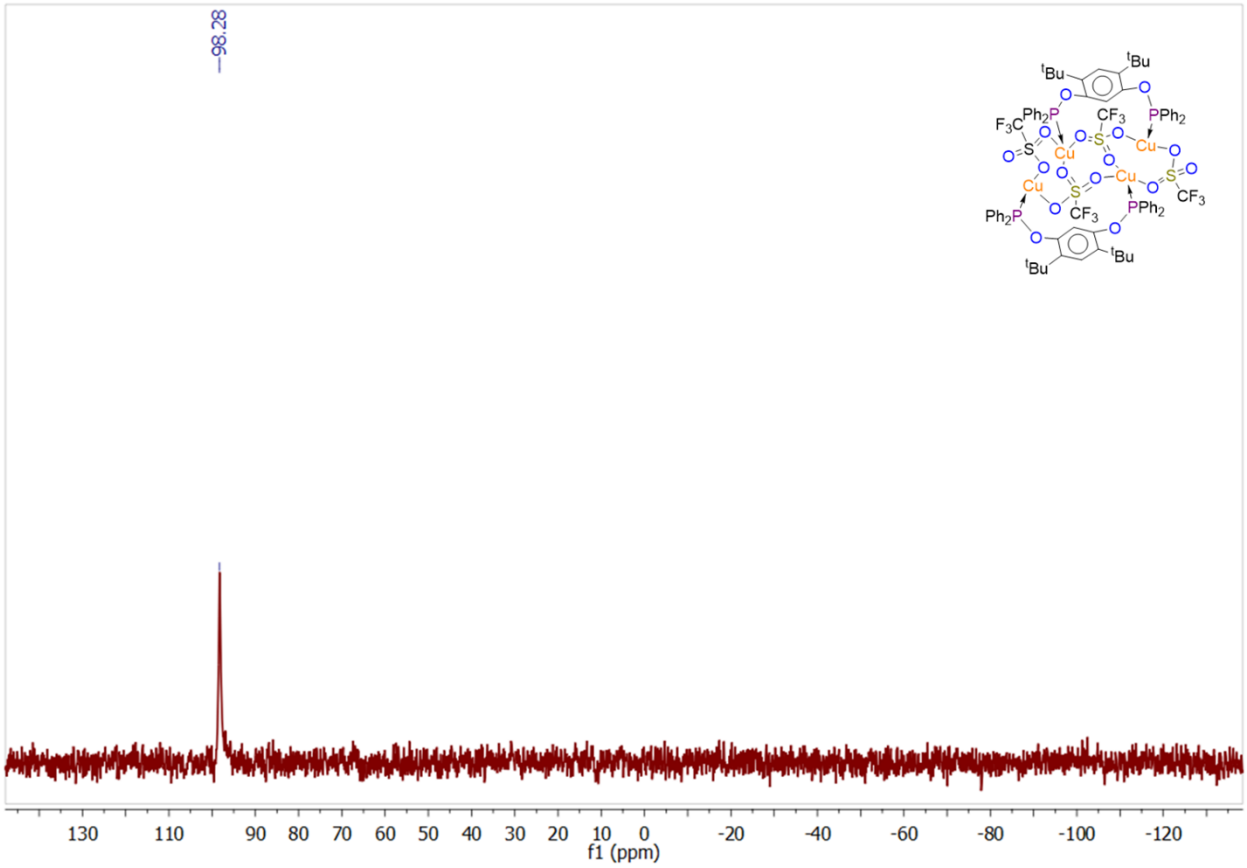

Figure S10. ^{31}P NMR spectrum of **5**

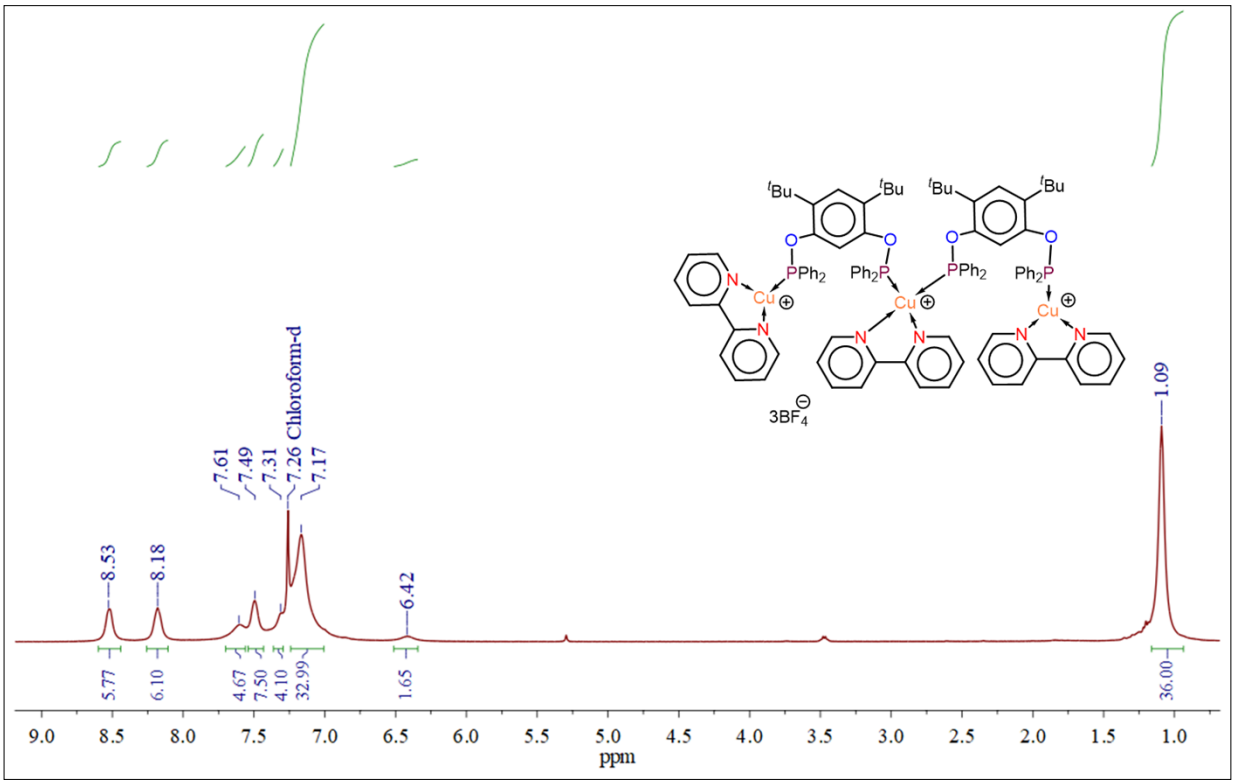

Figure S11. ^{1}H NMR spectrum of **7**

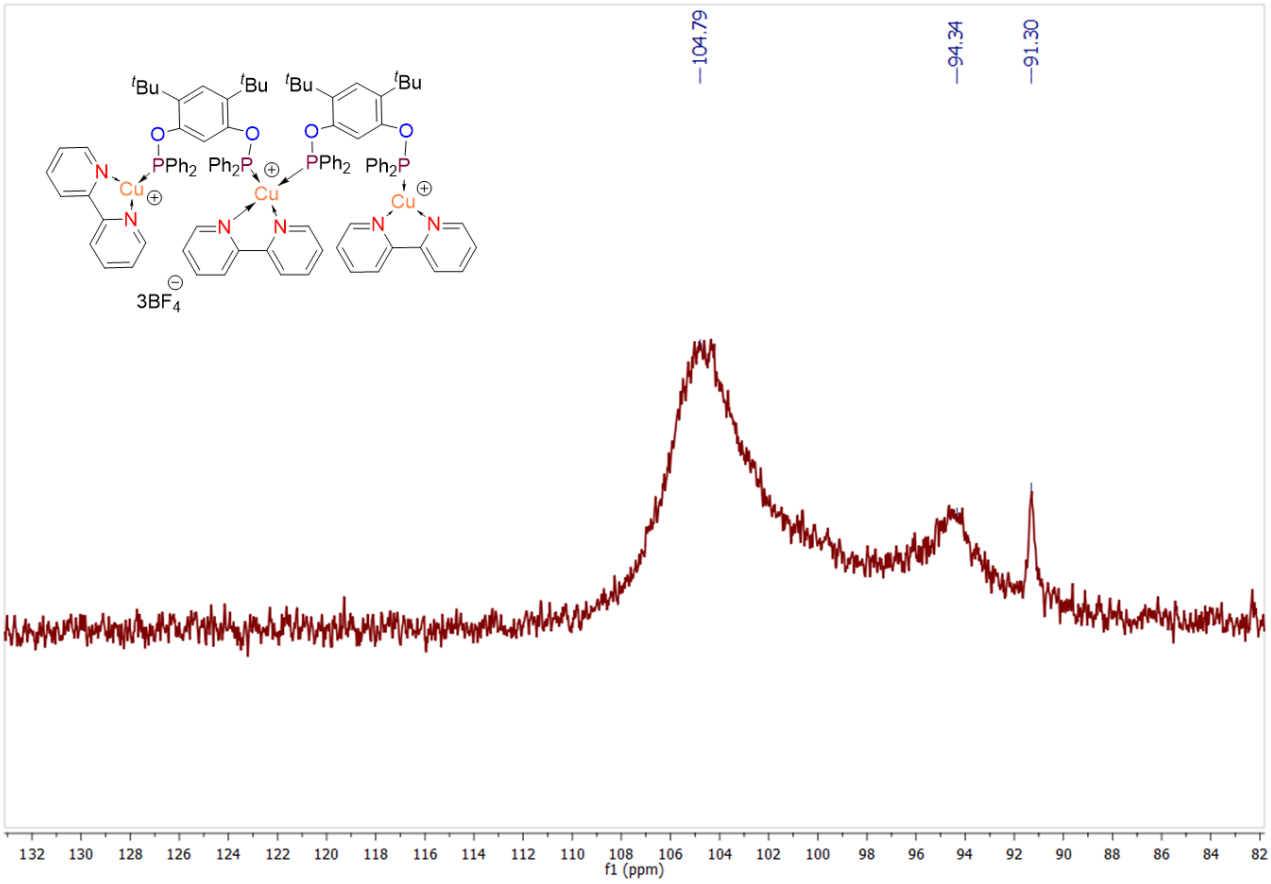

Figure S12. ^{31}P NMR spectrum of **7**

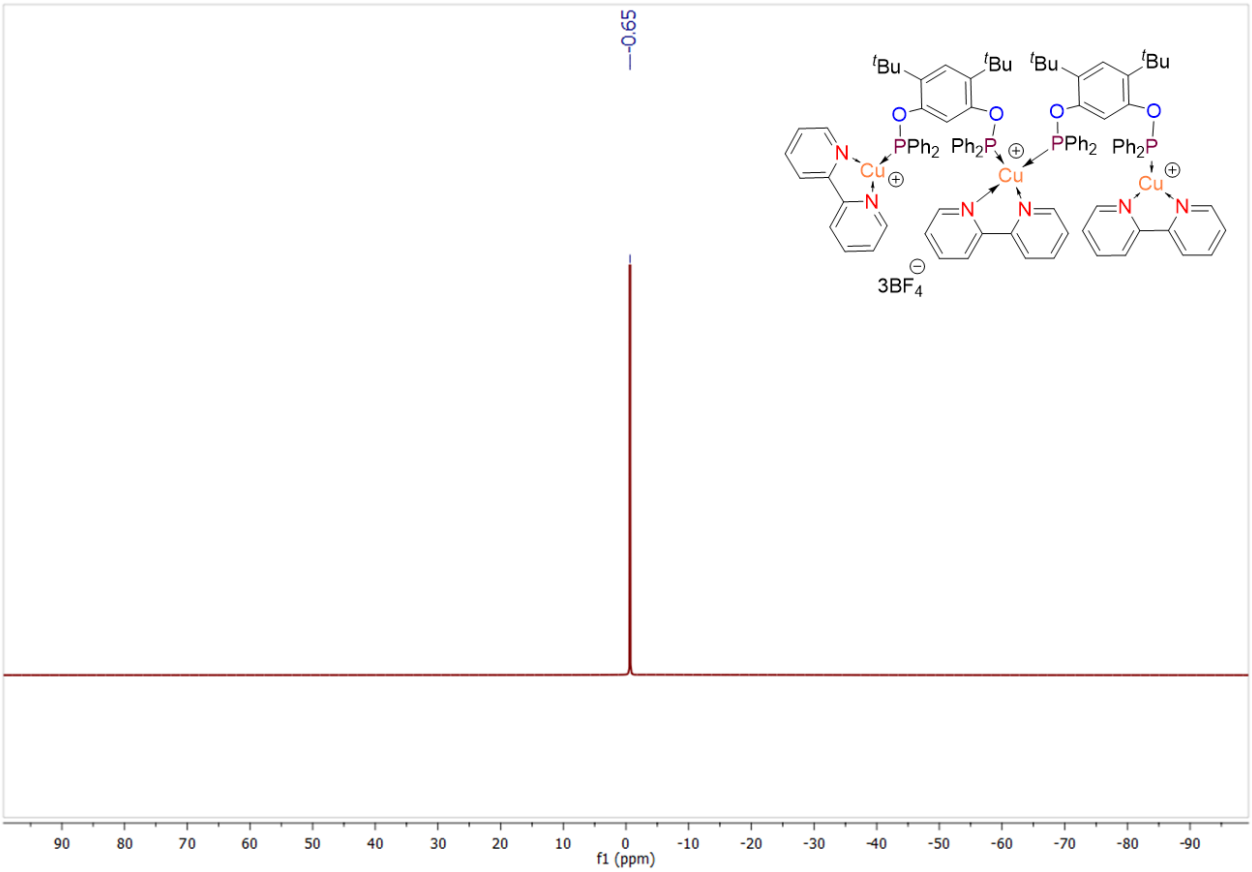

Figure S13. ^{11}B NMR spectrum of **7**

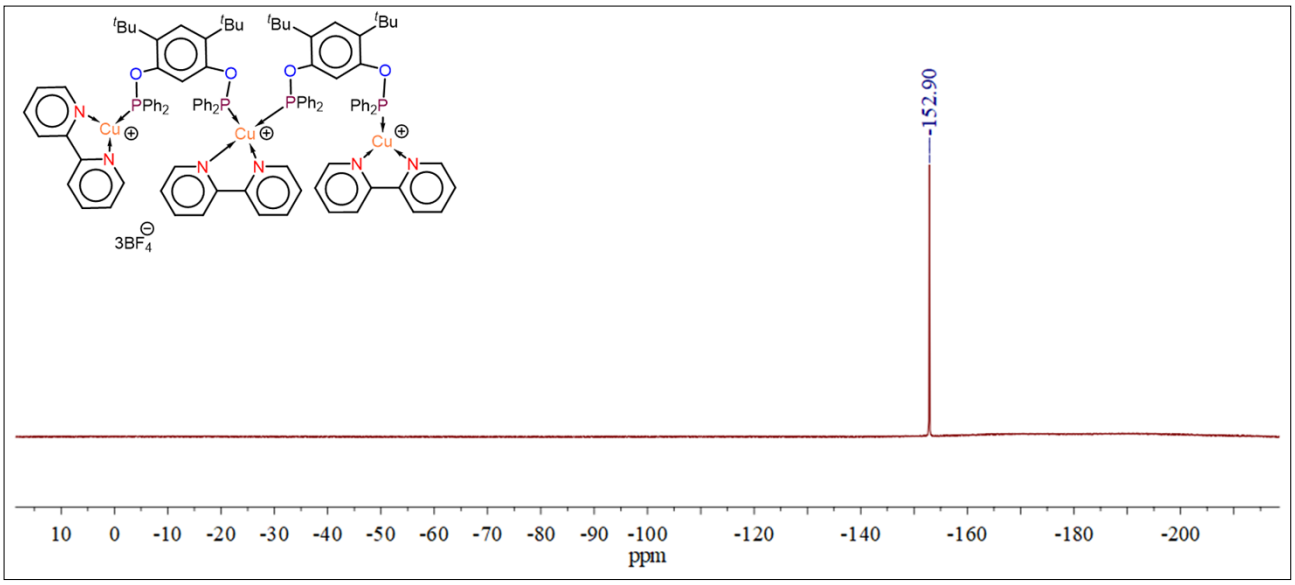

Figure S14. ^{19}F NMR spectrum of **7**

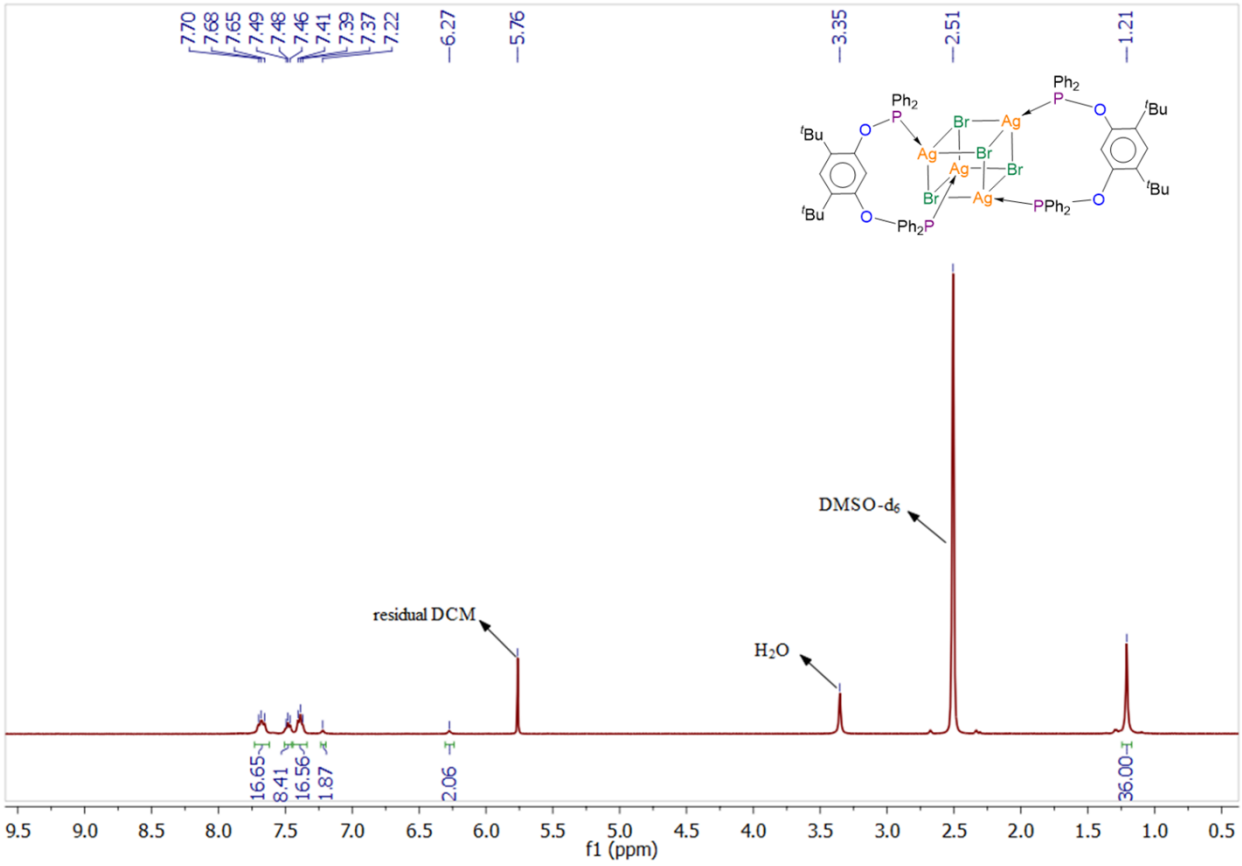

Figure S15. ^{1}H NMR spectrum of **8**

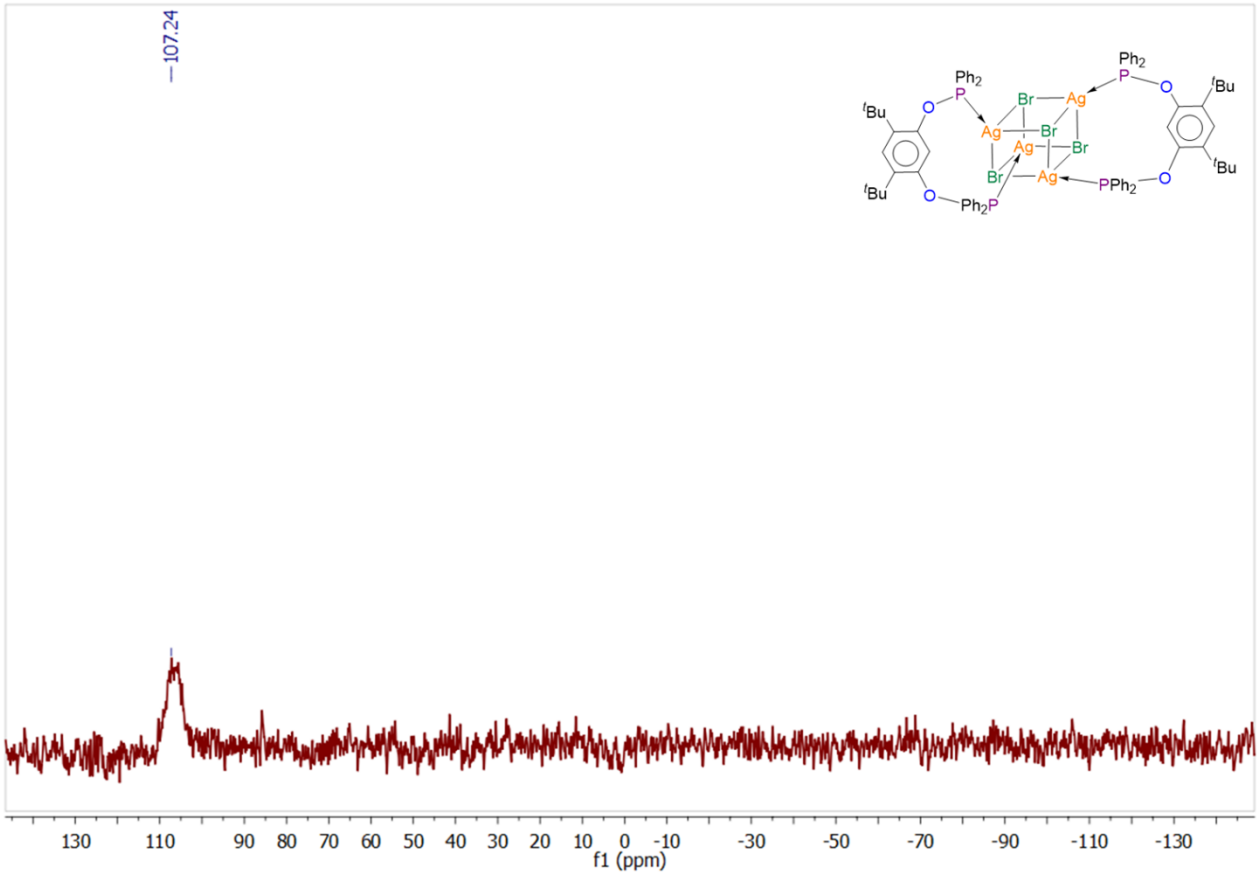

Figure S16. ^{31}P NMR spectrum of **8**

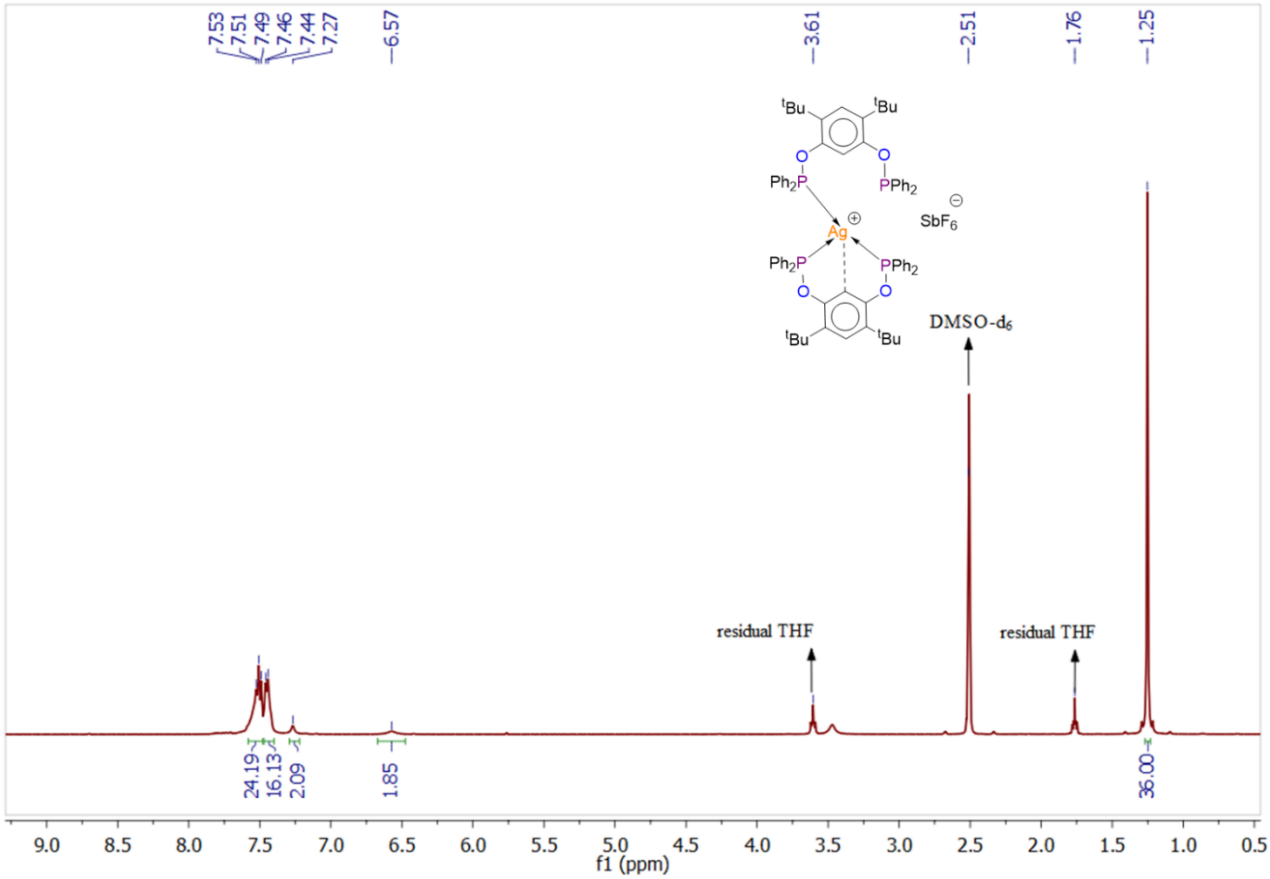

Figure S17. ^{1}H NMR spectrum of **10**

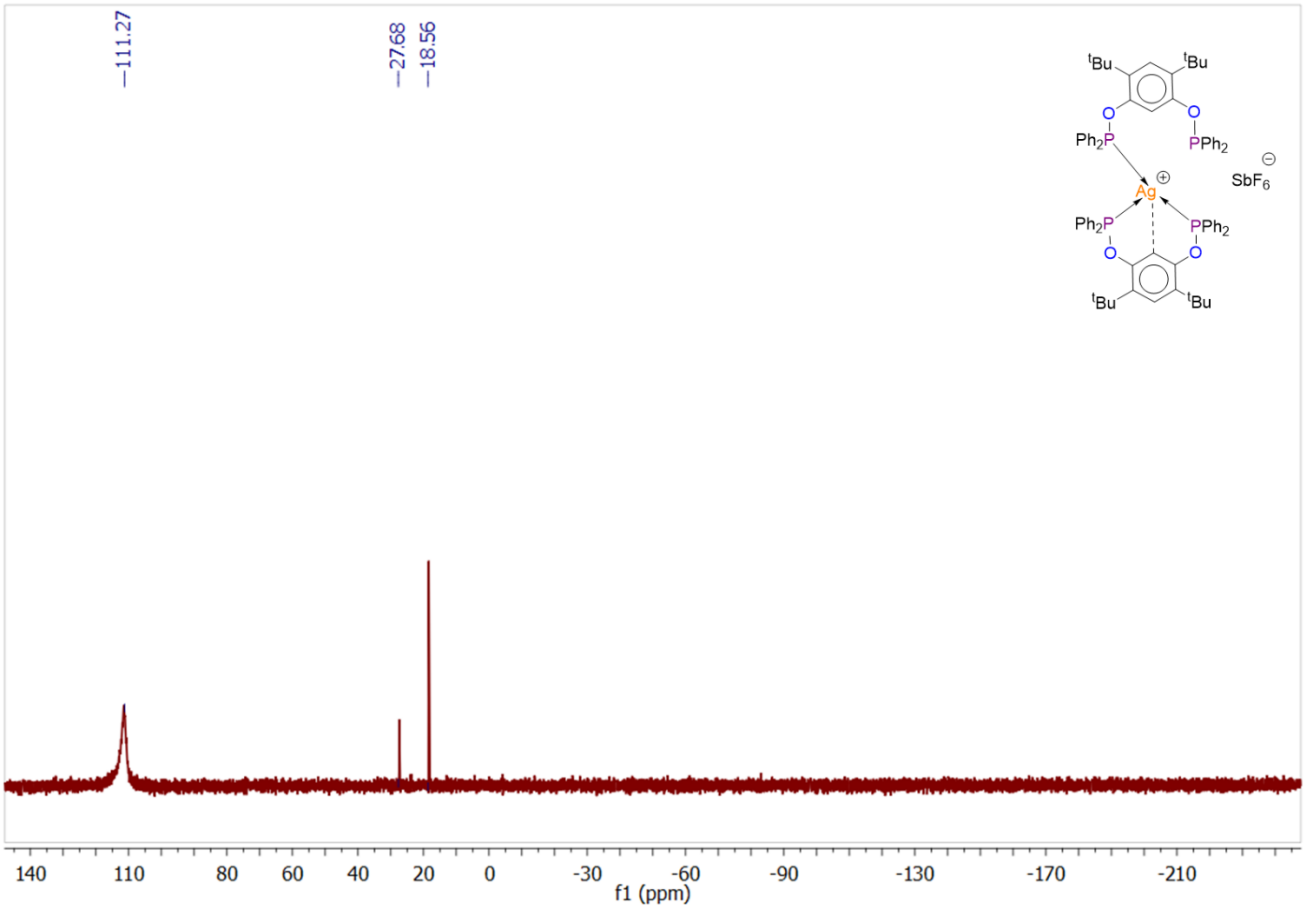

Figure S18. ^{31}P NMR spectrum of **10**

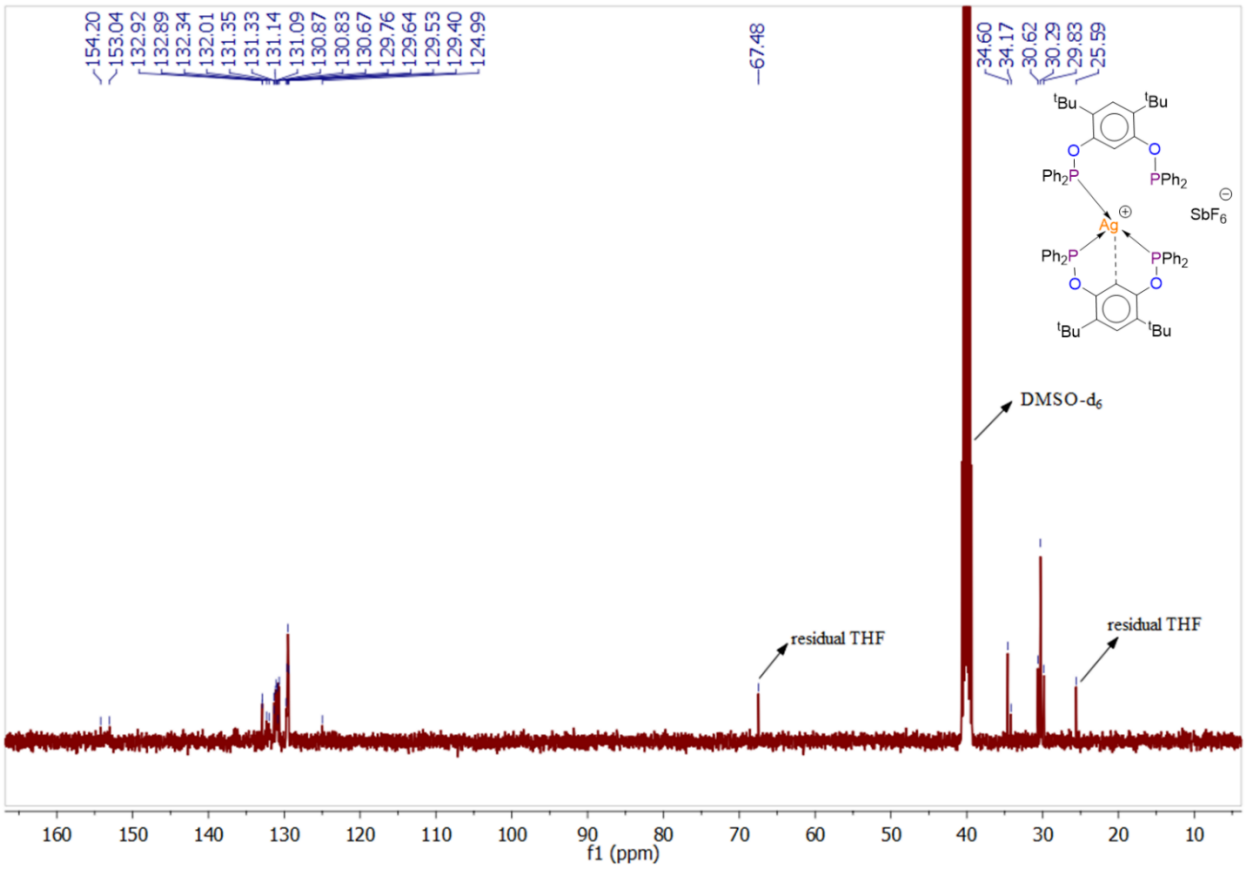

Figure S19. ^{13}C NMR spectrum of **10**

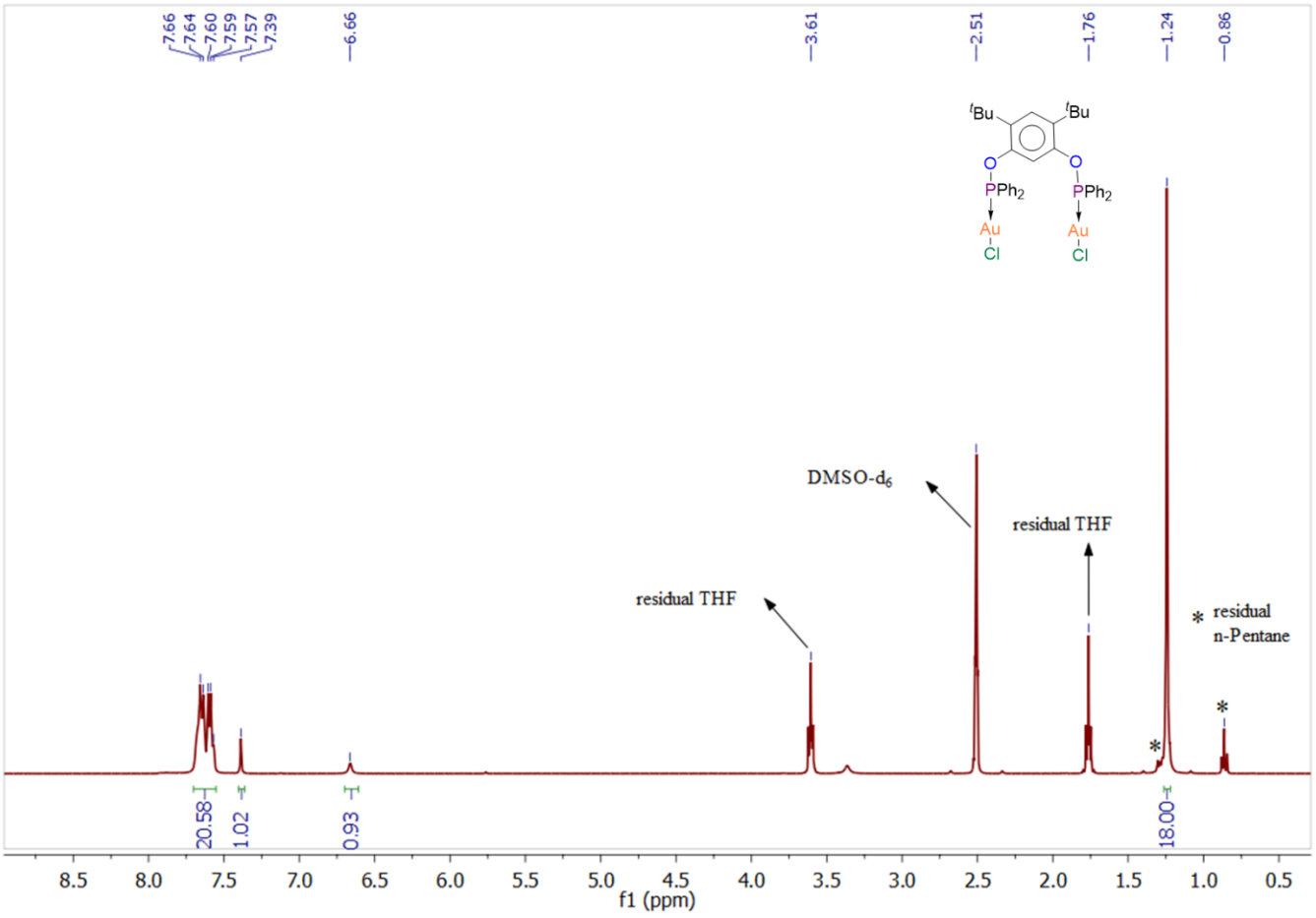

Figure S20. ^{1}H NMR spectrum of **11**

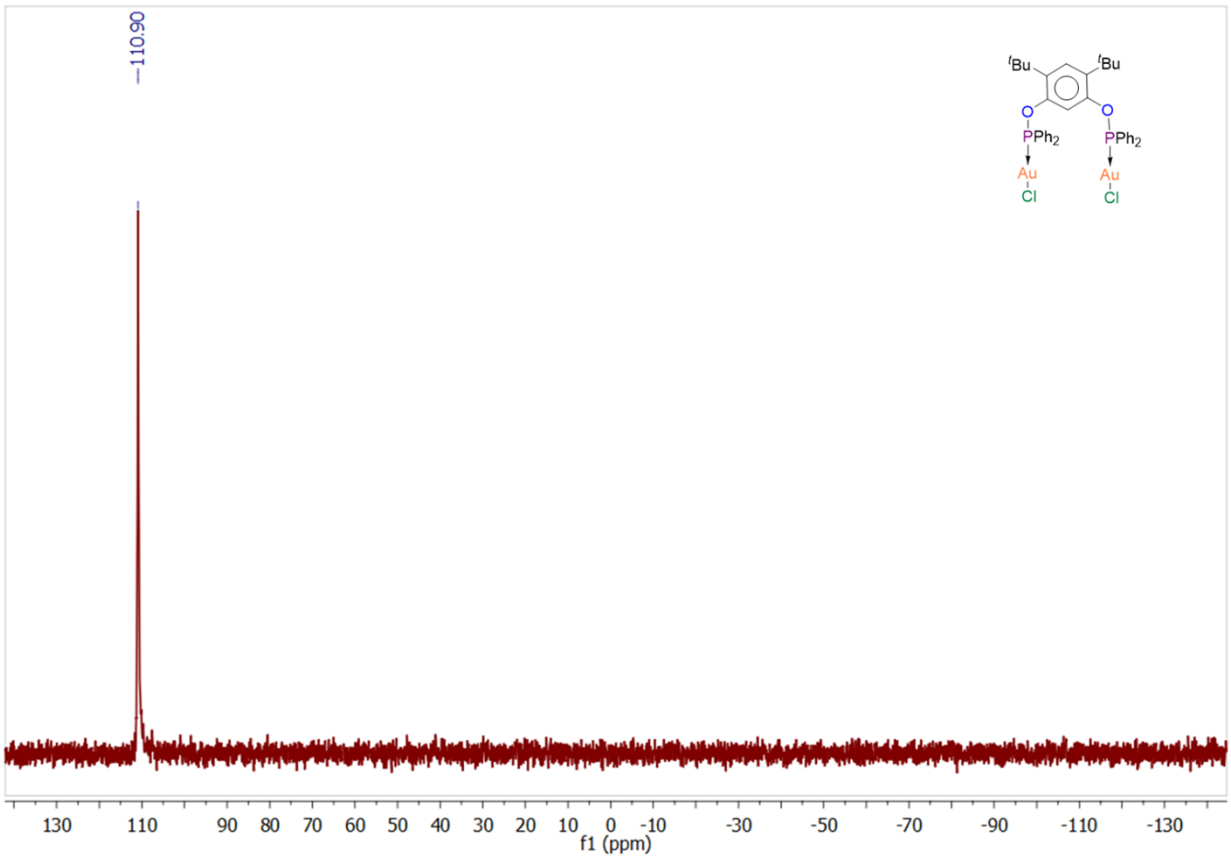

Figure S21. ^{31}P NMR spectrum of **11**

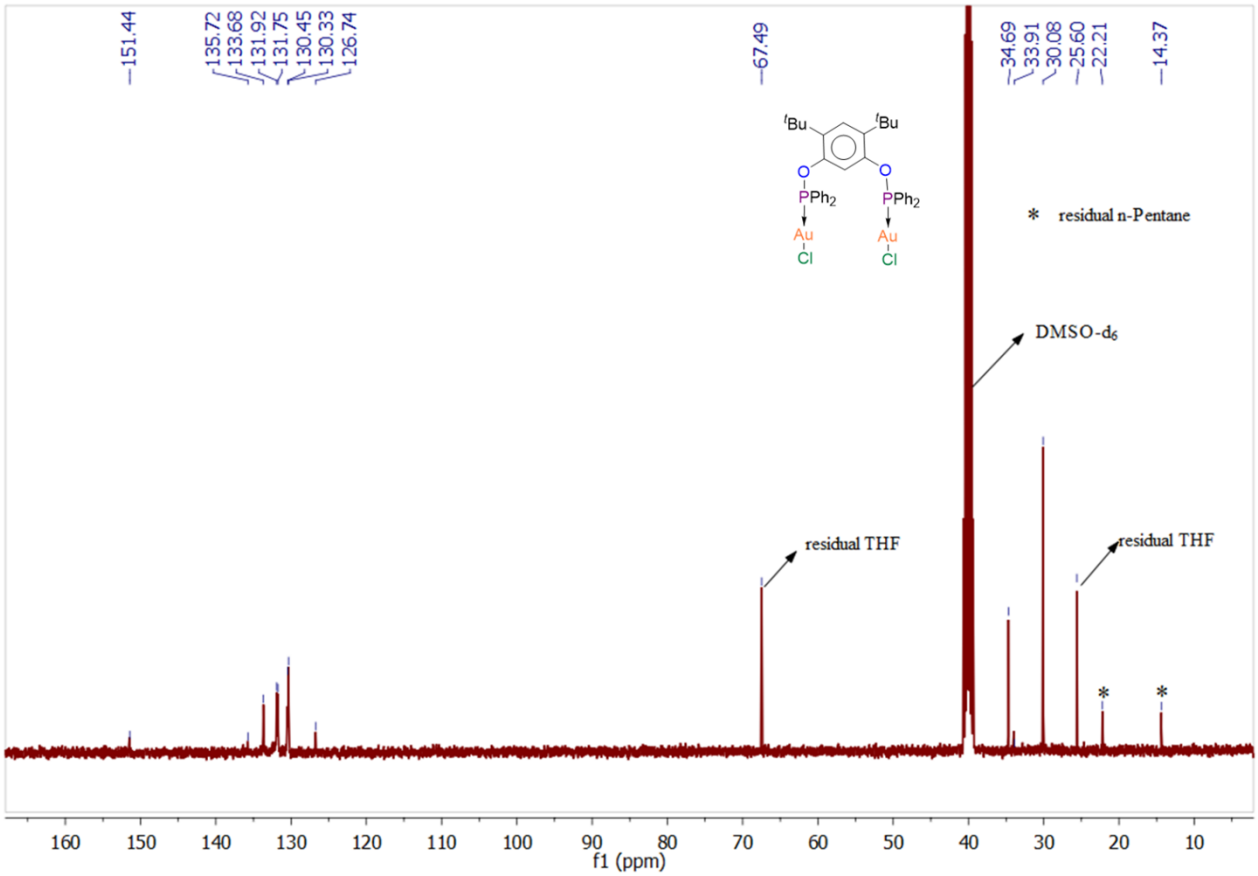

Figure S22. ^{13}C NMR spectrum of **11**

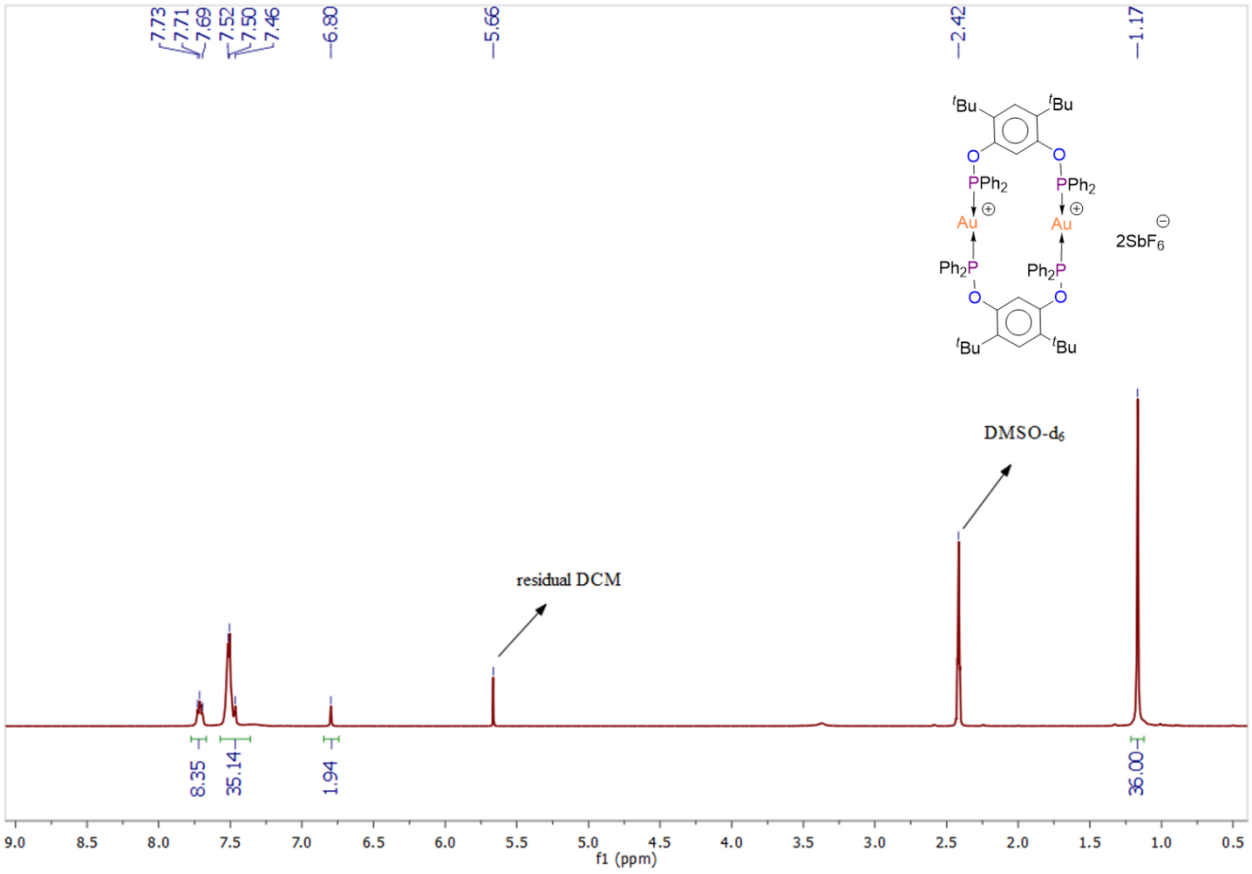

Figure S23. ^{1}H NMR spectrum of **12**

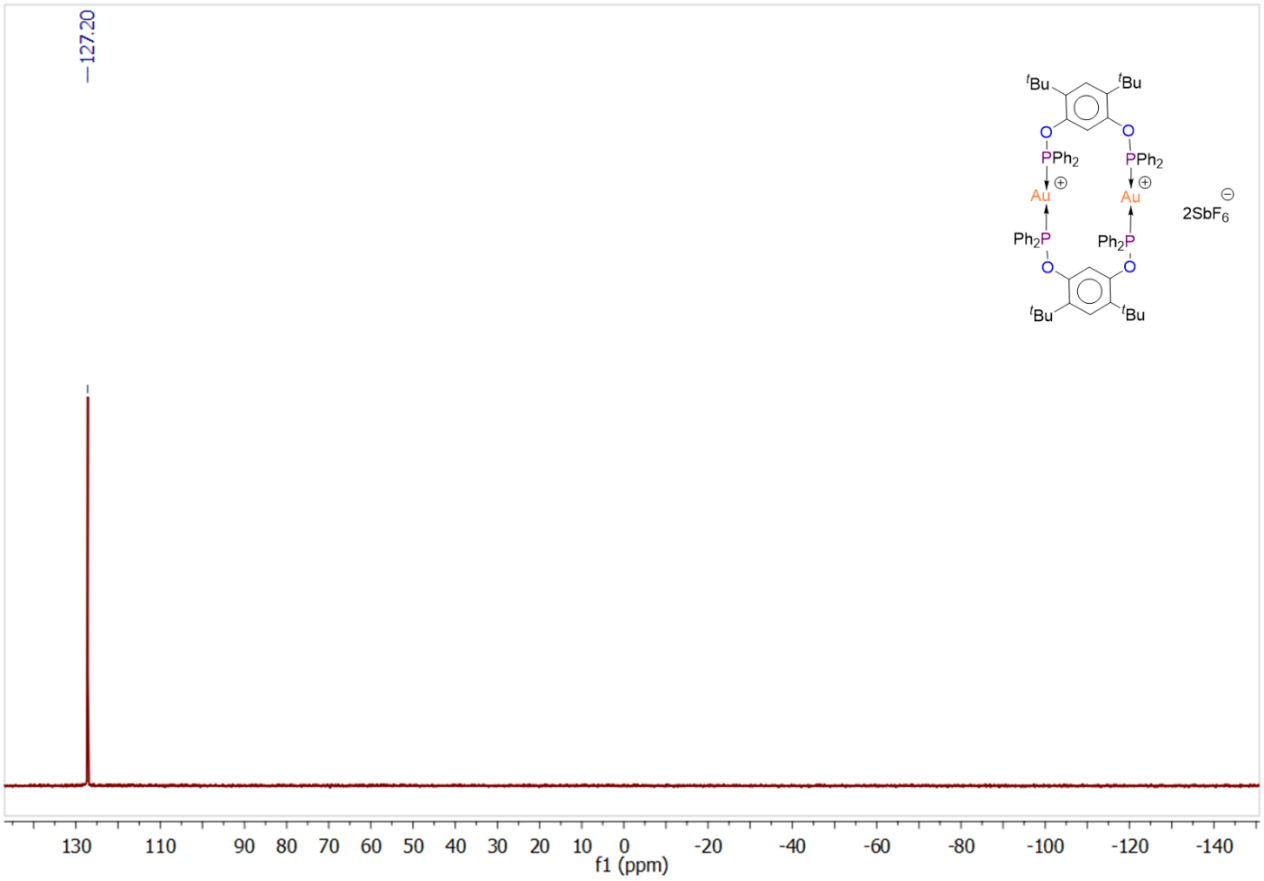

Figure S24. ^{31}P NMR spectrum of **12**

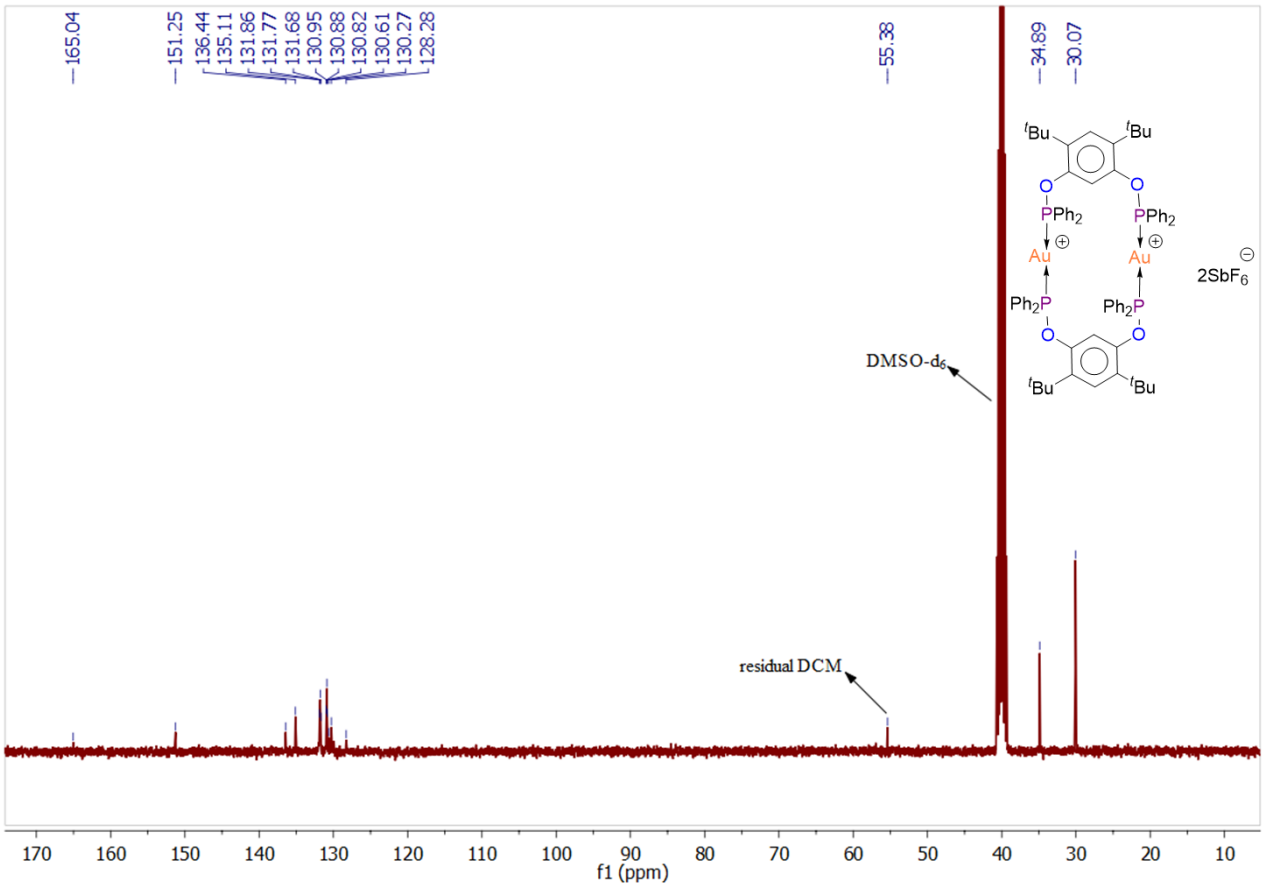

Figure S25. ^{13}C NMR spectrum of **12**

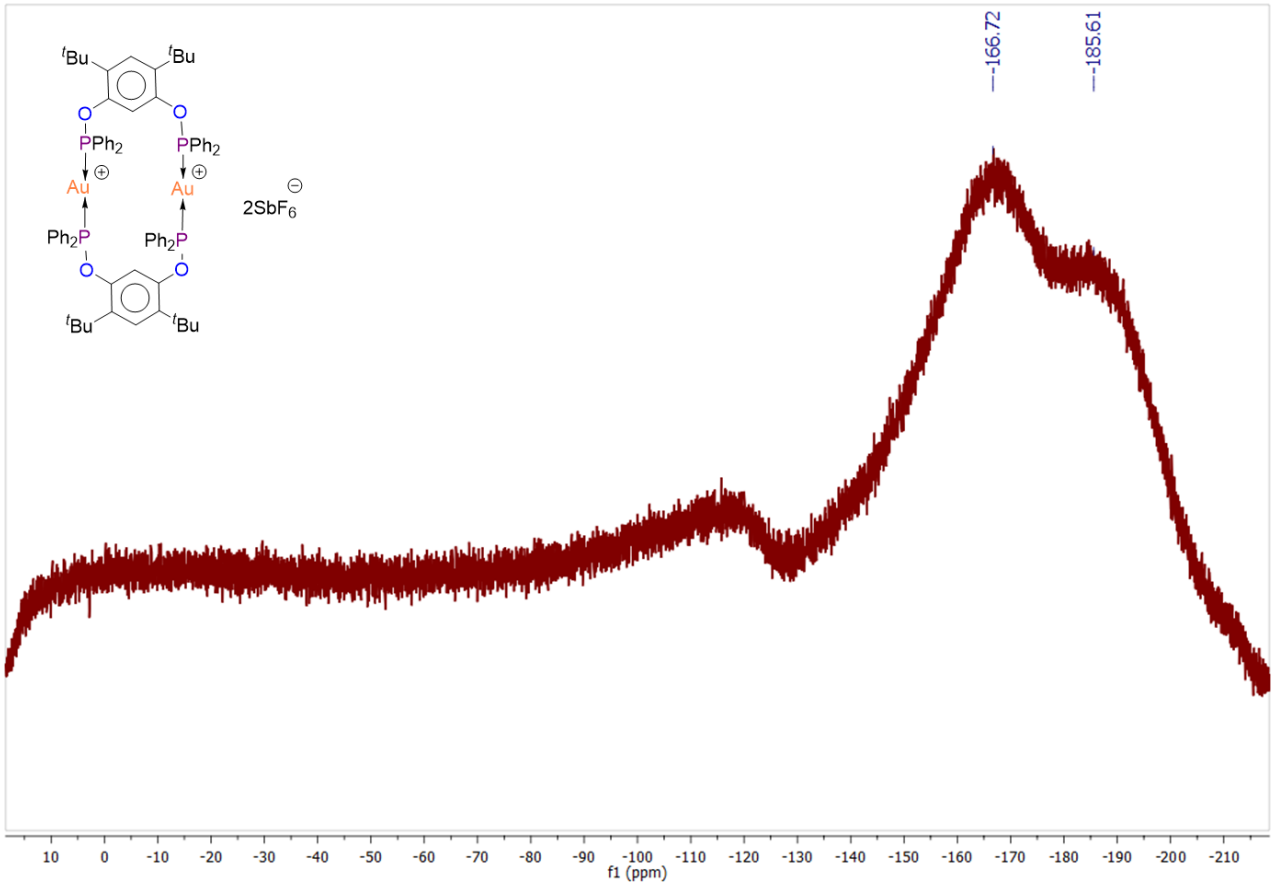

Figure S26. ^{19}F NMR spectrum of **12**

S3. Crystallographic Details of 2-12.

Crystal data for **2-12** were collected on a Bruker Smart Apex Duo diffractometer at 100 K using MoKα radiation (λ = 0.71073 Å). The absorption correction was done using the multi-scan method (SADABS). The structures were solved by direct methods and refined by full-matrix least-squares methods against F2 (SHELXL-2014/6) and Olex[2] with the ShelXT[3] structure solution program. Attempts to refine residual electron density peaks as disordered or partial occupancy solvent toluene carbon atoms were unsuccessful. The data were corrected for disordered electron density using the SQUEEZE procedure implemented in PLATON.[4] We used solvent masking for complexes **2, 3** and **4,** the solvent mask corresponds to CH_2Cl_2. Moreover, we also used solvent mask for **6,** the solvent mask corresponds to CH_2Cl_2 and toluene. Crystallographic data files for the **2-12** have been deposited with the Cambridge Crystallographic Data Centre. CCDC No.: 2244747 (**2**), 2244748 (**3**), 2244749 (**4**), 2244750 (**5**), 2244751 (**6**), 2244752 (**7**), 2244753 (**8**), 2244755 (**9**), 2244756 (**10**), 2244757 (**11**), 2244758 (**12**)

S3. Crystal Data and Structure Refinement Data for 2-12

	2	**3**	**4**	**5**
Sum formula	$C_{76}H_{80}Cl_2Cu_2O_4P_4$ [+solvent]	$C_{76}H_{80}Br_4Cu_4O_4P_4$[+ solvent]	$C_{78}H_{84}Cl_4Cu_4I_4O_4P_4$ [+ solvent]	$C_{80}H_{80}Cl_4Cu_4F_{12}O_{16}P_4S_4$
Mr	1379.28	1755.08	2112.93	2201.61
Temperature	100 K	100 K	100 K	100 K
Wavelength	0.71703 Å	0.71073 Å	0.71073 Å	0.71073 Å
Crystal system	Monoclinic	Triclinic	Triclinic	Monoclinic
Space group	*$P2_1/n$*	*P -1*	*P-1*	*$P2_1/n$*
Unit cell dimensions	*a* = 16.391(5) Å	*a* = 11.012(3) Å	*a* = 11.0314(18) Å	*a* = 14.262(4) Å
	b = 10.259(3) Å	*b* = 13.359(3) Å	*b* = 13.720(2) Å	*b* = 18.863(5) Å
	c = 22.237(7) Å	*c* =15.688(4) Å	c= 15.256(2) Å	c= 17.852(5) Å
	$\alpha = 90°$	$\alpha = 101.991(8)°$	$\alpha = 102.657(4)°$	$\alpha = 90°$
	$\beta = 91.976(9)°$	$\beta = 101.226(8)°$	$\beta = 101.013(5)°$	$\beta = 107.047(7)°$
	$\gamma = 90°$	$\gamma = 110.003(7)°$	$\gamma = 91.511(5)°$	$\gamma = 90°$
Volume	3737(2)	2030.7(9)	2205.7 (6)	4592(2)
Z	1	1	1	2
Density (calculated)	1.294 g/cm^3	1.506 g/cm^3	1.591 g/cm^3	1.592 g/cm^3
Absorption coefficient	0.827 mm^{-1}	3.190 mm^{-1}	2.587 mm^{-1}	1.278 mm^{-1}
F(000)	1515.0	929.10	1040.0	2240.0
Theta range for data collection	2.49 to 28.41°	2.45 to 28.29°	2.49 to 28.27°	2.42 to 26.11°
Index ranges	-19<=h<=19, -12<=k<=12, -26<=l<=26	-14<=h<=14, -17<=k<=17, -21<=l<=21	-14<=h<=14, -18<=k<=18, -20<=l<=20	-19<=h<=19, -25<=k<=25, -23<=l<=23
Reflections collected	128654	75600	94097	148346

Independent reflections	6522 [R(int) = 0.0412]	10201[R(int) = 0.0610]	11045 [R(int) = 0.0546]	11846 [R(int) = 0.1024]
Coverage of independent reflections	96.3%	99.5%	99.6%	99.9%
Function minimized	Σ w(Fo^2 - Fc^2)^2	Σ w(Fo^2 - Fc^2)^2	Σ w(Fo^2 - Fc^2)^2	Σ w(Fo^2 - Fc^2)^2
Data / restraints / parameters	6522/0/430	10201/ 0 / 477	11045 / 0 / 448	11846/ 0 / 584
Goodness-of-fit on F^2	1.218	1.031	1.031	1.025
Δ/σ max	0.002	0.001	0.001	0.001
Final R indices	6308 data[I>2σ(I)], R1 = 0.0309, wR2 = 0.0956	7541 data[I>2σ(I)], R1 = 0.0587, wR2 = 0.1401	3961 data[I>2σ(I)], R1 = 0.0368, wR2 = 0.0750	7743 data[I>2σ(I)], R1 = 0.0460, wR2 = 0.0766
	all data, R1 = 0.0321, wR2 = 0.0964	all data, R1 = 0.0884, wR2 = 0.1603	all data, R1 = 0.0554, wR2 = 0.0822	all data, R1 = 0.0912, wR2 = 0.0897
Largest diff. peak and hole	0.571 and -1.120 eÅ^{-3}	1.307 and -1.261eÅ^{-3}	1.511 and -1.436 eÅ^{-3}	0.737 to -0.694 eÅ^{-3}
R.M.S. deviation from mean	0.164 eÅ^{-3}	0.187 eÅ^{-3}	0.122 eÅ^{-3}	0.091 eÅ^{-3}

	6	7	8	9
Sum Formula	$C_{124}H_{120}Cu_4O_4P_8$ [+solvent]	$C_{214}H_{213}B_6Cl_4Cu_6F_{24}N_{12}O_9P_8$	$C_{77}H_{82}Ag_4Br_4Cl_2O_4P_4$	$C_{78}H_{83}Ag_4Cl_4I_4O_4P_4$
Mr	2176.17	4388.70	2017.32	2289.21
Temperature	100 K	100 K	100 K	100 K
Wavelength	0.71703 Å	0.71073 Å	0.71703 Å	0.71073 Å
Crystal system	Monoclinic	Triclinic	Monoclinic	Monoclinic
Space group	*C2/c*	*P-1*	*C2/c*	*C2/c*
Unit cell dimensions	*a* = 26.715(6) Å	*a* = 13.814(5) Å	*a* = 16.1275(5) Å	*a* = 27.384(8) Å
	b = 23.138(6) Å	*b* = 16.572(6) Å	*b* = 24.4987(8) Å	*b* = 28.232(8) Å
	c = 20.914(5) Å	*c* = 23.261(8) Å	*c* = 21.1870(9) Å	*c* = 11.836(3) Å
	α = 90°	α = 93.161(10) °	α = 90°	α = 90°
	β = 93.309(8) °	β = 90.315(11)°	β = 105.565(1)°	β = 112.454(8)°
	γ = 90°	γ = 103.514(10) °	γ = 90°	γ = 90°
Volume	12906(5) Å^3	5169(3) Å^3	8064.0(1) Å^3	8457 (4) Å^3
Z	4	1	4	4
Density (calculated)	1.120 g/cm^3	1.410 g/cm^3	1.662 g/cm^3	1.797 g/cm^3
Absorption coefficient	0.794 mm^{-1}	0.802 mm^{-1}	3.130 mm^{-1}	2.620 mm^{-1}
F(000)	4528.0	2260.0	3992.0	4440.0
Theta range for data collection	4.62 to 50°	4.328 to 50°	1.996 to 28.370°	2.40 to 28.61°
Index ranges	-31<=h<=31, -27<=k<=27, -24<=l<=24	-16<=h<=16, -19<=k<=19, -27<=l<=27	-21<=h<=21, -32<=k<=32, -28<=l<=28	-37<=h<=37, -38<=k<=38, -16<=l<=16
Reflections collected	183866	178187	174464	192252
Independent reflections	11346 [Rint = 0.1787]	18187 [Rint = 0.2358]	10039 [R(int) = 0.0636]	10813 [R(int) = 0.0533]
Coverage of independent	99.9%	99.9%	99.4%	94.1%

reflections				
Function minimized	Σ w(Fo^2 - Fc^2)^2	Σ w(Fo^2 - Fc^2)^2	Σ w(Fo^2 - Fc^2)^2	Σ w(Fo^2 - Fc^2)^2
Data / restraints / parameters	11346 /0 /637	18187 / 0 / 1291	10039 /0 /436	10813 / 0 / 453
Goodness-of-fit on F^2	1.038	1.074	1.071	1.126
Δ/σ max	0.002	0.001	0.002	0.002
Final R indices	[I>2σ(I)], R1 = 0.0507, wR2 = 0.1037	[I>2σ(I)], R1 = 0.0922, wR2 = 0.1745	8082 data[I>2σ(I)], R1 = 0.0266, wR2 = 0.0535	9701 data[I>2σ(I)], R1 = 0.0348, wR2 = 0.0971
	all data, R1 = 0.1004, wR2 = 0.1241	all data, R1 = 0.1677, wR2 = 0.2030	all data, R1 = 0.0434, wR2 = 0.0588	all data , R1 = 0.0426, wR2 = 0.1036
Largest diff. peak and hole	0.52 and -0.41 eÅ^{-3}	1.27 and -0.94 eÅ^{-3}	0475 and -0.678 eÅ^{-3}	1.031 and -1.809 eÅ^{-3}
R.M.S. deviation from mean	0.069 eÅ^{-3}	0.116 eÅ^{-3}	0.100 eÅ^{-3}	0.347 eÅ^{-3}

	10	**11**	**12**
Sum Formula	$C_{84}H_{95}AgF_6O_6P_4Sb$	$C_{42}H_{48}Au_2Cl_2O_3P_2$ [+solvent]	$C_{79}H_{85}Au_2Cl_6F_{12}$ $O_4P_4Sb_2$
Mr	1668.12	1127.59	2300.52
Temperature	100 K	100 K	100 K
Wavelength	0.71073 Å	0.71073 Å	0.71073 Å
Crystal system	Triclinic	Monoclinic	Orthorhombic
Space group	*P-1*	$P2_1/n$	*Pbca*
Unit cell dimensions	a = 14.6752(6) Å	a = 21.921(9) Å	a = 22.657(4) Å
	b = 15.9922(6) Å	b = 16.939(7) Å	b = 25.548(4) Å
	c = 17.7042(7) Å	c = 24.632(9) Å	c = 29.827(6)Å
	α = 103.034(2) °	α = 90°	α = 90°
	β = 91.157(2) °	β = 96.918(13)°	β = 90°
	γ = 103.181(2) °	γ = 90°	γ = 90°
Volume	3930.0(3) $Å^3$	9080 $Å^3$	17265(6) $Å^3$
Z	2	4	8
Density (calculated)	1.410 g/cm^3	1.650 g/cm^3	1.770 g/cm^3
Absorption coefficient	0.740 mm^{-1}	6.677 mm^{-1}	4.340 mm^{-1}
F(000)	1718.0	4368.0	8968.0
Theta range for data collection	2.18 to 22.16°	2.40 to 28.39°	2.37 to 25.14°
Index ranges	-17<=h<=17, -19<=k<=19, -21<=l<=21	-26<=h<=26, -20<=k<=20, -29<=l<=29	-27<=h<=27, -30<=k<=30, -35<=l<=35
Reflections collected	103417	248168	74303
Independent reflections	14238 [R(int) = 0.1183]	16446 [R(int) = 0.1064]	15600 [R(int) = 0.1526]
Coverage of independent	100%	99.9%	99.9%

reflections			
Function minimized	Σ w(Fo^2 - Fc^2)^2	Σ w(Fo^2 - Fc^2)^2	Σ w(Fo^2 - Fc^2)^2
Data / restraints / parameters	14238 / 0 / 960	16446/ 0 / 960	15600/ 0 / 984
Goodness-of-fit on F^2	1.025	1.017	1.050
Δ/σ max	0.001	0.001	0.001
Final R indices	9144 data [I>2σ(I)], R1 = 0.0633, wR2 = 0.1332	12689 data [I>2σ(I)], R1 = 0.0358, wR2 = 0.0709	9480 data [I>2σ(I)], R1 = 0.0630, wR2 = 0.0945
	all data, R1 = 0.1178, wR2 = 0.1572	all data, R1 = 0.0574, wR2 = 0.0808	all data, R1 = 0.1324, wR2 = 0.1126
Largest diff. peak and hole	2.51 to -0.85 eÅ^{-3}	1.847 to -1.387 eÅ^{-3}	1.740 to -1.475 eÅ^{-3}
R.M.S. deviation from mean	0.099 eÅ^{-3}	0.159 eÅ^{-3}	0.203 eÅ^{-3}

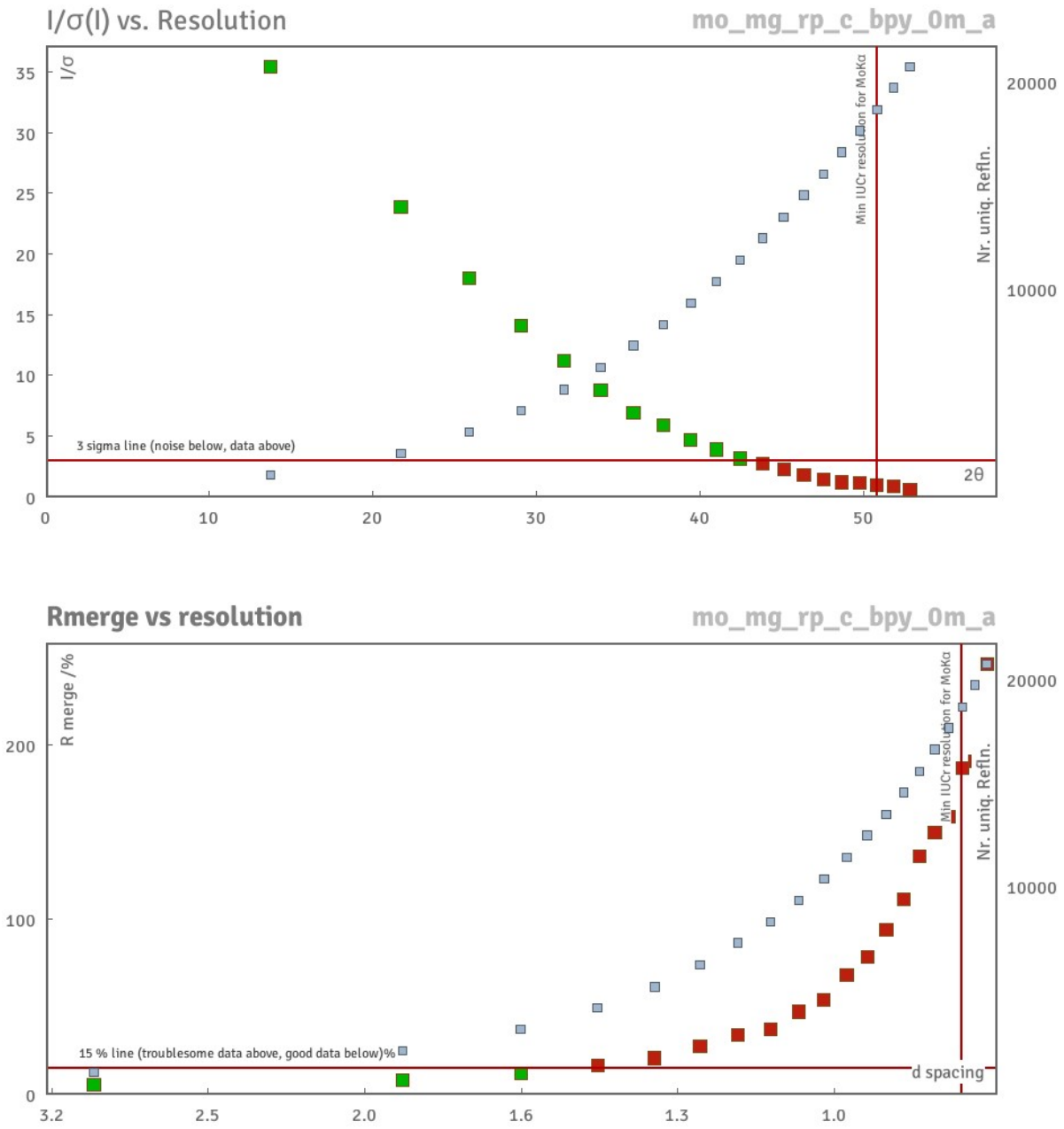

Figure S27. I/σ (I) (up) *vs.* Resolution and Rmerge *vs.* Resolution (down) for complex **7.** Concerning data quality, crystal quality is very poor; hence, that data quality is poor. We usually keep the scan at 0.5 to 1, and the exposure time is about 10-15 sec. depends on spot intensity at 0.84 Å resolution.

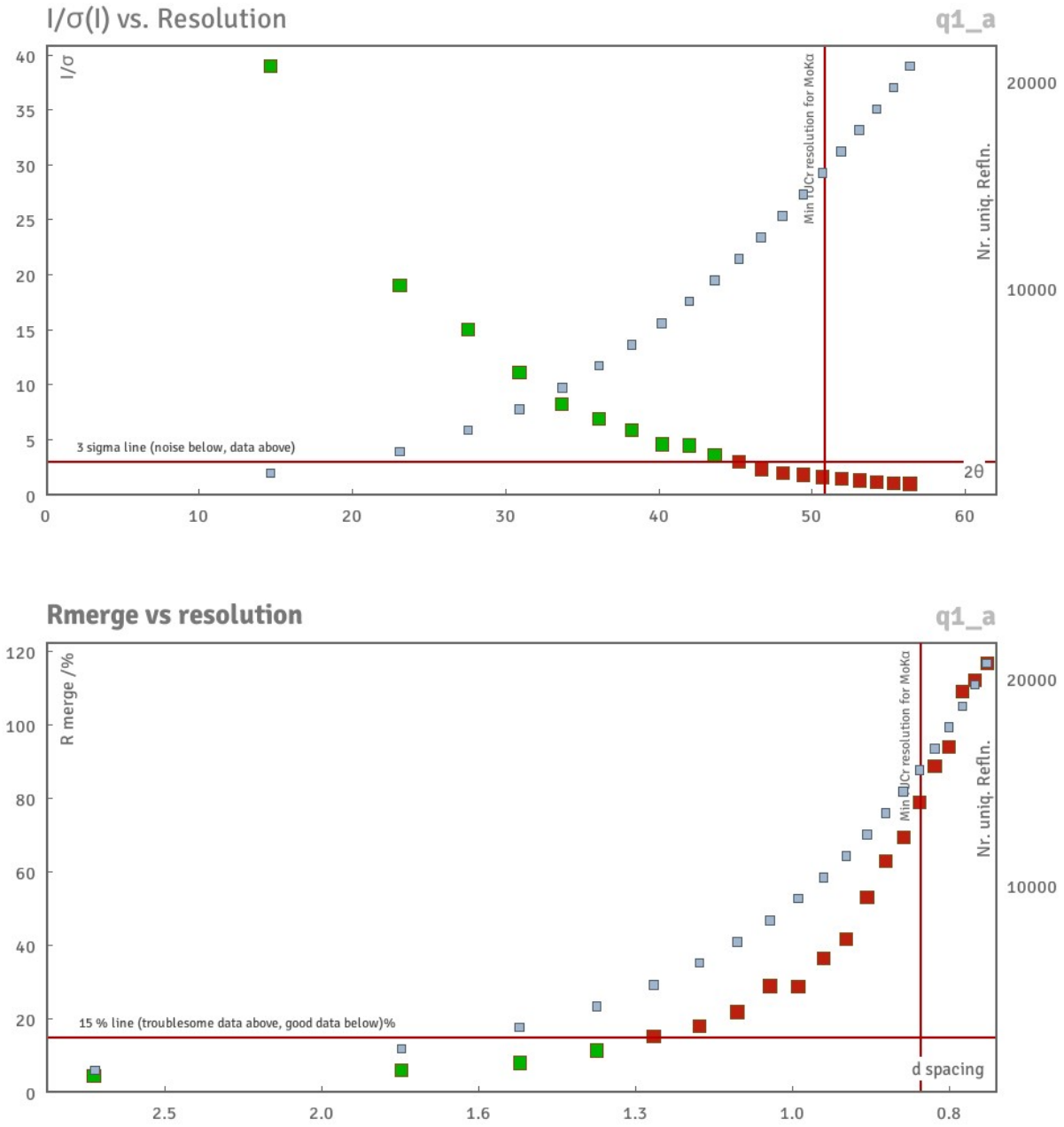

Figure S28. I/σ (I) (up) *vs.* Resolution and Rmerge *vs.* Resolution (down) for complex **12.** Concerning data quality, crystal quality is very poor; hence, that data quality is poor. We usually keep the scan at 0.5 to 1, with an exposure time of 40-45 sec. depends on spot intensity at 0.84 Å resolution.

S4. Photophysical Study

Steady state absorption spectra were recorded on Shimadzu, UV-2600 UV spectrophotometer. Microsecond flash lamp (of 1.5-2.5 μs bandwidth) and Edinburgh FLS980 instrument were

used during phosphorescence decay collection, and phosphorescence spectra measurement for complexes **4**, **6**, and **7** at 298 K. Steady State PL and lifetime was measured using an Edinburgh Instruments FS5 spectro-fluorometer and Xenon lamp for complexes **2**, **3**, **4** (variable temperature), **11** and **12**.

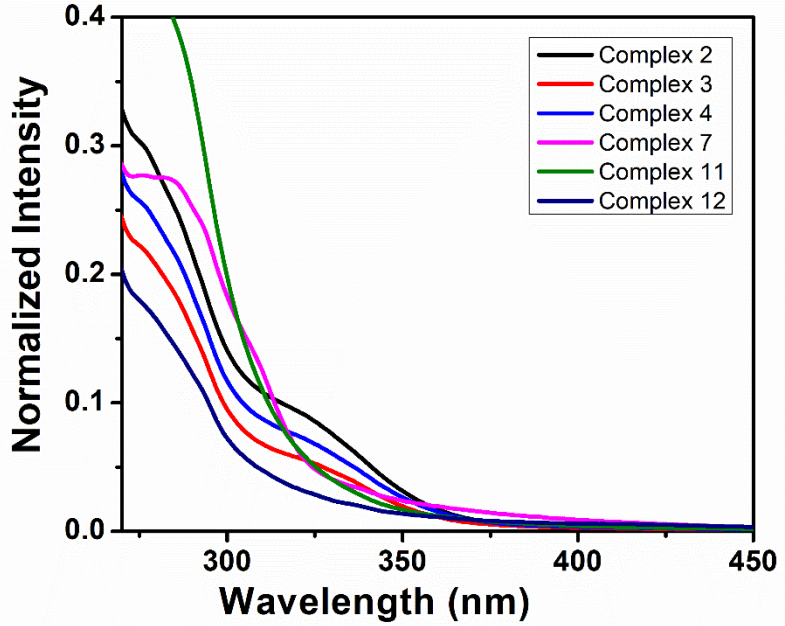

Figure S29. UV-visible spectra of Complexes **2**-**4**, **7**, **11**, **12** in THF.

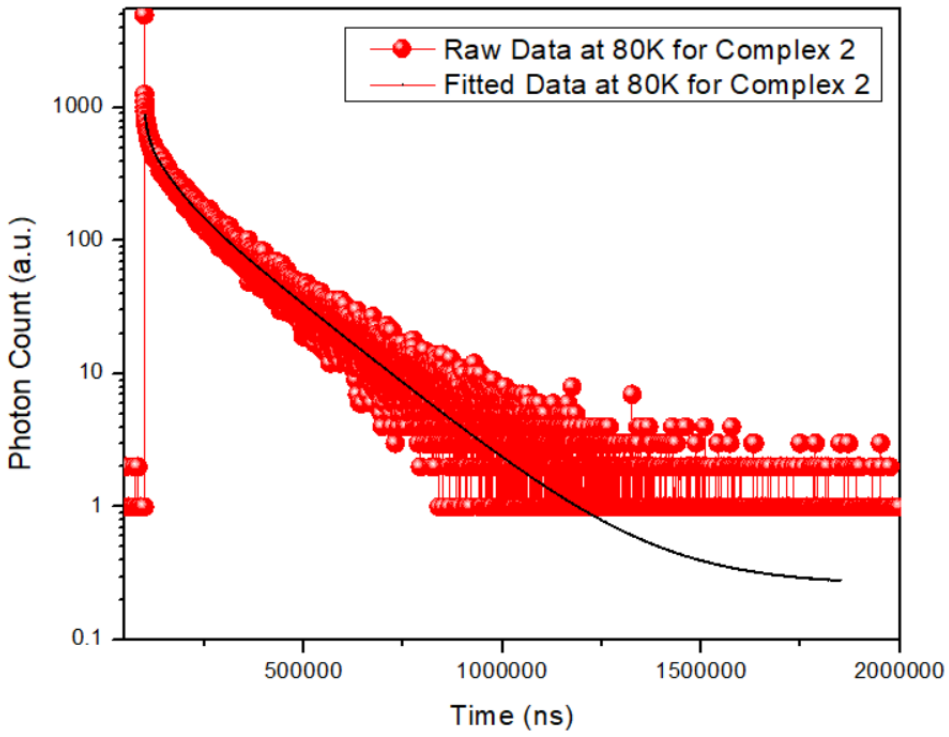

Figure S30. Decay profile for complex **2** at 80 K

Fit Results for complex **2**

Fit: $A+B1\exp(-t/\tau_1)+B2\exp(-t/\tau_2)+B3\exp(-t/\tau_3)$

T=80.00K

Parameter	Value	Std. Dev.	Rel %
τ_1	8.106E-006 s	6.037E-007 s	
τ_2	5.283E-005 s	1.990E-006 s	
τ_3	1.817E-004 s	1.194E-006 s	
B1	300.2333	11.8793	3.38
B2	296.3012	7.9292	21.75
B3	296.5236	4.9270	74.87
A	0.2593		
χ^2	0.7908		

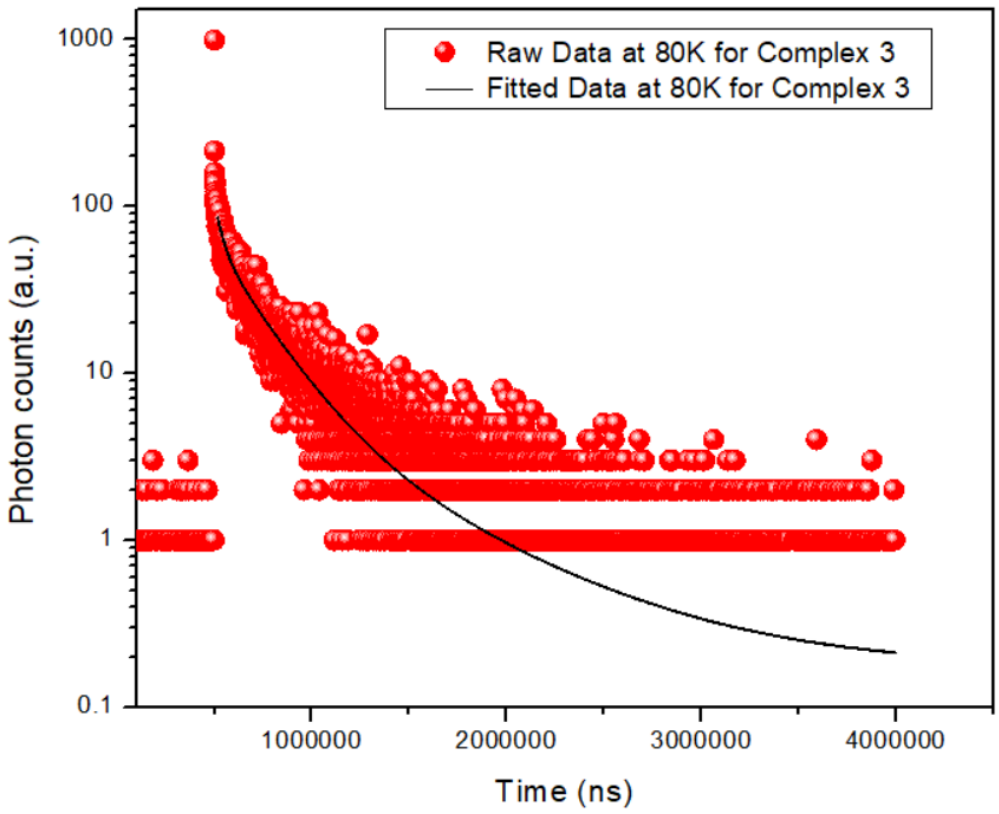

Figure S31. Decay profile for complex **3** at 80 K

Fit Results for complex **3**

Fit: A+B1exp(-t/τ_1) +B2exp (-t/ τ_2) +B3exp (-t/ τ_3)

T=80.00K

Parameter	Value	Std. Dev.	Rel %
τ_1	3.728E-005 s	5.451E-006 s	
τ_2	2.198E-004 s	1.447E-005 s	
τ_3	6.665E-004 s	1.103E-004 s	
B1	30.6288	2.5384	7.02
B2	48.2907	1.7237	65.30
B3	6.7503	2.2511	27.68
A	0.1752		
χ^2	0.6632		

Fit Results for complex **4**

Fit: A+B1exp(-t/ τ_1)+B2exp(-t/ τ_2)

T=80.00K

Parameter	Value	Std. Dev.	Rel %
τ_1	3.976E-006 s	2.161E-007 s	
τ_2	2.275E-005 s	3.449E-007 s	
B1	126.0995	4.2370	20.57
B2	85.0581	2.2877	79.43
A	0.3369		
χ^2	0.6961		

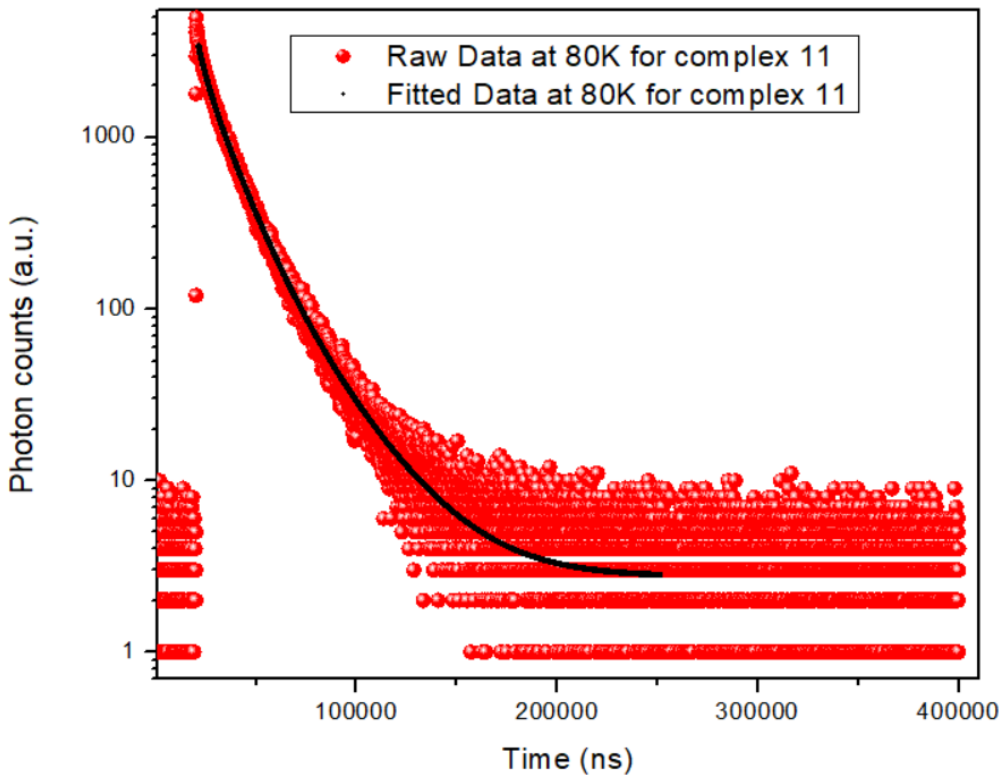

Figure S32. Decay profile for complex **11** at 80 K

Fit Results for complex 11

Fit: A+B1exp(-t/ τ_1)+B2exp(-t/ τ_2)+B3exp(-t/ τ_3)

T=80.00K

Parameter	Value	Std. Dev.	Rel %
τ_1	3.668E-006 s	2.113E-007 s	
τ_2	1.224E-005 s	3.206E-007 s	
τ_3	2.762E-005 s	1.029E-006 s	
B1	941.5818	54.8272	7.94
B2	2334.9937	33.9138	65.64
B3	416.2686	52.9845	26.42
A	5.6839		
χ^2	1.1185		

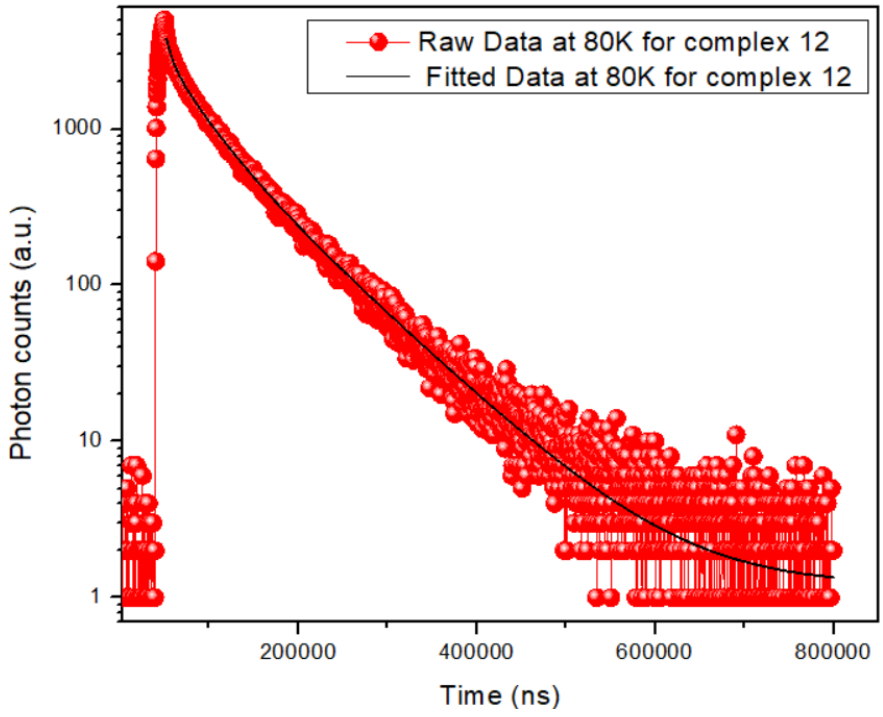

Figure S33. Decay profile for complex **12** at 80 K

Fit Results for complex **12**

T=80.00K

Fit: $A+B1\exp(-t/\tau_1)+B2\exp(-t/\tau_2)+B3\exp(-t/\tau_3)$

Parameter	Value	Std. Dev.	Rel %
τ_1	7.061E-006 s	5.189E-007 s	
τ_2	3.571E-005 s	1.449E-006 s	
τ_3	8.260E-005 s	9.529E-007 s	
B1	1052.1160	46.0087	4.39
B2	1532.7595	38.5037	32.38
B3	1294.0853	53.7412	63.23
A	1.1936		
χ^2	1.0896		

S5. Powder X-Ray Diffraction (PXRD) patterns of complex 2-4, 6 and 12

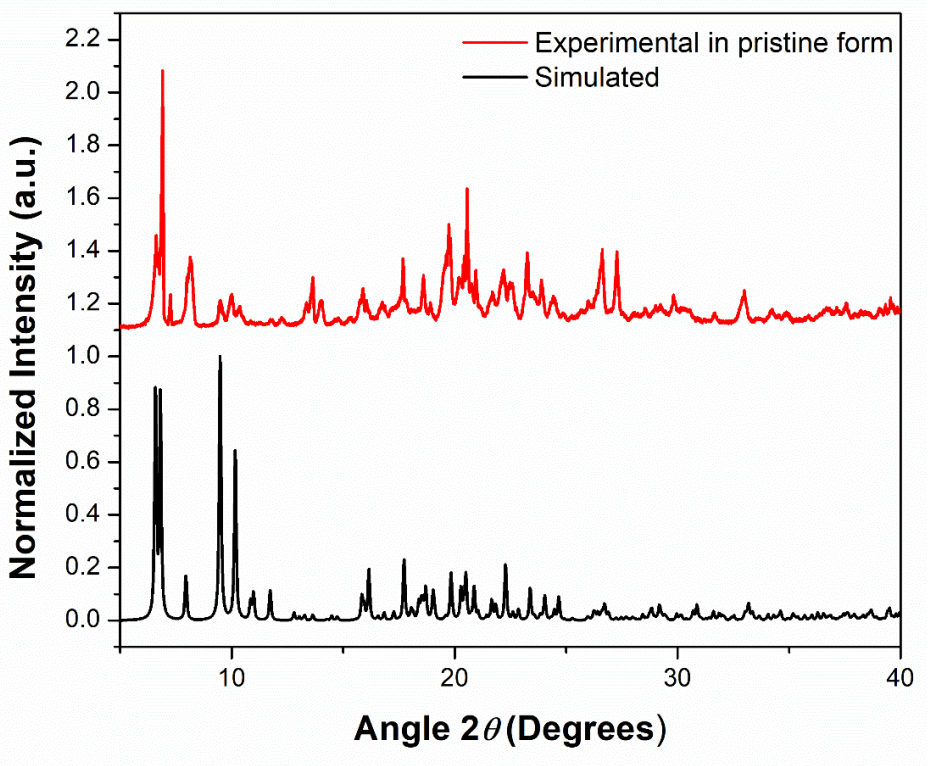

Figure S34. PXRD pattern of complex **2** at 298 K

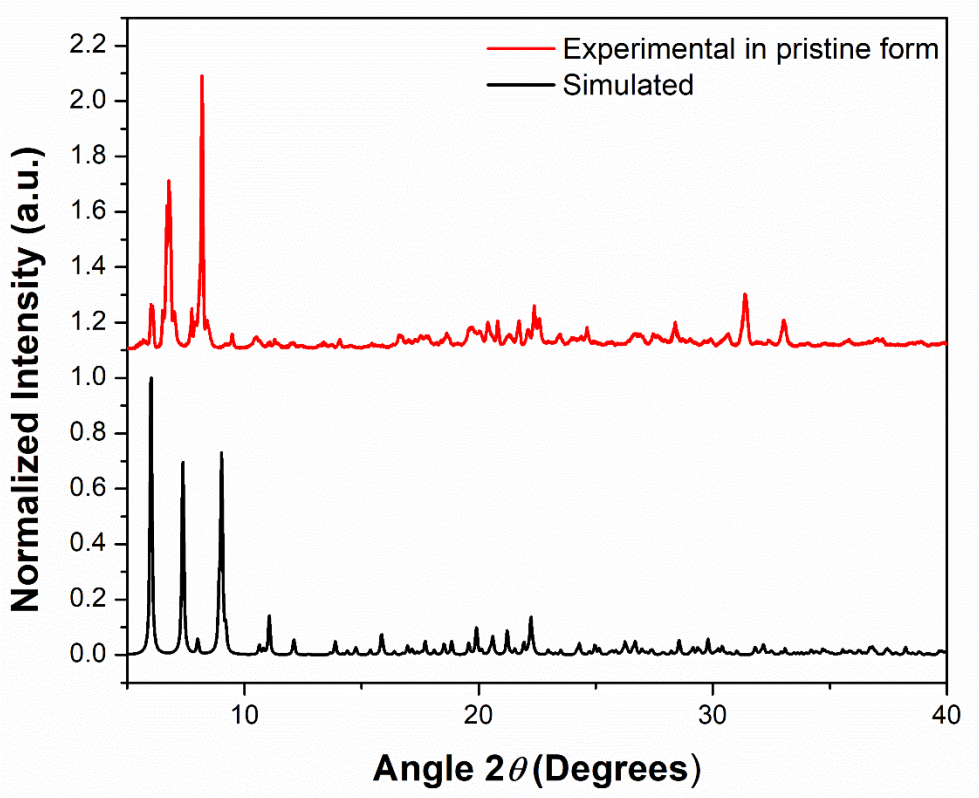

Figure S35. PXRD pattern of complex **3** at 298 K

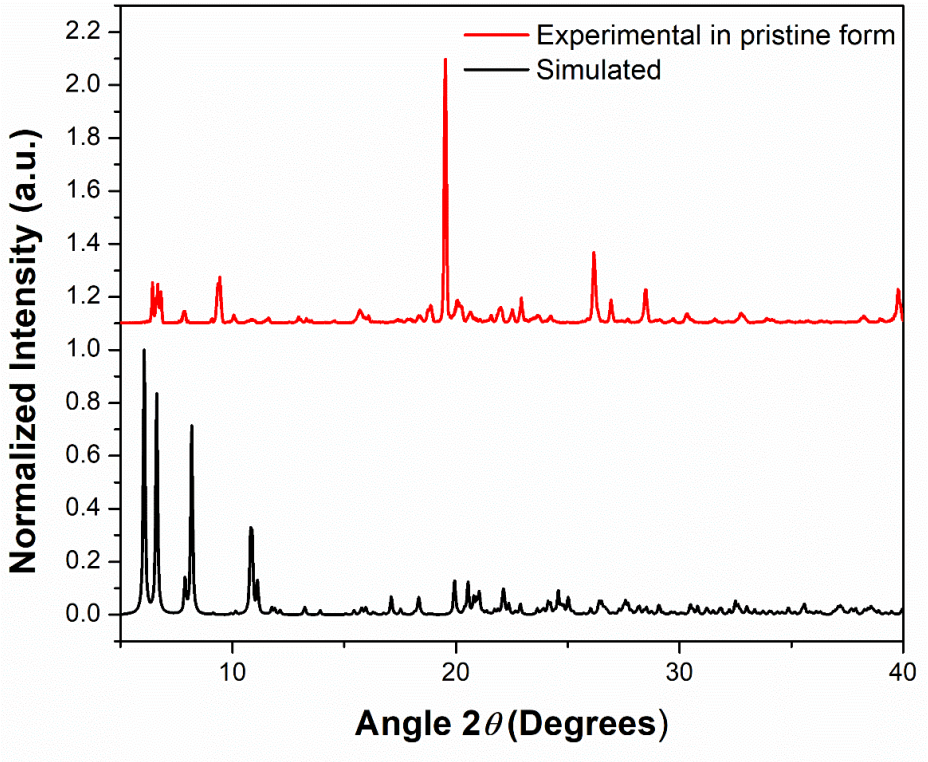

Figure S36. PXRD pattern of complex **4** at 298 K

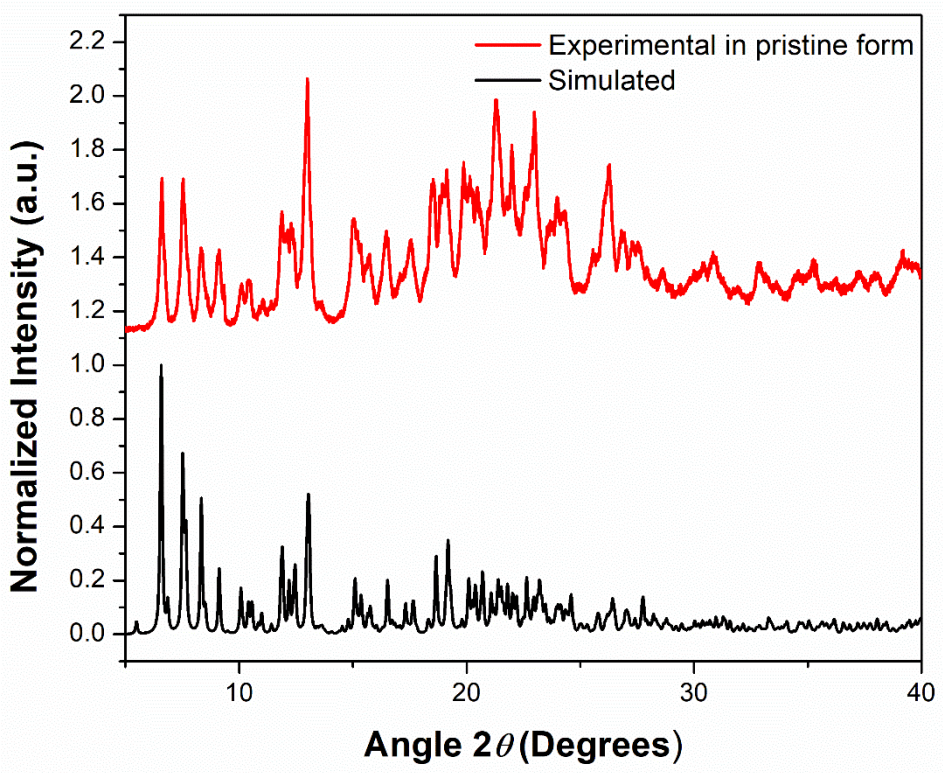

Figure S37. PXRD pattern of complex **6** at 298 K

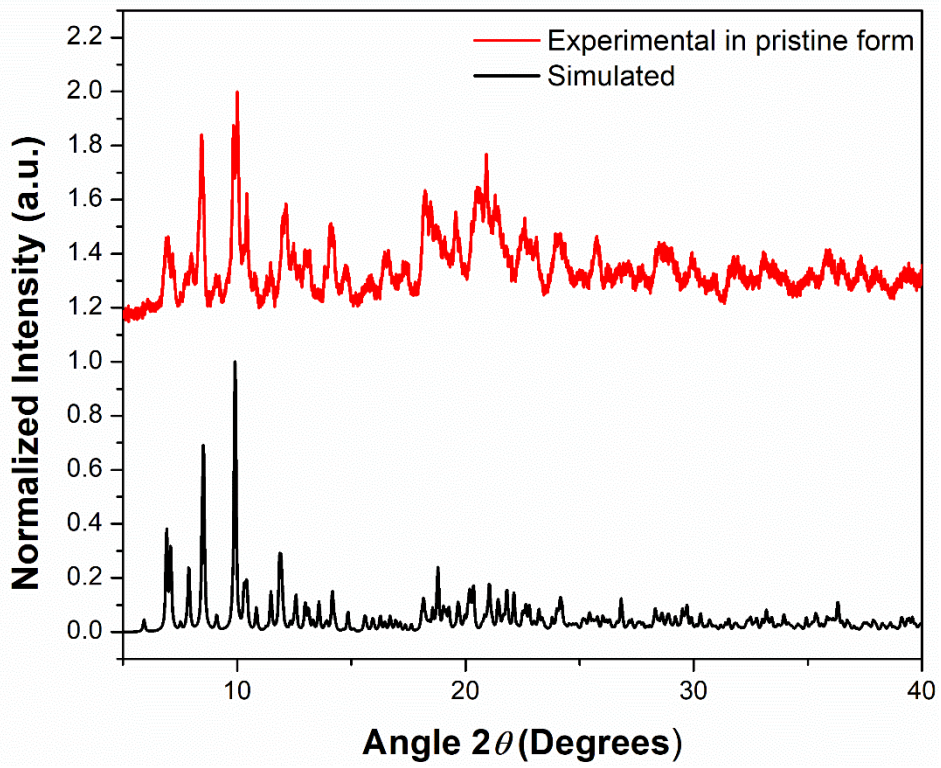

Figure S38. PXRD pattern of complex 1**2** at 298 K

S6. Mass Spectrometric Data for complexes 2-12

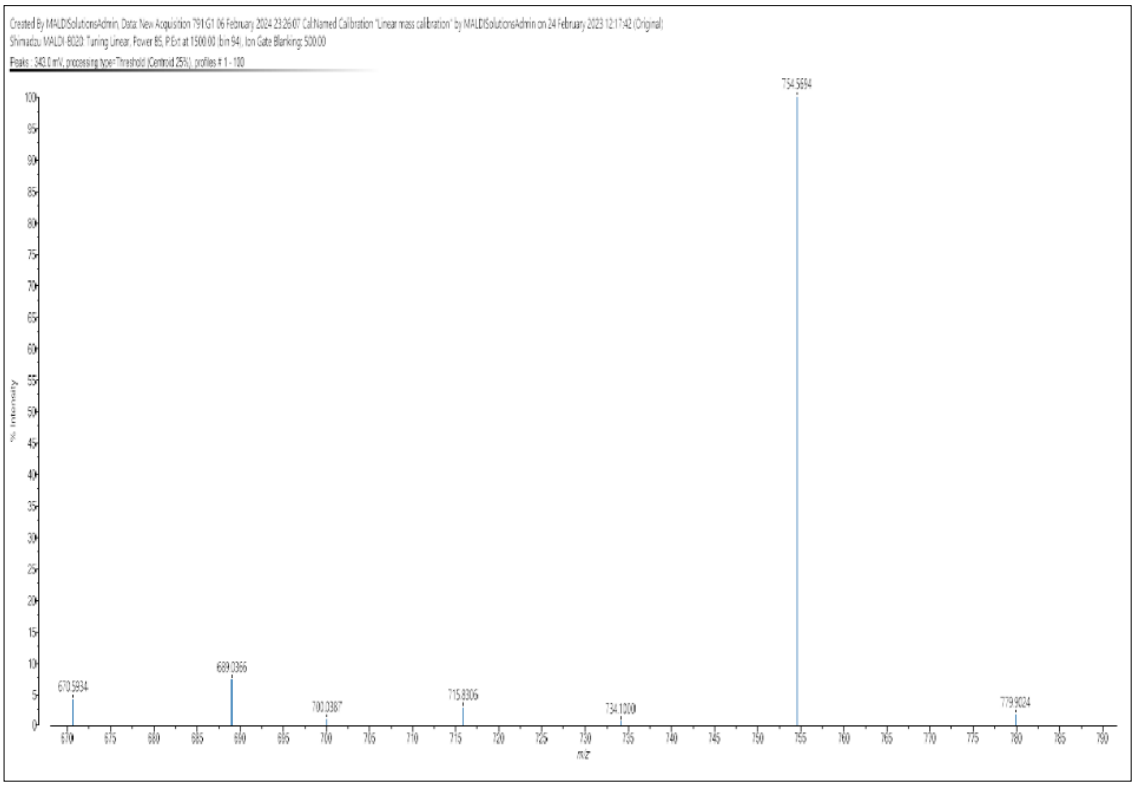

Figure S39. MALDI-TOF data of Complex **2**

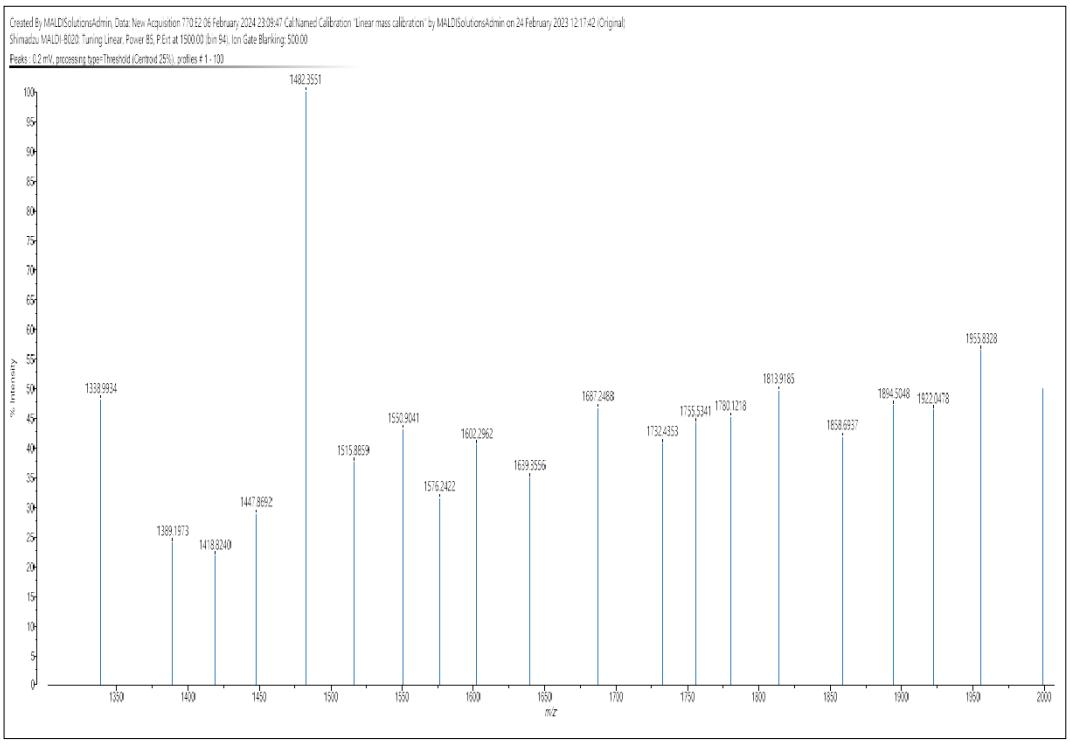

Figure S40. MALDI-TOF data of Complex **3**

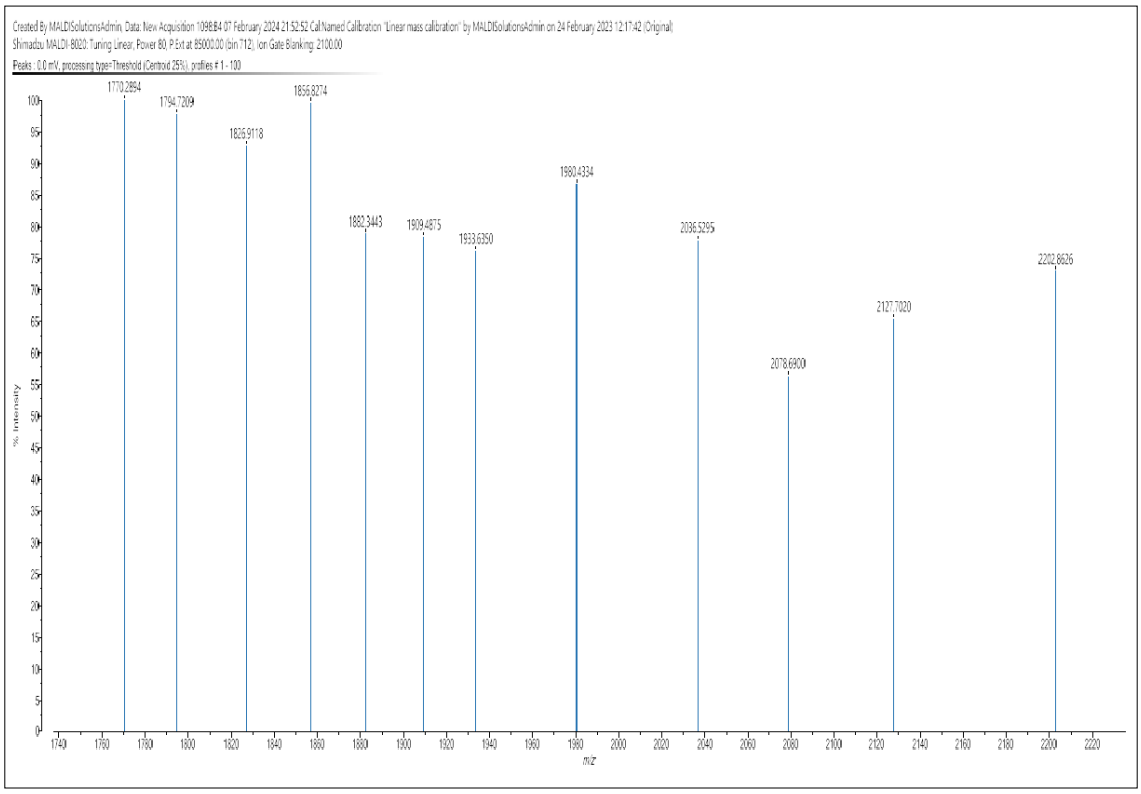

Figure S41. MALDI-TOF data of Complex **4**

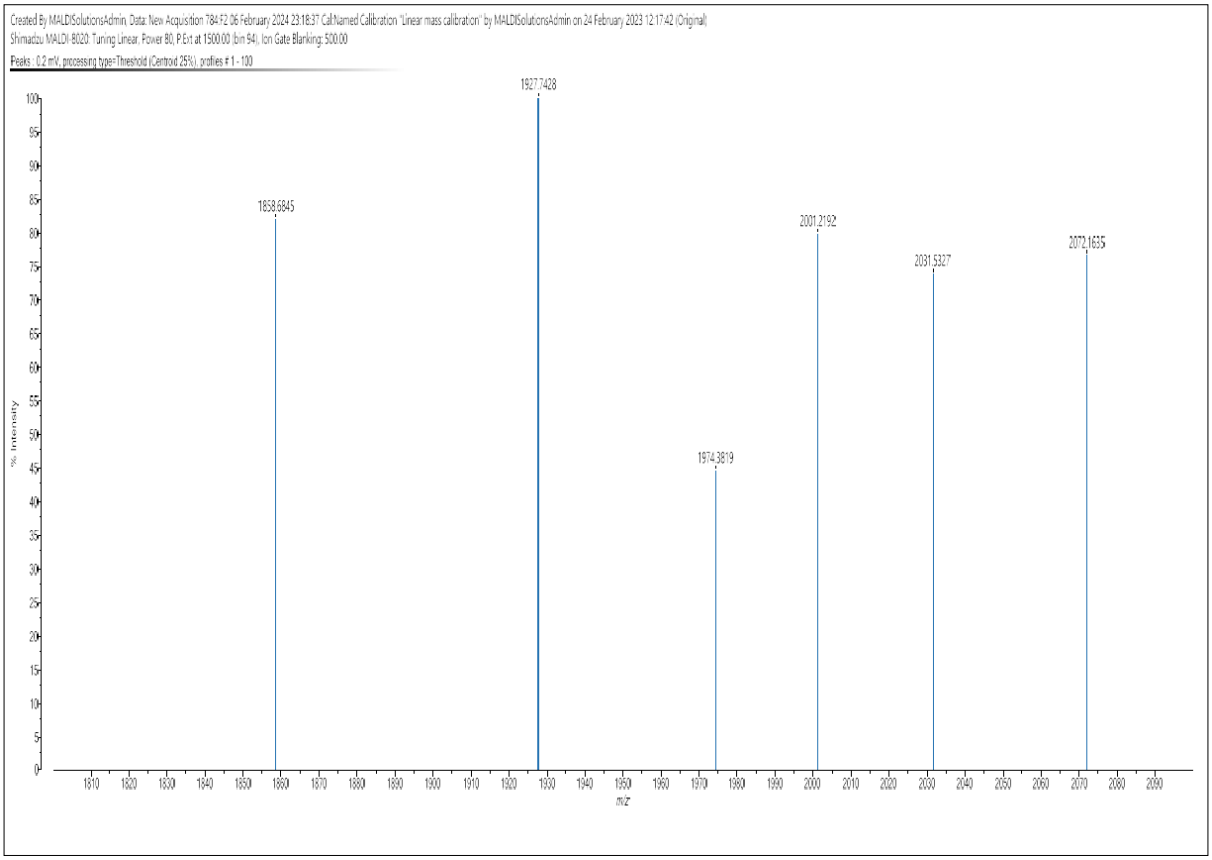

Figure S42. MALDI-TOF data of Complex **5**

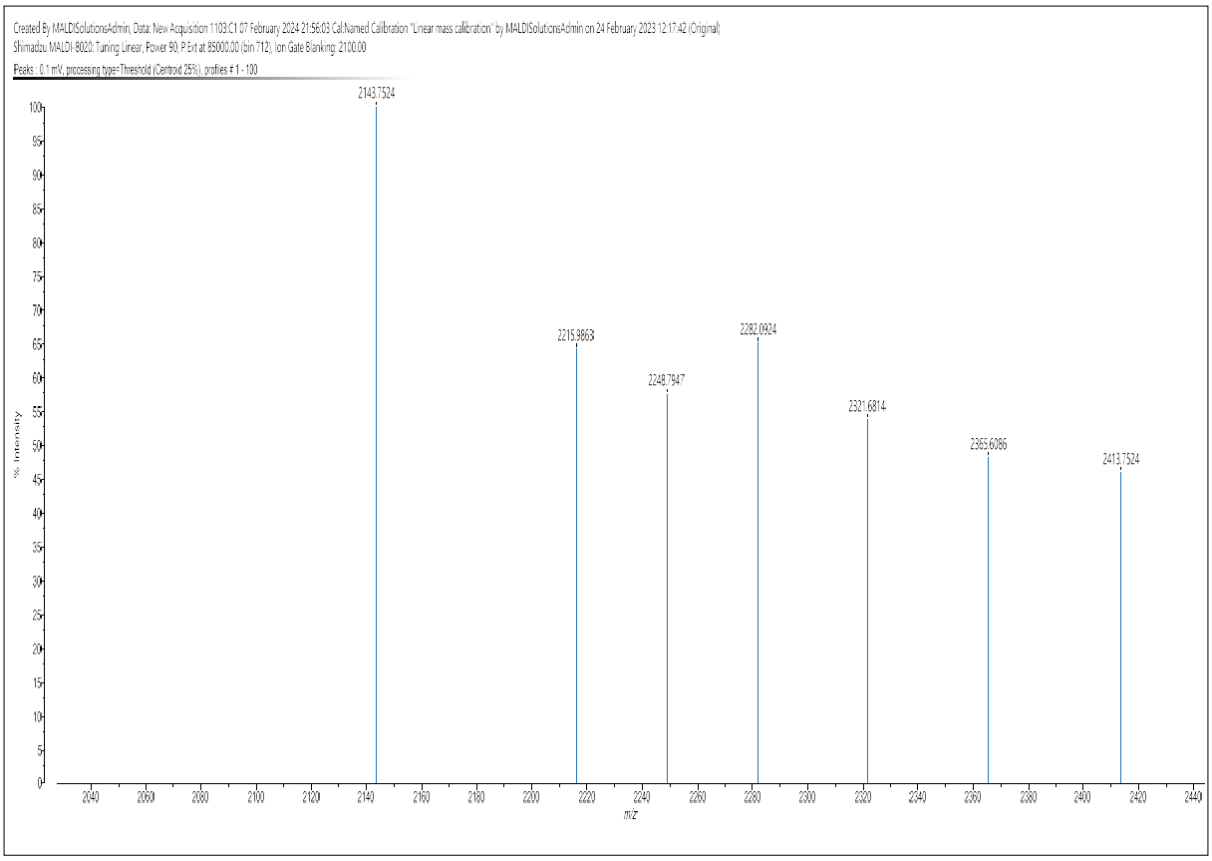

Figure S43. MALDI-TOF data of Complex **6**

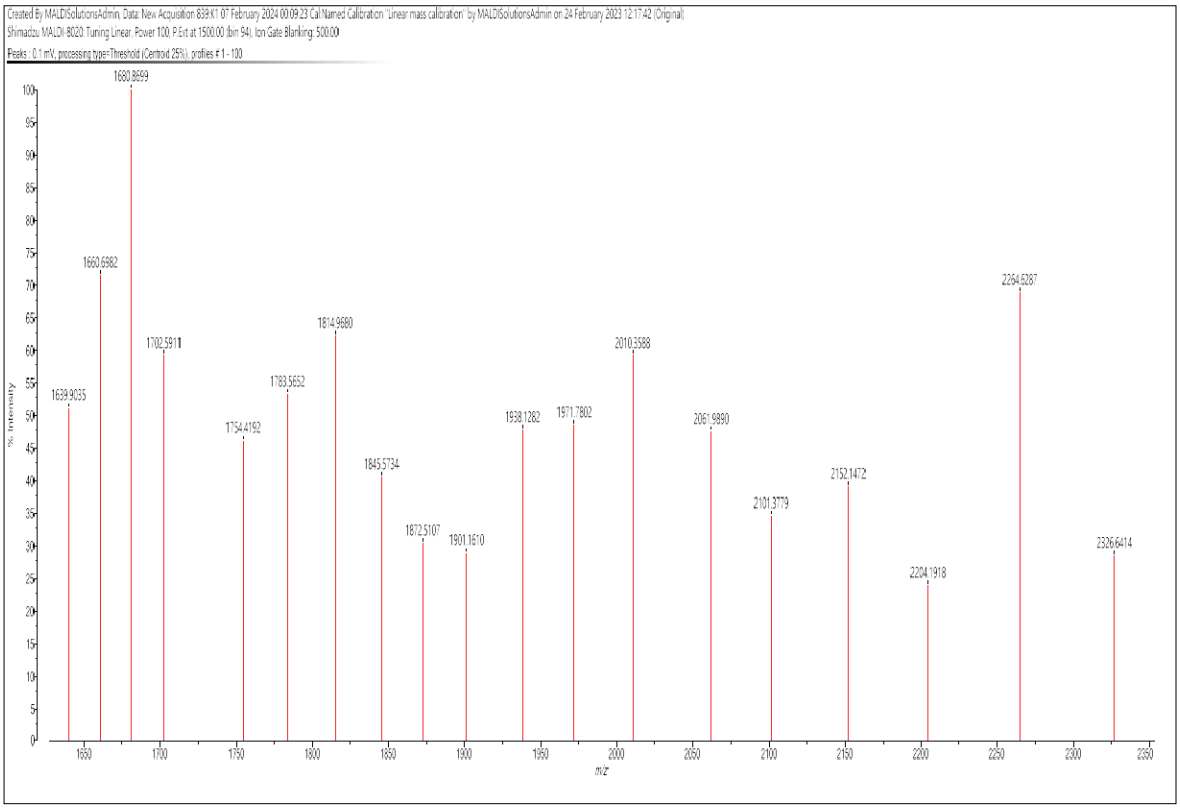

Figure S44. MALDI-TOF data of Complex **7**

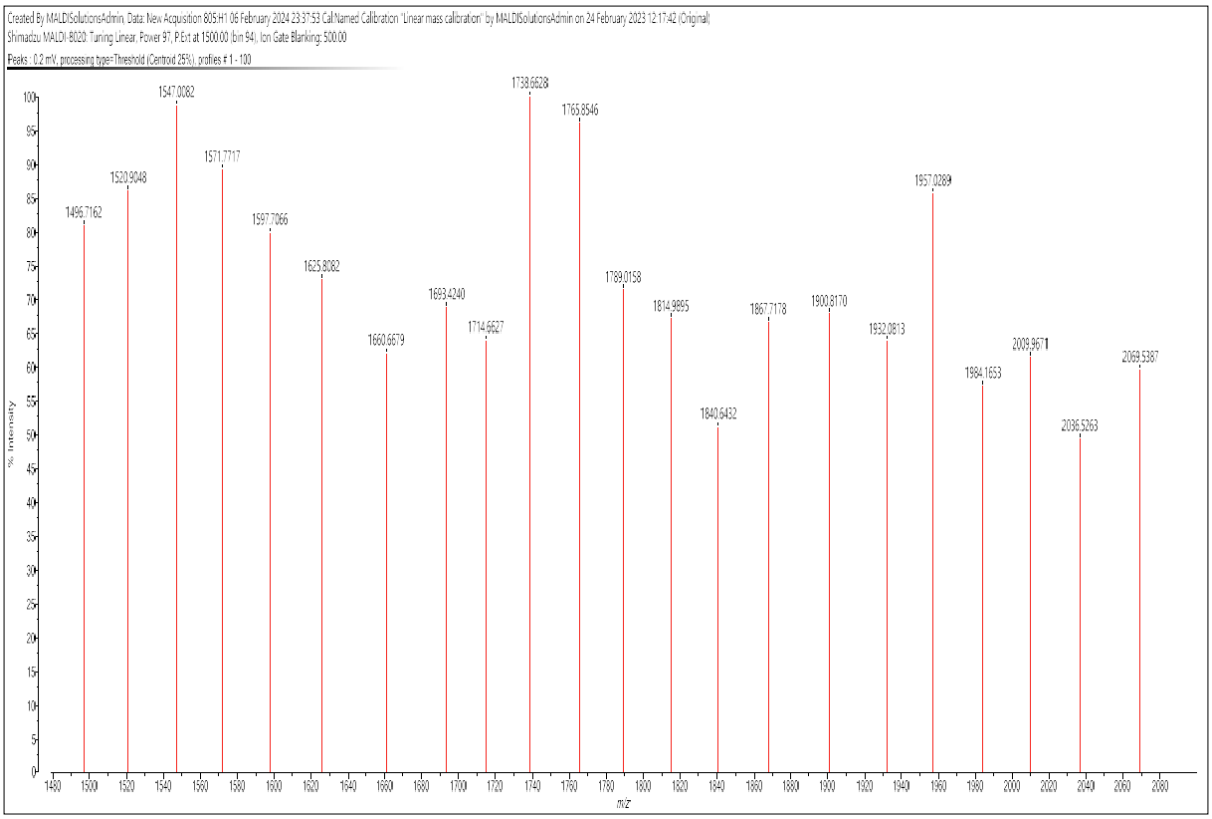

Figure S45. MALDI-TOF data of Complex **8**

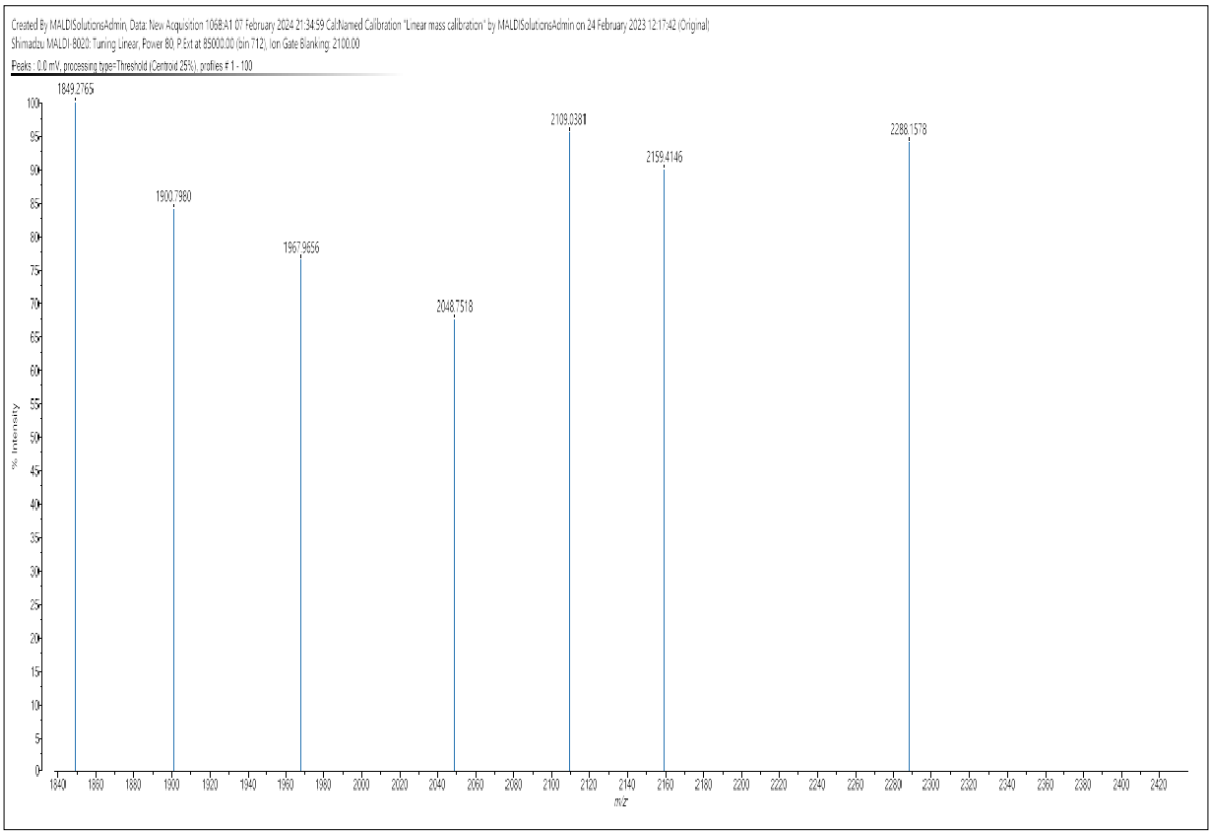

Figure S46. MALDI-TOF data of Complex **9**

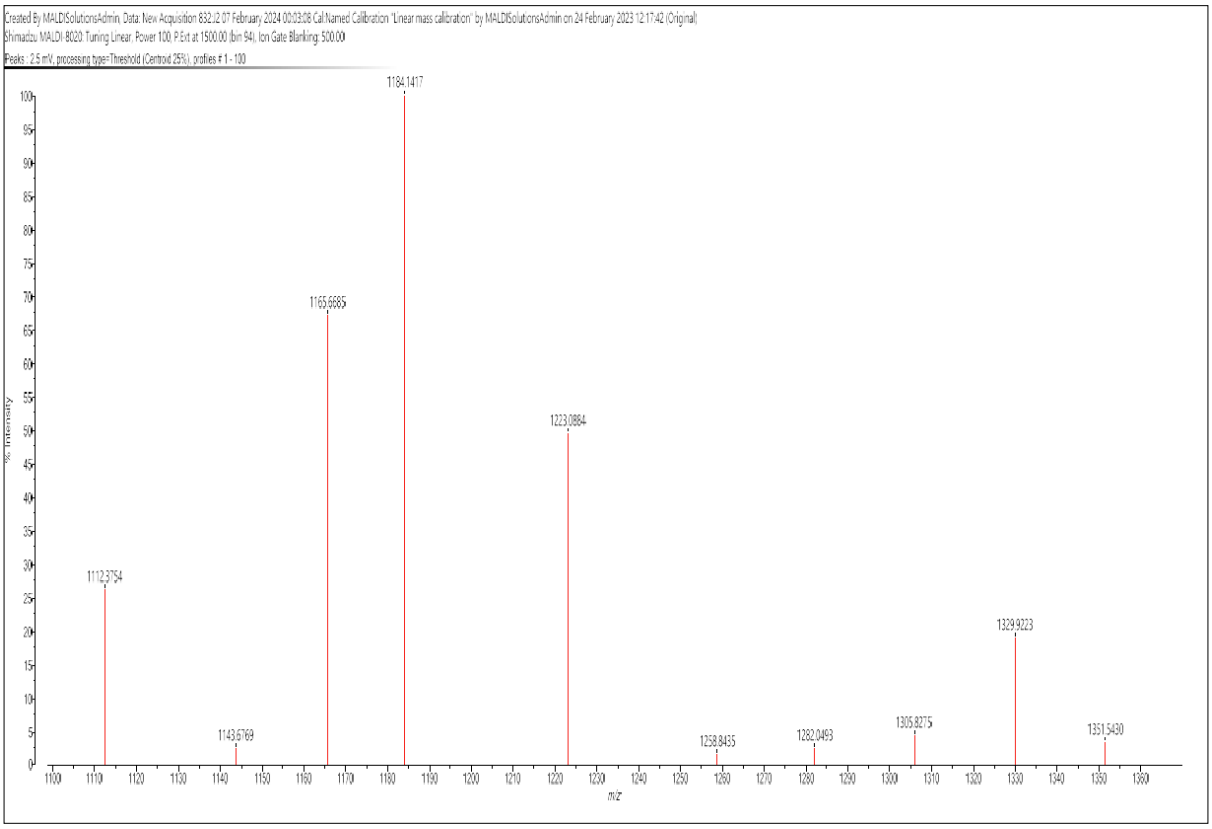

Figure S47. MALDI-TOF data of Complex **10**

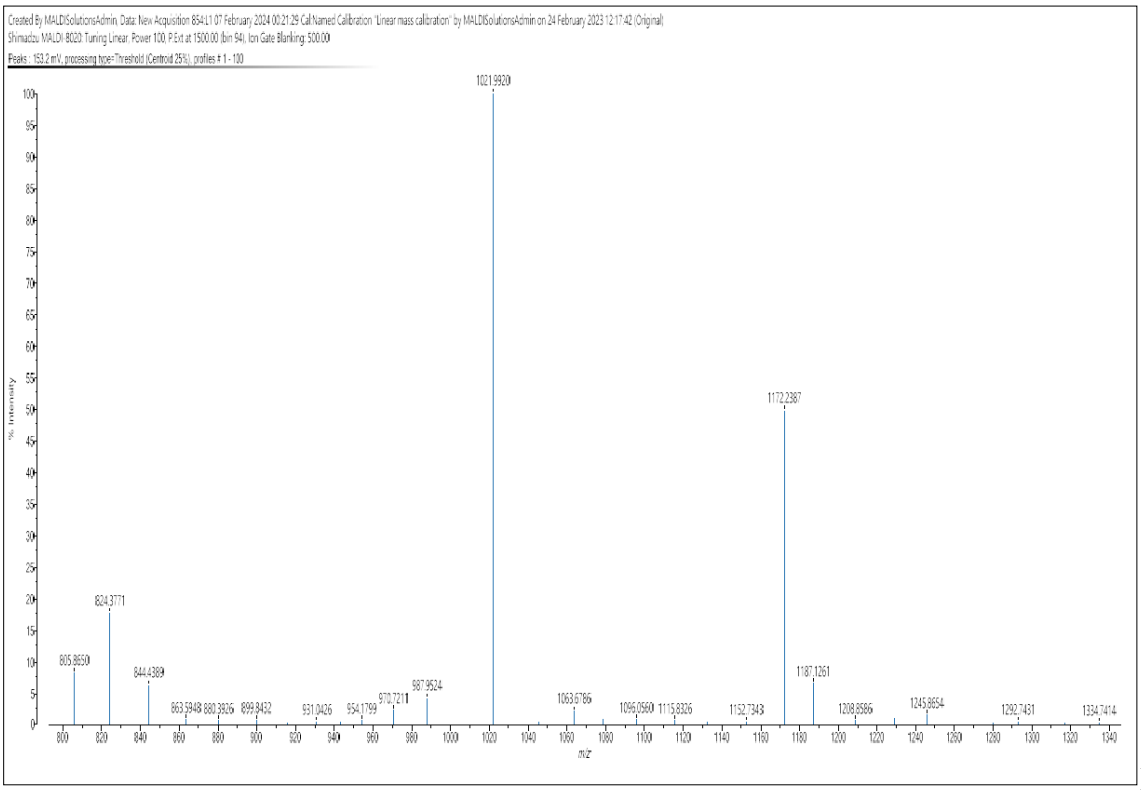

Figure S48. MALDI-TOF data of Complex **11**

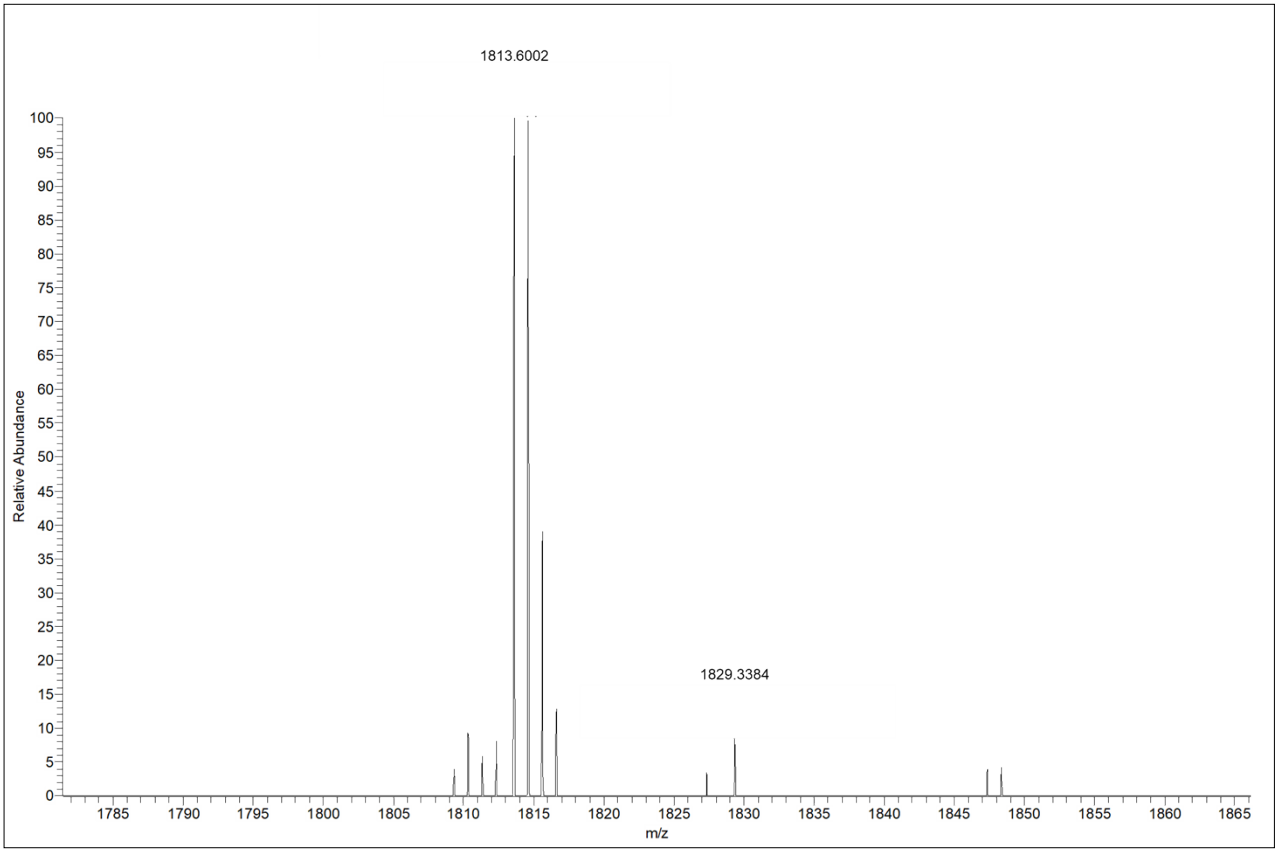

Figure S49. ESI-MS data of Complex **12**

S7. Quantum Chemical Calculation for Complexes 2-4, 6, 7, 11, and 12

Co-ordinates from crystal structures are used as initial geometries for obtaining the ground state (S_0) optimized geometries of these complexes. The Gaussian 09 program package was used to perform these calculations.[5] All these calculations are performed at the Grimme's dispersion corrected B3LYP functional (B3LYP-D3) using a def2-SVP basis set with ultrafine numerical integration grid and tight convergence criteria. Harmonic vibrational frequencies of these S_0 geometries were obtained to ensure the local minima of optimized structures. These geometries were further used to perform the TDDFT calculations to obtain further insights into the various singlet/triplet excited states, such as energies of excited states, oscillator strengths, and optical excitations.

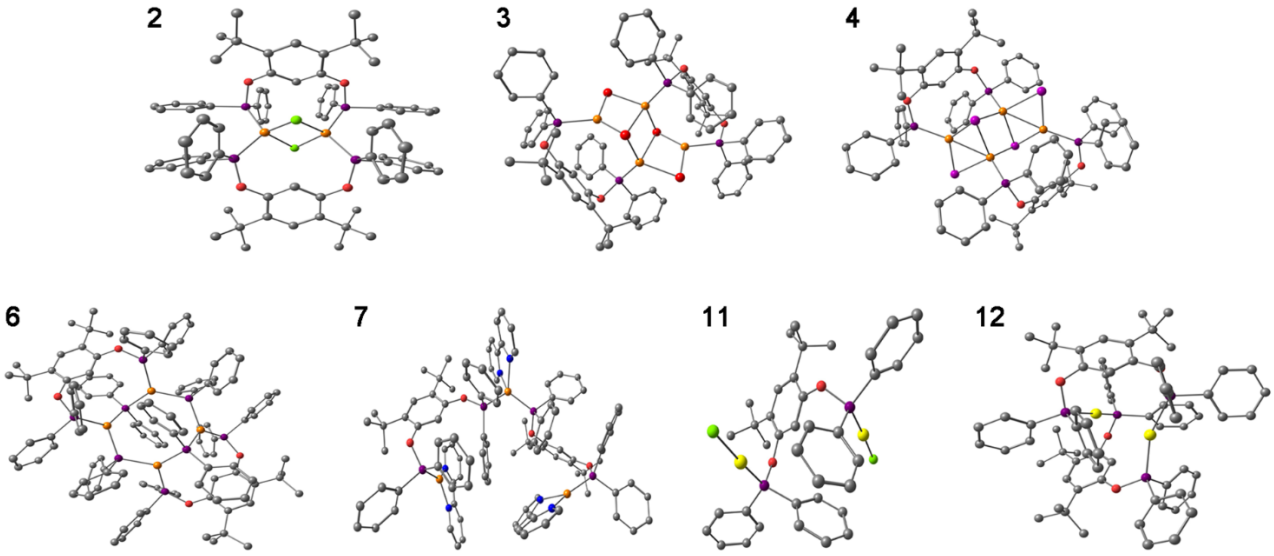

Figure S50. Ground state (S0) optimized geometries of the complexes **2-4**, **6**, **7**, **11**, and **12** calculated at the B3LYP-D3/def2-SVP level.

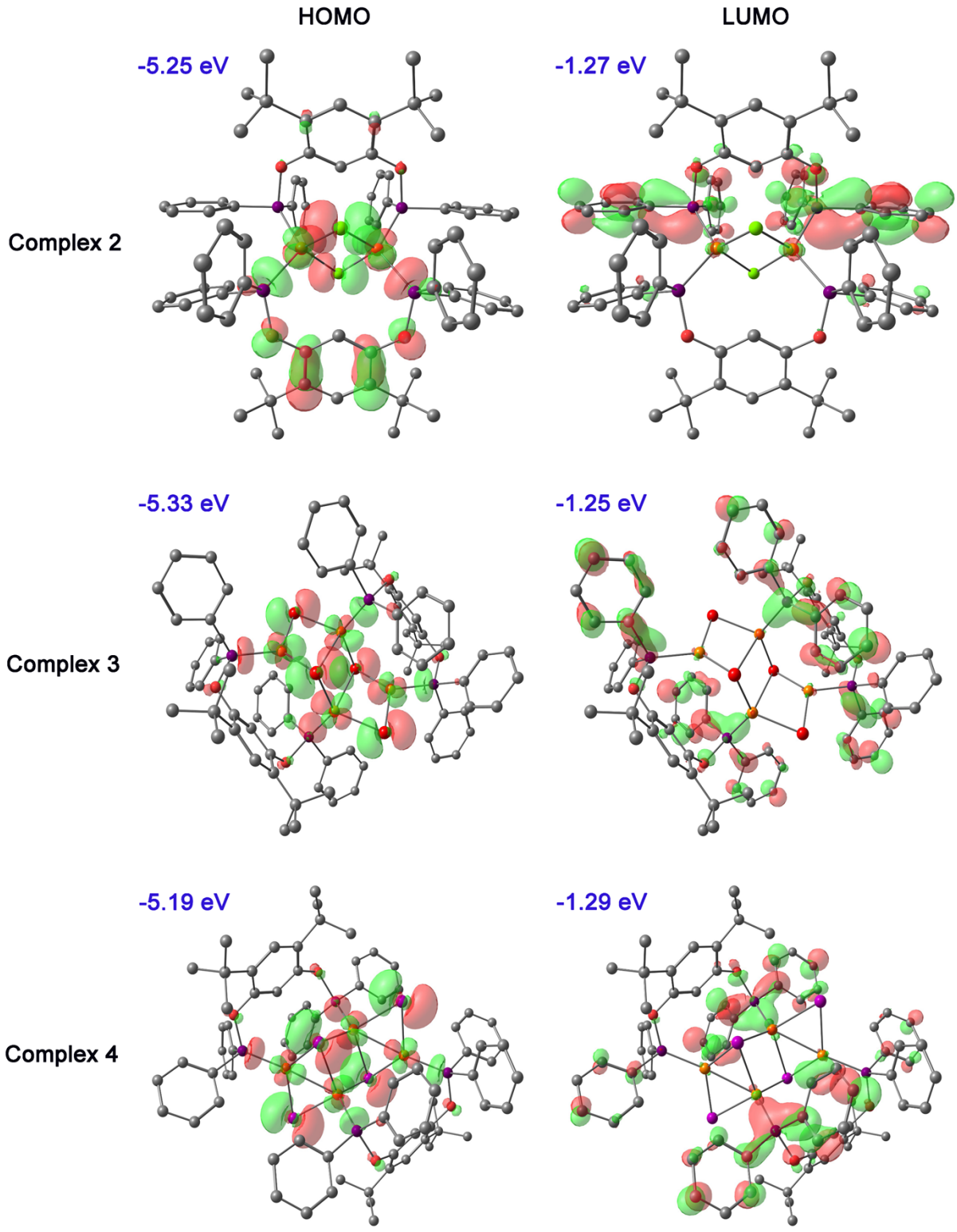

Figure S51. HOMO and LUMO of complexes **2-4** at ground state.

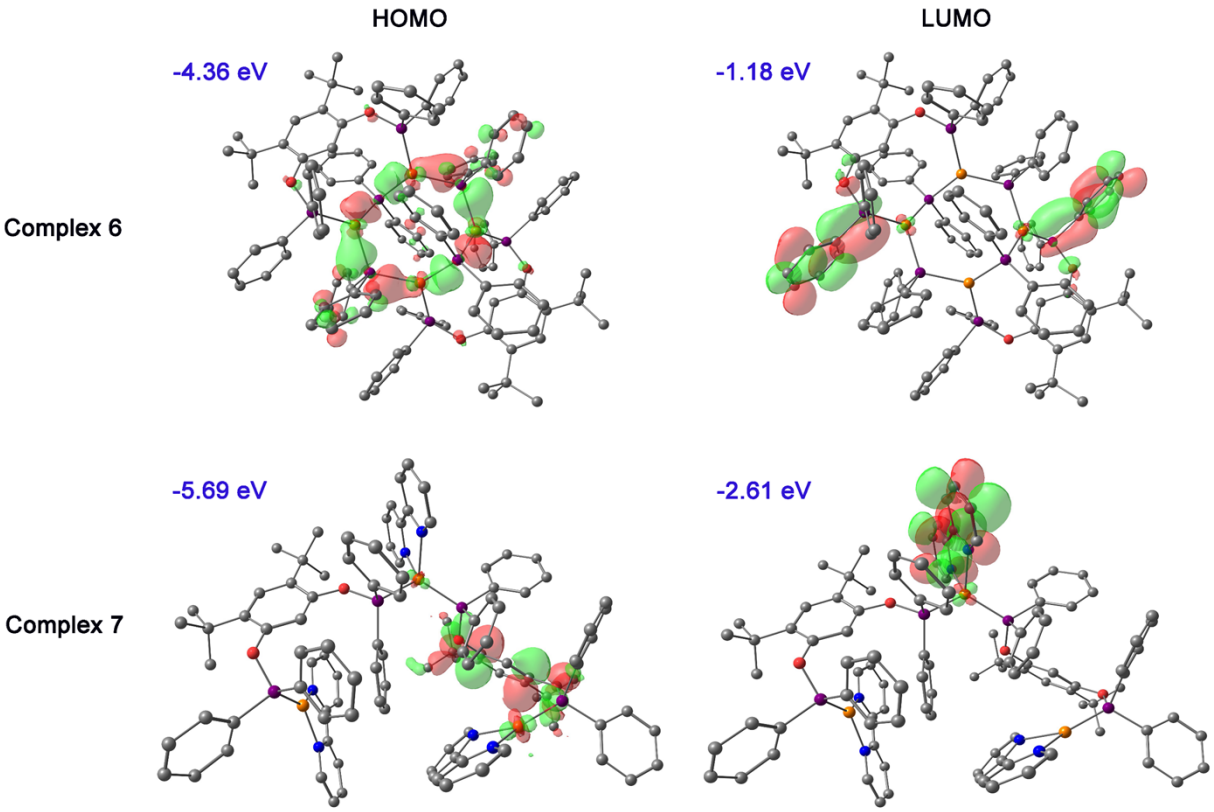

Figure S52. HOMO and LUMO of complexes **6** and **7** at ground state.

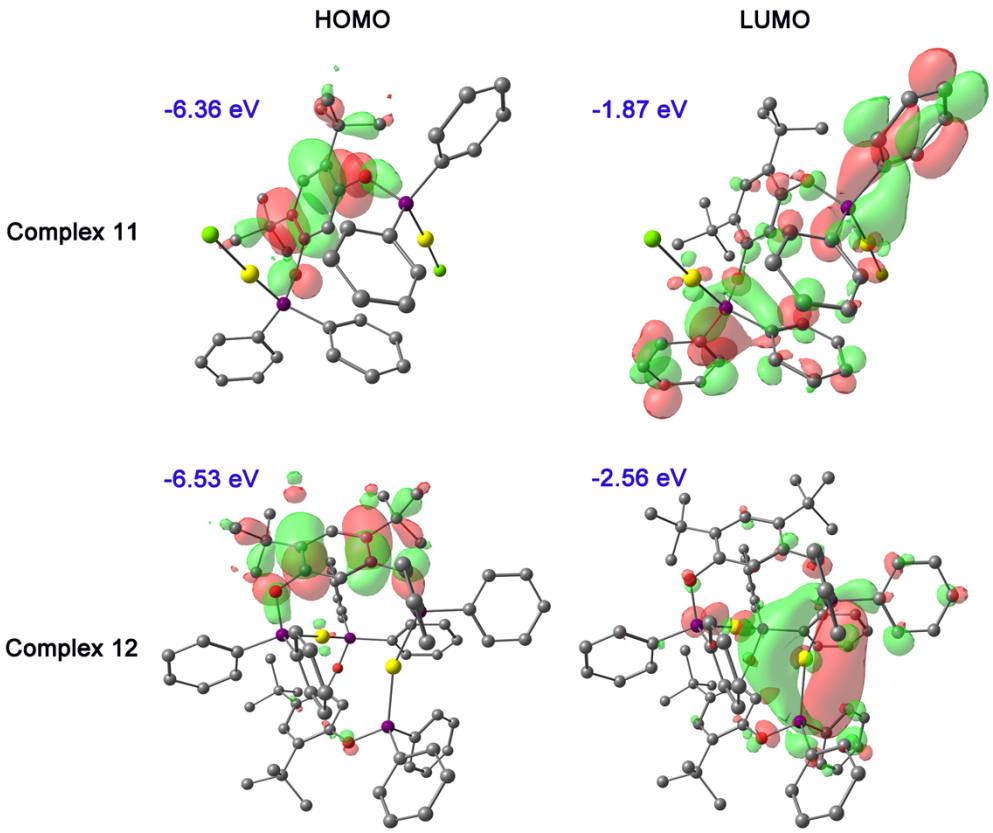

Figure S53. HOMO and LUMO of complexes **11** and **12** at the ground state.

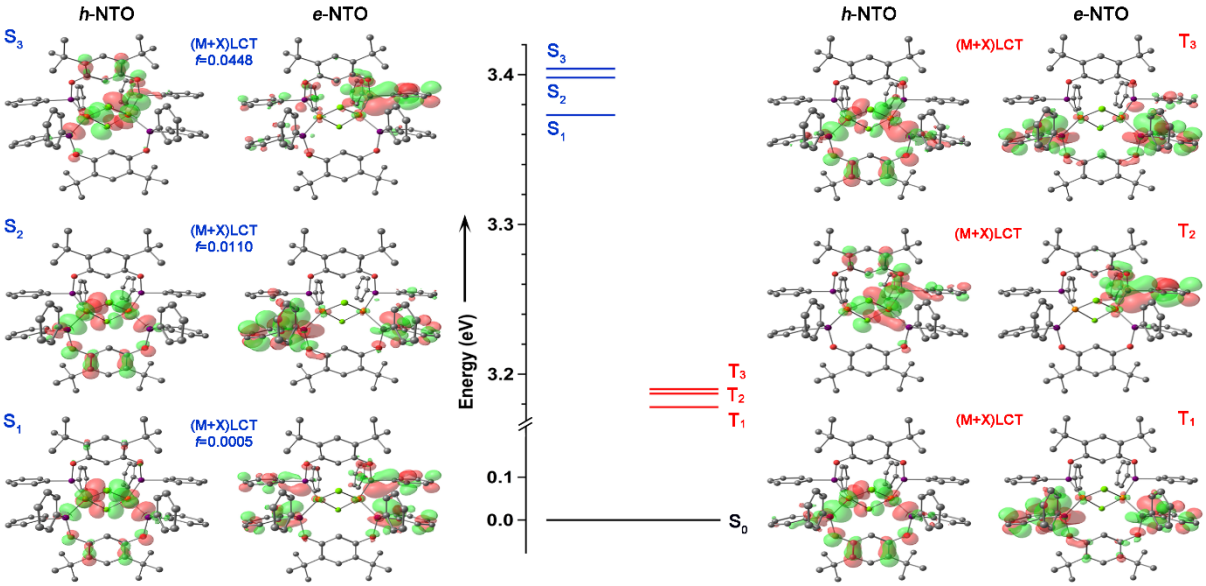

Figure S54. NTO analysis for complex **2**.

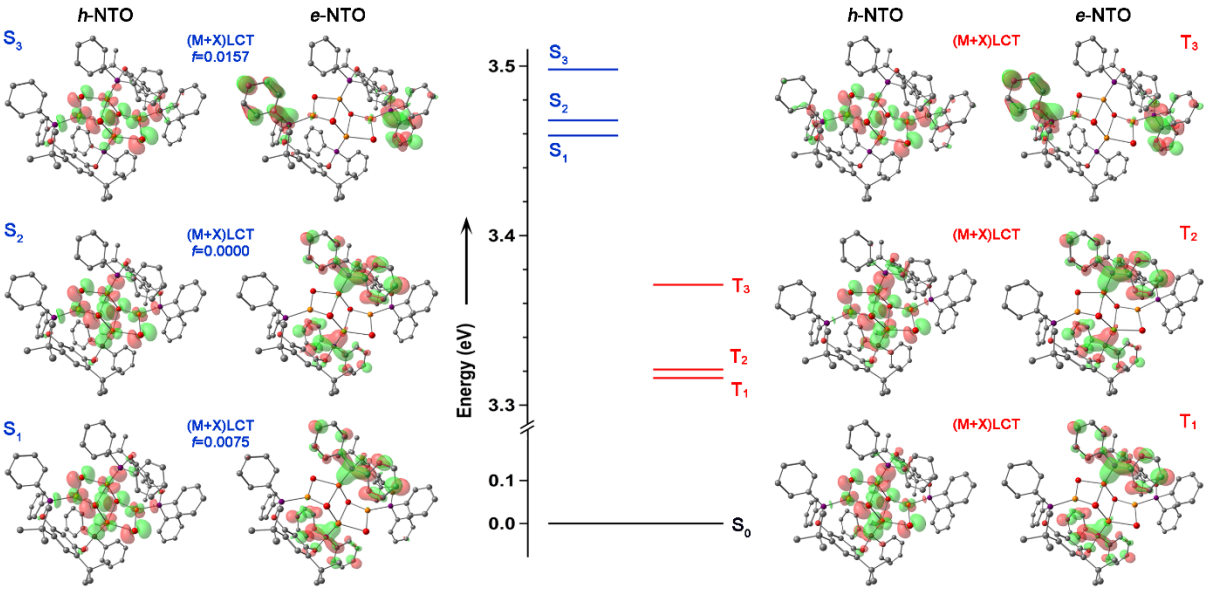

Figure S55. NTO analysis for complex **3**.

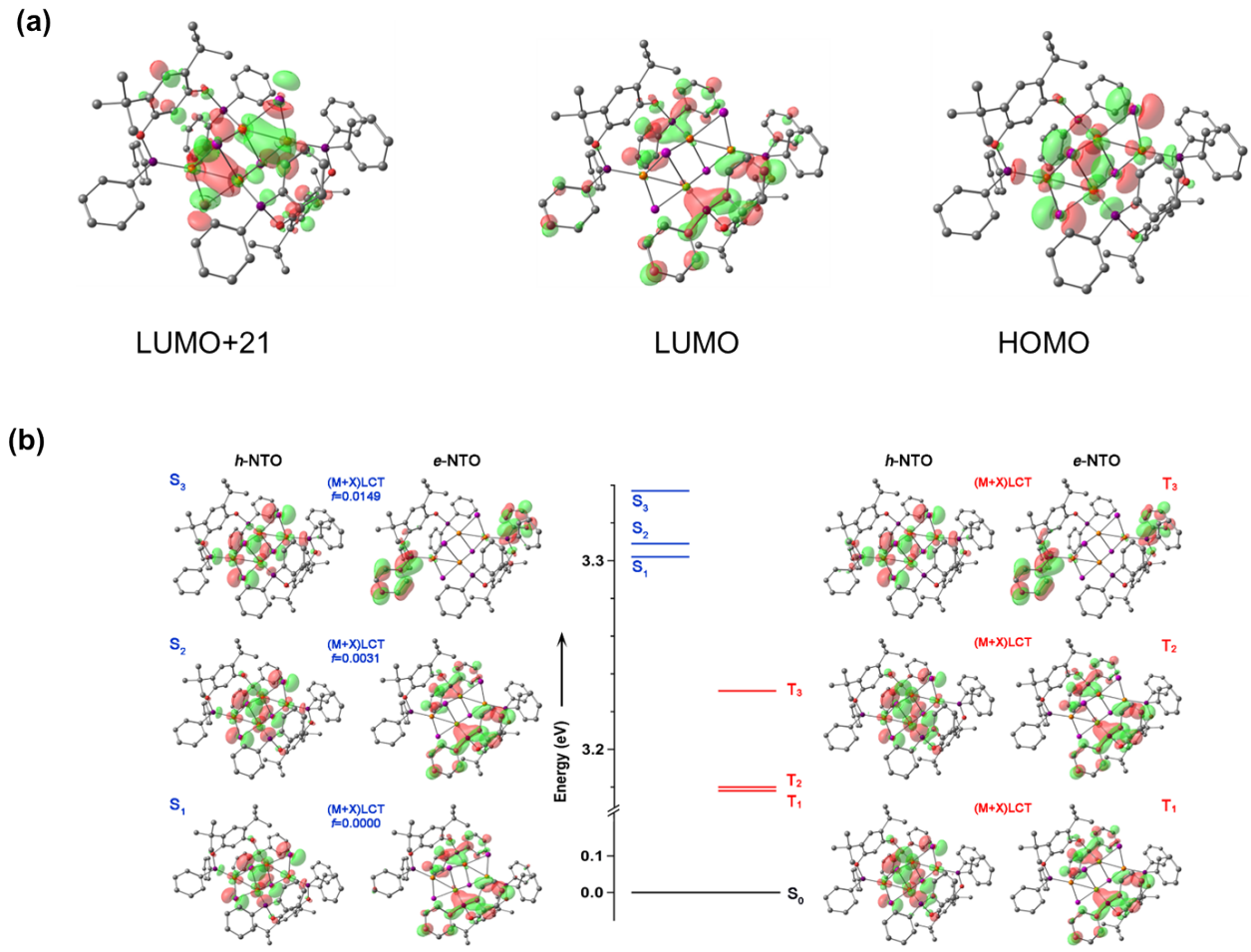

Figure S56. (a) MOs of complex **4** in the ground state; (b)NTO analysis for complex **4**.

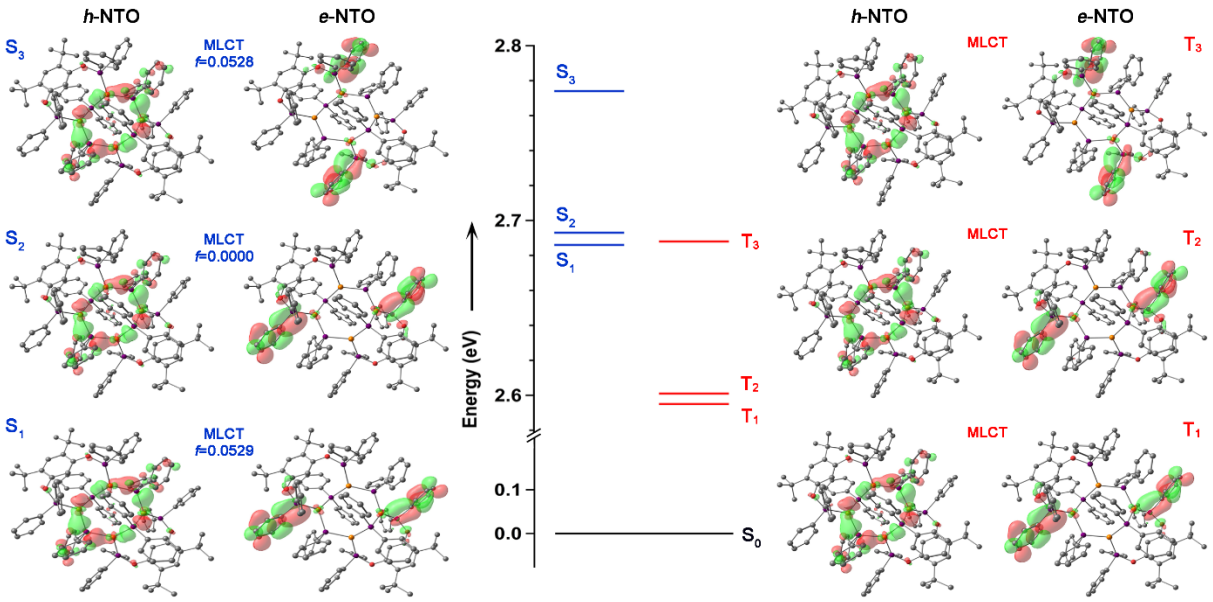

Figure S57. NTO analysis for complex **6**.

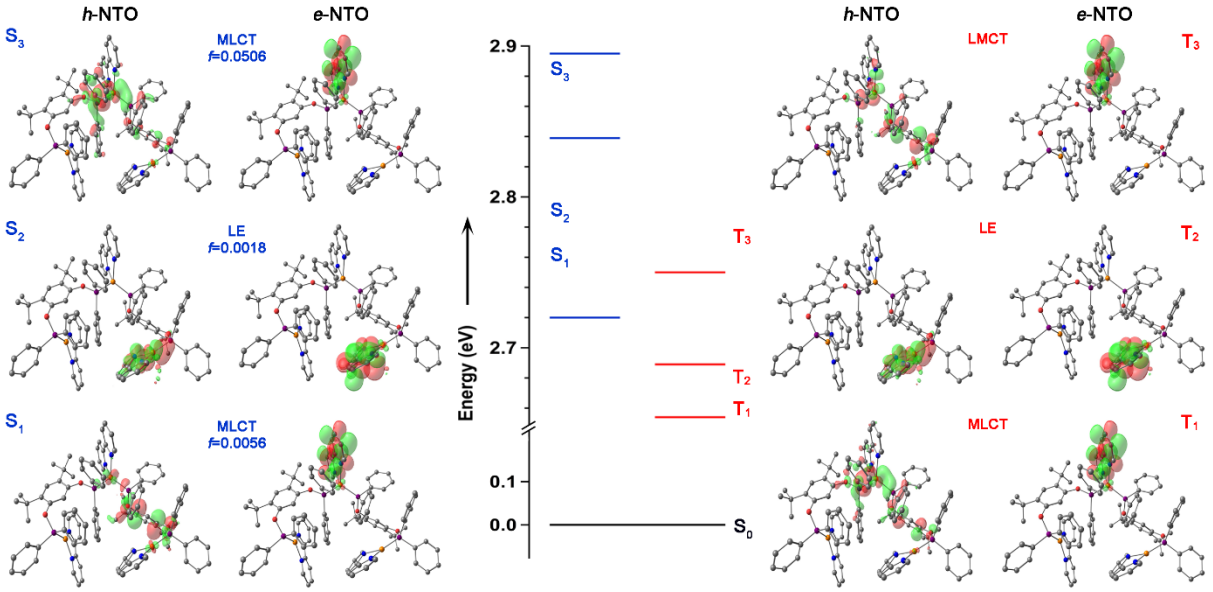

Figure S58. NTO analysis for complex **7**.

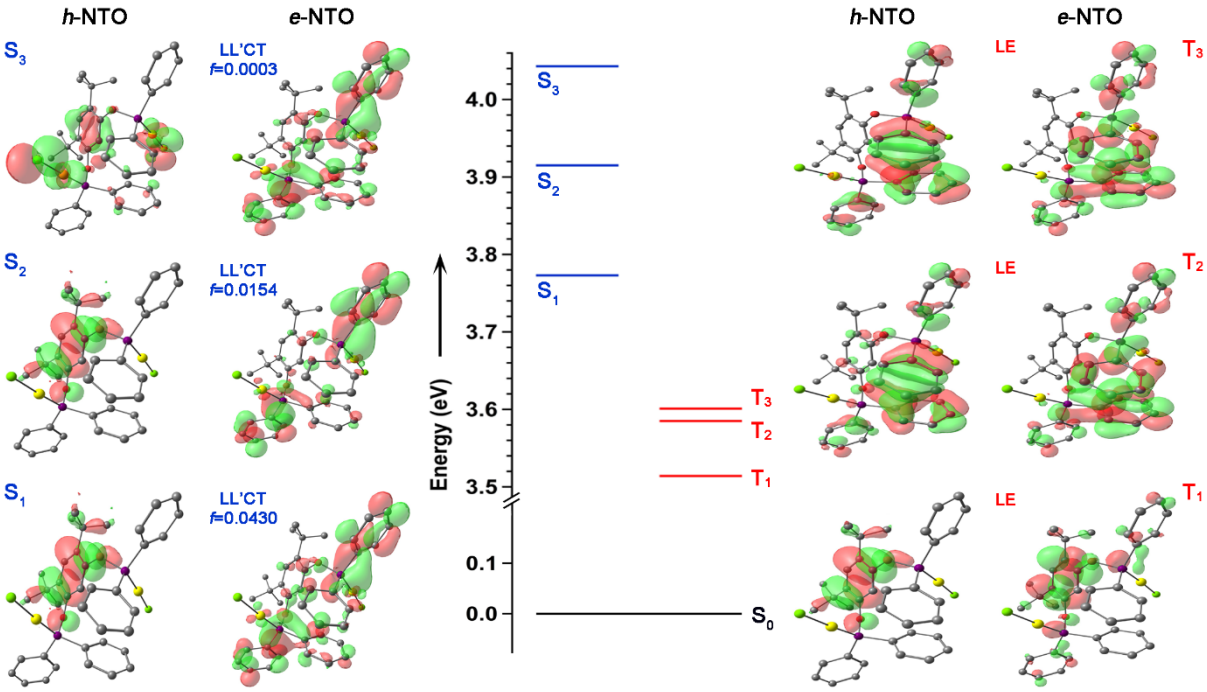

Figure S59. NTO analysis for complex **11**.

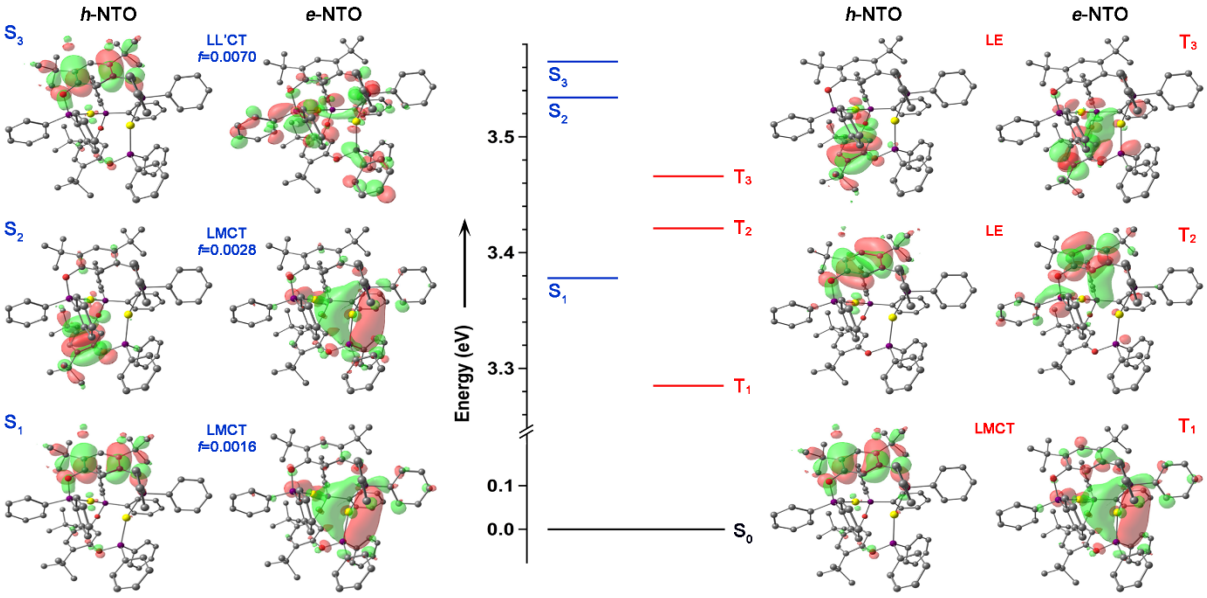

Figure S60. NTO analysis for complex **12**.

Table S1. Spin-orbit coupling (SOC) values for complexes **2**-**4** in cm^{-1}

	2	**3**	**4**
S_0-T_1	26.27527	1.01734	1.00089
S_0-T_2	100.0052	97.57894	73.17875
S_0-T_3	34.08661	0.46184	1.40215
S_1-T_1	6.68691	14.55867	0.13333
S_1-T_2	4.73363	0.16354	5.42224
S_1-T_3	7.21313	14.94565	0.07077
S_2-T_1	4.06299	0.16193	7.58012
S_2-T_2	7.65177	16.99998	0.15399
S_2-T_3	4.42956	0.142	8.11849
S_3-T_1	9.03803	12.19809	3.38845
S_3-T_2	8.60884	0.46646	0.06677
S_3-T_3	12.77628	7.99878	5.87418

Table S2. Excitation energies and oscillator strengths of emission properties

Complex number	**Excited state**	**Excitation involved**	**Oscillator strength**
2	S_1	(M+X)LCT	f=0.0005
	S_2	(M+X)LCT	f=0.0110
	S_3	(M+X)LCT	f=0.0448
	T_1	(M+X)LCT	f=0.0000
	T_2	(M+X)LCT	f=0.0000
	T_3	(M+X)LCT	f=0.0000
3	S_1	(M+X)LCT	f=0.0075
	S_2	(M+X)LCT	f=0.0000
	S_3	(M+X)LCT	f=0.0157
	T_1	(M+X)LCT	f=0.0000
	T_2	(M+X)LCT	f=0.0000
	T_3	(M+X)LCT	f=0.0000
4	S_1	(M+X)LCT	f=0.0000
	S_2	(M+X)LCT	f=0.0031
	S_3	(M+X)LCT	f=0.0149

	T_1	(M+X)LCT	f=0.0000
	T_2	(M+X)LCT	f=0.0000
	T_3	(M+X)LCT	f=0.0000
6	S_1	MLCT	f=0.0529
	S_2	MLCT	f=0.0000
	S_3	MLCT	f=0.0528
	T_1	MLCT	f=0.0000
	T_2	MLCT	f=0.0000
	T_3	MLCT	f=0.0000
7	S_1	MLCT	f=0.0056
	S_2	LE	f=0.0018
	S_3	MLCT	f=0.0506
	T_1	MLCT	f=0.0000
	T_2	LE	f=0.0000
	T_3	LMCT	f=0.0000
11	S_1	LL'CT	f=0.0430
	S_2	LL'CT	f=0.0154
	S_3	LL'CT	f=0.0003
	T_1	LE	f=0.0000
	T_2	LE	f=0.0000
	T_3	LE	f=0.0000
12	S_1	LMCT	f=0.0016
	S_2	LMCT	f=0.0028
	S_3	LL'CT	f=0.0070
	T_1	LMCT	f=0.0000
	T_2	LE	f=0.0000
	T_3	LE	f=0.0000

References

1. R. B. Bedford, M. Betham, M. E. Blake, S. J. Coles, S. M. Draper, M. B. Hursthouse and P. N. Scully, *Inorganica Chim. Acta*, 2006, **359**, 1870-1878.

2. O. V. Dolomanov, L. J. Bourhis, R. J. Gildea, J. A. K. Howard and H. Puschmann, *J. Appl. Crystallogr.*, 2009, **42**, 339-341.
3. G. M. Sheldrick, *Acta Crystallogr. C Struct.*, 2015, **71**, 3-8.
4. A. L. Spek, *J. Appl. Crystallogr.*, 2003, **36**, 7-13.
5. M. J. Frisch, G. W. Trucks, H. B. Schlegel, G. E. Scuseria, M. A. Robb, J. R. Cheeseman, G. Scalmani, V. Barone, B. Mennucci, G. A. Petersson, H. Nakatsuji, M. Caricato, X. H. Li, H. P., A. F. B. Izmaylov, J., G. Zheng, J. L. Sonnenberg, M. Hada, M. Ehara, K. Toyota, R. Fukuda, J. Hasegawa, M. Ishida, T. Nakajima, Y. Honda, O. Kitao, H. Nakai, T. Vreven, J. Montgomery, J. A., J. E. Peralta, F. Ogliaro, M. Bearpark, J. J. Heyd, E. Brothers, K. N. Kudin, V. N. Staroverov, R. Kobayashi, J. Normand, K. Raghavachari, A. Rendell, J. C. Burant, S. S. Iyengar, J. Tomasi, M. Cossi, N. Rega, N. J. Millam, M. Klene, J. E. Knox, J. B. Cross, V. Bakken, C. Adamo, J. Jaramillo, R. Gomperts, R. E. Stratmann, O. Yazyev, A. J. Austin, R. Cammi, C. Pomelli, J. W. Ochterski, R. L. Martin, K. Morokuma, V. G. Zakrzewski, G. A. Voth, P. Salvador, J. J. Dannenberg, S. Dapprich, A. D. Daniels, Ö. Farkas, J. B. Foresman, J. V. Ortiz, J. Cioslowski and D. J. Fox, *Revision D.01, Gaussian, Inc., Wallingford CT **(2009)***.

.